Universiteit Leiden
The Netherlands

Toxicity, bioaccumulation and trophic transfer of engineered nanoparticles in the aquatic environment
Yu, Q.

Toxicity, bioaccumulation and trophic transfer of engineered nanoparticles in the aquatic environment

Qi Yu

于 棋

Toxicity, bioaccumulation and trophic transfer of engineered nanoparticles in the aquatic environment

Toxicity, bioaccumulation and trophic transfer of engineered nanoparticles in the aquatic environment

Proefschrift

ter verkrijging van

de graad van doctor aan de Universiteit Leiden,

op gezag van rector magnificus prof.dr.ir. H. Bijl,

volgens besluit van het college van promoties

te verdedigen op dinsdag 31 januari 2023

klokke 11.15 uur

door

Qi Yu

Geboren te Heilongjiang, China

in 1992

Promotores:

Prof.dr.ir. W.J.G.M. Peijnenburg

Prof.dr.ing. M.G. Vijver

Dr.ir. T. Bosker

Promotiecommissie:

Prof.dr.ir. P.M. van Bodegom

Prof.dr. N.J. de Voogd

Dr. S.H. Barmentlo

Prof.dr. M.S. Sepúlveda

Prof.dr. Z. Wang

Table of contents

Chapter 1

General Introduction

Nanomaterials (NMs) are defined as materials containing 50% or more particles with at least one dimension on the nanoscale level. The European Commission Regulation 2011/696/EU (Science for Environment Policy, 2017; The European Commission recommendations, 2010) has defined nanoscale between 1 and 100 nm. Nanoparticles (NPs) are NMs with all three external dimensions in the nanoscale (ISO, 2008; *Terminology for nanomaterials*, 2007). Nanotechnology is the use of matter at the nano scale and is an emerging technology. The development of nanotechnology not only brings the promise of radical technological development– for example, clean energy, highly effective medicines and lightweight products - but also brings its own safety challenges (Science for Environment Policy, 2017). In this thesis, ecological hazard risk of engineering nanoparticles (ENPs) in the aquatic environment was assessed.

1.1 Application and release of ENPs

The applications for ENPs are numerous, with use in cosmetics, fuel additives, electronics, pharmaceuticals, clothing, biomedicine, catalysis and materials, and environmental remediation (Ju-Nam and Lead, 2008; Keller and Lazareva, 2013; Thomas et al., 2013). The common use of ENPs relies on their nanoscale size and relative large surface area, which result in extraordinary and tuneable nature of optical, electrical, chemical, thermal, magnetic, and mechanical properties (Dolez, 2015; Ju-Nam and Lead, 2008; Rai et al., 2018).

The global nanomaterials market (GNM) size has been expanding rapidly. The Project on Emerging Nanotechnologies (PEN, 2013)

reported that the number of products had a 25-fold growth between 2005 and 2010. The GNM value was estimated to be €20 billion (aroung 11 million tonnes NMs) in 2012 by European Commission Communication (European Commission, 2012). Furthermore, the GNM is expected to expand at a compound annual growth rate of more than 19% from 2022 to 2027 (Mordor Intelligence, 2022). In order to meet the growing market demand and potential applications, a number of ENPs are currently manufactured to arrange the size, shape, and crystal structure of NPs, as well as composition (single or mixture) (Peralta-Videa et al., 2011). Especially, more and more complex and functional ENPs such as gold-silica NPs for medical treatment and silicon–organic hybrid nanostructures for electro-optic nanomodulators, are predicted to dominate the market (Camboni et al., 2019; Wolf et al., 2018). **The complex nanomaterial systems are currently in short of risk assessment and evaluation under the REACH Regulation.**

Given the worldwide use and production of ENPs, their release into freshwater ecosystems is inevitable during their lifecycle (Bundschuh et al., 2016; Peng et al., 2017). Keller and Lazareva (2013) estimated the global mass flow of ENPs to be over 69,200 metric tons per year disposed or released into aquatic environments as of 2010. ENPs in freshwater ecosystems can interact with organisms due to their small size, which may lead to trophic transfer into food chains. To address this, it is essential to determine the fate and behavior of ENPs in the aqueous environment (Batley et al., 2013; Klaine et al., 2008; Williams et al., 2019).

1.2 Fate of ENPs in the aquatic environment

The stability and fate of ENPs in the aquatic environment are influenced by physical, chemical and biological processes (Lowry et al., 2012; Peijnenburg et al., 2015). Dwivedi et al. (2015) further proposed that physicochemical processes (comprising of aggregation, sedimentation, and dissolution of the particles) also play a vital role in affecting the behavior of ENPs in water as illustrated in Figure 1.1 (Rocha et al., 2016; Van Koetsem et al., 2015).
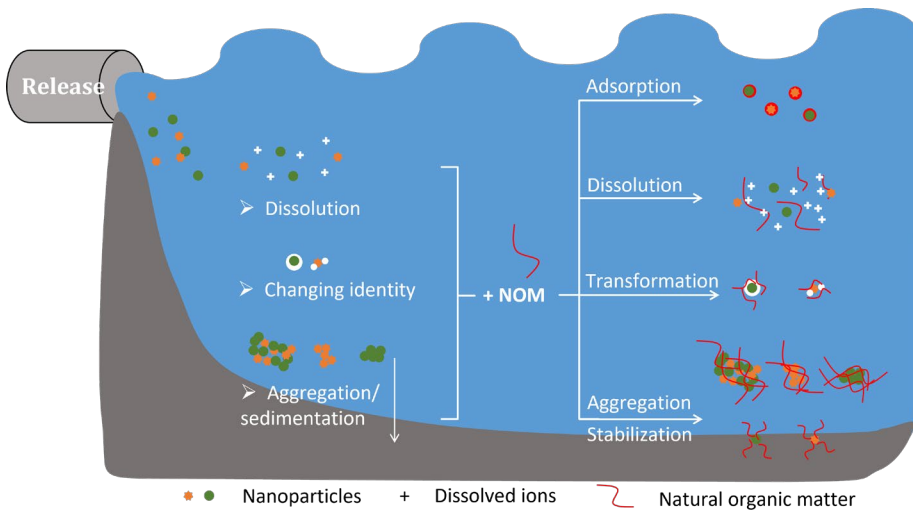

Figure 1.1 Schematic diagram showing the physicochemical transformation and the influence of natural organic matter (NOM) in the aquatic environment.

1.2.1 Aggregation and sedimentation

Aggregation describes the dynamics of nano-sized particles that bounded or fused together into larger clusters (Garner and Keller, 2014). Sedimentation occurs when the particles or aggregated particles have a higher density than the exposure medium (Alstrup Jensen et al., 2009). The degree of aggregation and the rate of sedimentation are determined by the properties and concentrations of the NPs, and the characteristics of the aqueous system (for example the presence of natural organic matter (NOM)) (Du et al., 2019; Dunphy Guzman et al., 2006; Farkas et al., 2010; Garner and Keller, 2014; Phenrat et al., 2007). The aggregation and sedimentation of NPs will dictate mobility and fate in the aquatic environment, and thus bioavailability and possible ecotoxicological effects (Liu and Cohen, 2014; Velzeboer et al., 2008).

1.2.2 Dissolution of soluble ENPs

Some ENPs can dissolve, e.g. ZnONPs and CuNPs, and as a result both ions as well as particles occur within exposure media influencing toxicological effects (Lowry et al., 2012; Van Koetsem et al., 2015; Williams et al., 2019). The rate and extent of dissolution mainly depends on the surface functionalization (e.g. surface to volume ratios and surface charge) (Peijnenburg et al., 2015; Quik et al., 2011). Dissolution is concentration dependent (Lead et al., 2018; Merrifield et al., 2017), and the dynamics are influenced by solubility, size and composition of particles as well as environmental conditions (for example pH, temperature and the concentrations of NOM) (Jiang

et al., 2015; Levard et al., 2012; Peralta-Videa et al., 2011; Quik et al., 2011; Zhang et al., 2010).

1.2.3 Influence of NOM

Ubiquitous and abundant NOM can alter the aggregation, sedimentation and dissolution progresses of ENPs in the aquatic environment (Bo et al., 2017; Carapar et al., 2022; Grillo et al., 2015; Tortella et al., 2020; Wang et al., 2018, 2016).

The interactions between NOM and ENPs contain hydrophobic interactions, electrostatic interactions, steric interactions, hydrogen bonding, and bridging (Li et al., 2022). For example, on the one hand, the presence of NOM may inhibit the aggregation and enhance the stability of ENPs, as a reason of electrostatic and steric interactions (Baalousha et al., 2013; Bo et al., 2017; Mohd Omar et al., 2014; Wang et al., 2018). On the other hand, the presence of NOM, may promote the aggregation due to bridging interactions (Akaighe et al., 2012; Li et al., 2022). Moreover, the existence of NOM was reported to slow down the dissolution progress of AgNPs via sulfidation due to the formation of a passivating coat on the surface (Reinsch et al., 2012), or via making the surface charge more negatively charged (Fabrega et al., 2009).

Although several mechanisms of NOM-ENPs interactions have been investigated, up till now there is limited knowledge on realistic fresh water system containing the mixtures of ENPs, and the further interactions with water chemistry parameters that all may impact the ecotoxicity to organisms (Levard et al., 2012). The above statements highlight that the environmental behavior of ENPs in the aquatic

ecosystem is quite complex (Carapar et al., 2022) and a challenging research topic.

1.3 Uptake, bioaccumulation and trophic transfer of ENPs

1.3.1 Uptake and bioaccumulation of ENPs from aquatic environment

Uptake routes embody direct ingestion and entry across surface epithelia such as gills and body walls (Moore, 2006). There are researchers reporting uptake and accumulation of different kinds of ENPs (e.g. metal-based NPs, metal oxide NPs and nanoplastics, etc.) into organisms in various trophic levels (Gupta et al., 2017; Mateos-Cárdenas et al., 2021; Nam et al., 2014; Nowack and Bucheli, 2007; Tortella et al., 2020; Wang et al., 2016).

Particles can be ingested or incorporated into organisms, e.g. the uptake of polystyrene nanoplastics in zebrafish embryos (Pakrashi et al., 2014; van Pomeren et al., 2017). Aggregates of particles are less mobile, yet ingestion by animals, like *Daphnia magna,* still occurred (Xiao et al., 2015). Moreover, filter-feeder, benthic, sediment-dwelling organisms have shown to be prone to uptake of ENPs (Carocci et al., 2015; Gupta et al., 2016; Nowack and Bucheli, 2007).

Uptake and accumulation of ENPs depend on the particle size and the presence of NOM (Bundschuh et al., 2016; Limbach et al., 2005; Mateos-Cárdenas et al., 2021; Nowack and Bucheli, 2007; Wang et al., 2016). Generally, the smaller the particle size is, the more uptake and accumulation of ENPs. However, an opposite finding was observed on the uptake of AuNPs, which increased along with an increasing

particle size (Pan et al., 2012). This highlights that further investigations on size relations are needed. Likely, the relationship between the presence of NOM and uptake of ENPs is not elucidated, but several studies have found some impacts as summarized by Wang et al. (2016).

Previous studies mostly focused on the impact of particle size and NOM on a certain ENP or a certain organism. The conclusion from different studies were not consistent, highlighting the complex relationship and mechanisms between NOM and ENPs. Therefore, more research is needed.

1.3.2 Trophic transfer of ENPs

Evidence has been found on transfer of ENPs through aquatic food chains (Chae and An, 2016; Lee et al., 2015; Wang et al., 2017; Yan and Wang, 2021; Zhao et al., 2017; Zhu et al., 2010). To evaluate the environment risk of ENPs, trophic transfer is a crucial aspect, especially when biomagnification (tropic transfer factor > 1) occurs (Shi et al., 2020).

A series of factors can affect trophic transfer of ENPs through food chains in aquatic environments. As concluded by Dang et al. (2021) and Tangaa et al. (2016), the main factors include (1) the ENP characteristics, (2) prey and predator species, (3) the exposure route of the prey, (4) the uptake and internalization of ENPs in preys, and (5) the digestive physiology of predators and the subcellular fractionation of ENPs. To the best of our knowledge, few studies have looked at above five aspects. For instance, uptake of AgNPs in *D.*

magna depended on dietary exposure instead of aqueous exposure. In the case of the relationship between digestive physiology with trophic availability, experiments using soluble metals have shown that when bound to organelle particles were more readily available to predator than those partitioned to insoluble components (Chen et al., 2016). As is concluded by in previous studies (Chang and Reinfelder, 2000; Wallace et al., 1998), dissolved metals associated with organelles or cytosolic proteins are more easily solubilized by the digestive processes of predators. The position organisms in the food chains has shown to impact the magnitude of transfer, namely ENP concentration increased between the first and the second trophic level organism (Gupta et al. 2017). Whereas, the extent of transfer decreased to several fold from the second to the third trophic level organism To investigate the multistage trophic transfer of ENPs, research on a three-level food chain could provide more information compared with research on a two-level food chain (Shi et al., 2020), yet so far poorly studied. It remains also a question if the particulate or the ions of the ENPs transfer across organisms, and how the size and concentration alter this transfer. Ionic metal shedded from ENPs were found to move along food chains according to the total mass concentration (Bhuvaneshwari et al., 2017; Gambardella et al., 2014; Lammel et al., 2014; Wu et al., 2017).

For particle transfer the techniques are nowadays in their infancies and therefore limited information was found. Earlier reports showed measurements based on the total mass concentration including both the particles and the dissolved ions of ENPs in the biota (Baccaro et al., 2018; Chen et al., 2015; Lee et al., 2015; Yan and Wang, 2021). With the development of single particle inductively coupled plasma

mass spectrometry (sp-ICP-MS) and single cell ICP-MS, the first attempts to quantify particulate ENPs are available. For example, Gray et al. (2013) successfully established and verified a method to determine the particle number concentration of gold nanoparticles (AuNPs) and AgNPs in *Daphnia magna* and *Lumbriculus variegatus* samples. Particle number-based assessment was also applied in the trophic transfer of AuNPs from algae to daphnia to fishes (Monikh et al., 2021). Despite the fact that these techniques are in their infancies, they have great potential for furthering this field of research.

1.4 Toxicity of ENPs

Although quite some toxicity tests with aquatic organisms have been executed and published (overview for instance in Chen et al (2015)), the majority of studies have focused on acute endpoints (Balraadjsing et al., 2022) using standard organisms (Chen et al., 2015). Understanding the processes at the interface of exposure, uptake, effects and trophic transfer requires more attention especially with considering the fate of metallic NPs that are in exposure media as ions and particles in suspension. To discuss these gaps, single and joint toxicity, as well as the influence of NOM on the toxicity are summarized as shown below.

1.4.1 Single toxicity

The toxic action of soluble and insoluble ENPs can be roughly described with three pathways or mechanisms (Besseling et al., 2019;

Brunner et al., 2006; Ma et al., 2013; Peng et al., 2017; Santschi et al., 2017): (1) surface interactions or internalization of particles, (2) shedding toxic ions from soluble ENPs (e.g. CuNPs and ZnONPs), and (3) oxidative stress caused by chemical radicals or reactive oxygen species (ROS).

These responses can be impacted by the surface functionality and surface charge (Garner and Keller, 2014). As described in section 1.2, the environmental behavior of ENPs (aggregation, sedimentation and dissolution) in the water column play an important role in determining the surface chemistry and stability of ENPs, and thus determine the bioavailability and potential ecotoxicological effects on aquatic organisms (Borm et al., 2006; Holden et al., 2016). The type of organisms used – which all have their own requirements related to exposure medium composition and the multiplicity of experimental methods and conditions will also affect the toxicity values reported (Libralato et al., 2017). Hence, different exposure conditions to different trophic level organisms should be considered in the studies of toxic effect.

Another key area of research is the contribution to toxicity of particles compared to the released/dissolved ions for soluble ENPs. It is debated that in nanotoxicity the total toxic effect generated from particulate part (ENPs themselves) and/or the ionic metal part released from metal-based or metal oxide-based ENPs both should be accounted for (Libralato et al., 2017; Ma et al., 2013; Malhotra et al., 2020). Several studies have demonstrated that the effects of soluble ENPs result not solely from dissolved ions or particles (Carocci et al., 2015; Griffitt et al., 2008; Wang and Wang, 2014). The contribution of particles versus ions might vary on the basis of the physicochemical

processes especially the dissolution, and the exposure conditions such as the presentence of NOM (Malhotra et al., 2020; Saleh et al., 2014). Therefore, further studies are hence devoted to quantitative clarify the interaction and contribution of particles and ions, and to understand the mechanism of soluble ENPs toxicity under different parameters and conditions.

1.4.2 Joint toxicity

"*There is no such thing as a single chemical exposure*" (Yang et al., 1998). Aquatic organisms are mostly co-exposed to ENP mixtures in the real scenario due to the release of individual ENPs as introduced in front, and the emerging of hybrid nanoparticles consisted of multiple components (Deng et al., 2017; Maji et al., 2019; Pacheco et al., 2018). More knowledge is needed on the joint toxicity of multiple ENPs to provide basis to assess the risk of ENPs in the realistic and complex natural systems.

The behavior and toxicity of ENP mixtures may differ from exposure to single ENPs. Interactions of ENPs in a mixture can result in different toxic actions including increasing (synergistic) or decreasing (antagonistic) effects as compared with summed (additive) behavior (Altenburger et al., 2003). The existing literature on joint toxic actions of ENPs and the contribution of individual component to the joint effect is rather limited (Deng et al., 2017; Pacheco et al., 2018). Deng et al. (2017) reviewed the joint toxicity of NPs together with another contaminants involving organic medicals, metal ions, NPs. In this review, several cases for the joint toxicity of ENPs to

bacteria and human cells are reported. Here, current literatures on the joint toxicity upon freshwater organisms' exposure to two types of NPs are collected and summarized in Table 1.1.

As shown in Table 1.1, the toxic actions of multiple ENP mixtures varied in different exposure systems. However, information on the mechanisms of action is an aspect that is still scarce in literature, especially for the soluble metal-based or metal oxide ENPs (Hernández-Moreno et al., 2019; Ogunsuyi et al., 2019). Note that the suspensions of soluble ENP mixtures are complicated due to the coexistence of different kinds of particulate and ionic ENPs. The interaction between multiple particles and released metal ions might alter the additive toxicity. It is, thus, necessary to unravel if one of the particulate or ionic components dominates the toxic action, or if the contribution to total toxicity depend on interactions of multiple components. Moreover, previous studies have investigated the joint toxicity of metal salts. It is important to elucidate if the toxic effect of metal-based or metal oxide ENP mixtures can be dealt with in a similar way as with the responses of biota to mixtures of metal salts.

Table 1.1 List of published studies (to date) conducted on joint toxicity of ENPs to organisms in freshwater

ENP mixture	Exposure species	Exposure time	Endpoint	Joint effect	References
CuNPs+CrNPs	Waterflea *Daphnia magna*	48 hours 7 days 21 days	survival, reproduction, growth, feeding behavior, four biomarkers	comparable to nCu on feeding behavior and biomarker responses.	(Lu et al., 2017)
AgNPs+hematite (HemNPs)	Alga *Chlamydomonas reinhardtii* and *Ochromonas danica*	24 hours	cell-specific growth rate	antagonistic 1) decreasing the bioavailability of Ag ions through adsorption 2) competitively inhibiting AgNP uptake.	(Huang et al., 2019)
AgNPs+polystyrene (PsNPs)	Alga *Chlamydomonas reinhardtii* and *Ochromonas danica*	24 hours	cell-specific growth rate	synergistic	(Huang et al., 2019)

AgNPs+CuONPs	African mud catfish *Clarias gariepinus*	28 days	oxidative stress analyses, biomarkers	antagonistic genotoxicity and oxidative damage	(Ogunsuyi et al., 2019)
ZnONPs+graphene oxide nanoplatelets (GONPs)	Alga *Scenedesmus obliquus* Waterflea *Daphnia magna* Fish larva *Danio rerio*	96 hours 48 hours 96 hours	growth inhibition, lethality tests, Embryo–larval toxicity bioassays	additive to S. obliquus and D. magna antagonistic to D. rerio.	(Ye et al., 2018)
AuNPs+microplastics	Waterflea *Daphnia magna*	21 days	lethality tests, reproduction	High concentrations: synergistic Low concentrations: antagonistic	(Pacheco et al., 2018)
CuNPs+ZnONPs	rainbow trout	96 hours	behaviour, lethality tests, oxidative stress, accumulation	CuNPs increase the uptake of Zn. Co-exposure alters of the GST activity and GSH/GSSG ratio in gill and liver.	(Hernández-Moreno et al., 2019)
30 combinations (CuONPs, ZnONPs, NiONPs, TiO$_2$NPs, Fe$_2$O$_3$NPs)	Alga *Chlorella vulgaris*	72 hours	growth inhibition (cell count and chlorophyll content)	additive (67%) antagonistic (16.5%) synergistic (16.5%)	(Ko et al., 2018)

1.4.3 Influence of NOM

Numerous studies have reported the influence of NOM on the single toxicity of ENPs (Farner et al., 2019; Wang et al., 2016, 2011). The presence of NOM mostly modulate the original toxic effect (Cerrillo et al., 2016; Saleh et al., 2014). For instance, Suwannee River NOM can alleviate the adverse effects of NPs on algal growth (Cerrillo et al., 2016). Deng et al. (2017) concluded that the mechanism of the impact of NOM on the availability and toxic action of ENPs accounts for altered electrostatic repulsion between ENPs and/or between ENPs and cells, scavenging of ENPs-induced reactive oxidative species, and the formation of complexes with released ions. However, the relationship between NOM influenced ENP single toxicity to different trophic level has not been clearly understood. In addition, there is a research gap on the impact of NOM on the joint toxicity of multiple ENPs and the alteration on the contributions of particulate/ionic components. To fill these gaps, more concern should be focused on the relationship of the presence of NOM and the single or joint toxic effect of ENPs. The exposure condition such as the presence of NOM is the key factor affecting the behavior and stability of ENPs, as well as a factor affecting the toxicity of ENPs.

1.5 Test organisms

In order to determine the bioaccumulation, trophic transfer, and toxicity of ENPs in aquatic organisms, different trophic level test species were selected as follows. Images of these species are shown in Figure 1.2.
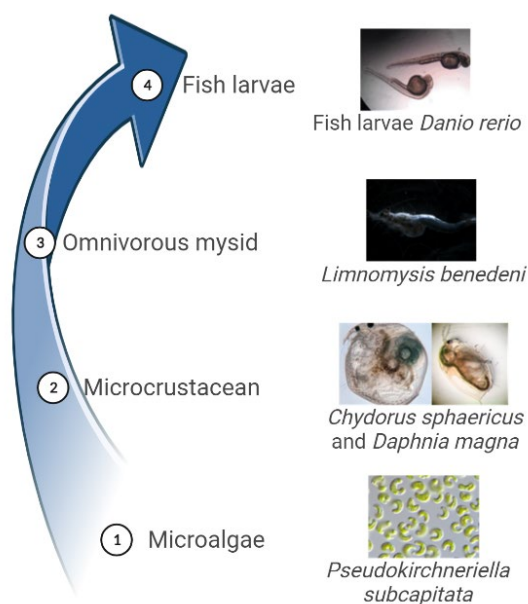
Figure 1.2 Images of test organisms in different trophic levels.

1.5.1 Microalgae *Pseudokirchneriella subcapitata*

As primary producers, microalgae contain species important to freshwater ecosystems and those that have potential applied usages (Suzuki et al., 2018). In particular, *Pseudokirchneriella subcapitata* (= *Raphidocelis subcapitata*), shown in the first image of Figure 1.2, is an unicellular, sickle-shaped, freshwater green microalga (Machado and Soares, 2014; Yamagishi et al., 2017). Compared with other algae, *P. subcapitata* has been widely and most frequently used for bioassays in toxicological risk assessments accounting for its high growth rate, sensitivity to toxicants, and good reproducibility (Yamagishi et al., 2017). Hence, *P. subcapitata* was recommended as an ecotoxicological bioindicator by the Organization for Economic

Cooperation and Development (OECD) (Andrews and Walsh, 2007; Suzuki et al., 2018). Here, *P. subcapitata* was selected as the first trophic level as the food for microcrustaceans and mysids.

1.5.2 Microcrustacean *Chydorus sphaericus* and *Daphnia magna*

Microcrustacean is composed of species that are important components of freshwater food webs. Two species of planktonic genera microcrustacean, *Chydorus sphaericus* and *Daphnia magna*, were used in the research presented in this thesis. They are vital components in food and energy relationships between primary produces and higher-level consumers, especially within lakes and ponds (de los Ríos-Escalante et al., 2011).

C. sphaericus is found worldwide in water bodies, from the equator to the Arctic Circle (Kotov et al., 2016). It is generally found in lakes or ponds with eutrophication and around the bottom sediments (Central Michigan University, n.d.). It can swim well for only short distances, but is most likely to be found clinging to various filamentous algae with its modified limbs (Central Michigan University, n.d.; Fryer. G, 1968). *C. sphaericus* is tolerant of a wide range of pH levels (from 3.4 to 9.5) and varying levels of dissolved oxygen, including very low levels of oxygen (Fryer. G, 1968).

D. magna is model species for toxicity test recommended by OECD guidelines 202 (OECD, 2004). It is widespread in a variety of freshwater systems from acidic swamps to lakes, ponds, and streams. The body of daphnia is usually 1–5 millimeters long, and is divided into segments, although this division is not visible. Daphnids are

typically filter feeders, ingesting suspended particles (mainly unicellular algae) as large as 70 μm (Geller and Müller, 1981). Moreover, as a result of the high efficiency of filtering water, *D. magna* are sensitive to pollutants in aquatic environment.

As experimental organisms, *C. sphaericus* and *D. magna* are suitable to culture in the laboratory for their short generation time and strong adaptability to the environment. Furthermore, observation with the microscope is possible due to their transparency and small sizes. Thus, *C. sphaericus* and *D. magna* are good choice as test organisms to construct aquatic food chains and to determine the toxicity of ENPs (Baun et al., 2008). It is closely related to algae present which is one of its major food sources (i.e., Anabaena).

1.5.3 Omnivorous mysid *Limnomysis benedeni*

Limnomysis benedeni is a freshwater mysid originally located in the area of the Black Sea and the lower Danube river (Gergs et al., 2008). As an invasive species, it has spread in freshwater systems globally (Yohannes and Rothhaupt, 2017). *L. benedeni* is an omnivorous species ingesting both microalgae and microcrustaceans in the laboratory (Gergs et al., 2008). It is a perfect predator to construct a food chain with different food sources, and then to compare the trophic transfer of ENPs in these food chains. Meanwhile, it is a beneficiary food source for fish (Gergs et al., 2008; Kelleher et al., 1999). *L. benedeni* thus plays an important role as a bridge to connect the lower trophic levels to the higher trophic levels. Moreover, its

transparency makes the visualization of the biodistribution of fluorescent NPs inside convenient.

1.5.4 Fish larvae *Danio rerio*

Zebrafish (*Danio rerio*) is regarded as a model freshwater species for studying genetic effects in vertebrate development (David P. Clark, Nanette J. Pazdernik, 2019). It has been widely used in toxicity studies to evaluated the effect of pollutants. The advantages of *D. rerio* include their ease of culturing and in the laboratory, the large amount of embryos that females produce, and the optically transparent embryos which develop externally (Internal Control Genes, 2017; Xu et al., 2016). We used zebrafish larvae up to 5 days post fertilization.

1.6 Objectives and research questions

Taken together, the toxicity, bioaccumulation, and trophic transfer of selected ENPs are still poorly studied, especially when considering the realistic conditions such as the exposure of ENP mixtures and the influence of NOM. Therefore, this thesis aimed to (scheme as shown in Figure 1.3):

  1) investigate the fate, toxicity and bioaccumulation of both individual and mixture ENPs to aquatic organisms, and the impact of NOM on these processes;

2) evaluate the trophic transfer of ENPs through simulated aquatic food chains, and the following biodistribution and toxic effect of ENPs on the predators;

3) assess the key factors affecting the extent of trophic transfer among particle sizes and food chain types.

According to the objectives, the research questions were addressed:

1) How does NOM affect the stability and toxicity of **individual ENP** to aquatic organisms? (Chapter 2)

2) How does NOM affect the fate, accumulation and toxicity of **ENP mixtures** (Chapter 3)?

3) To what extent do ENPs **transfer** in particulate, and ionic forms and how does the particle size and number change in different organisms? (Chapter 4)

4) How do **particle sizes** and **food chain types** affect the trophic transfer of ENPs and their subsequently biodistribution and toxicity to the predators? (Chapter 4 and 5)
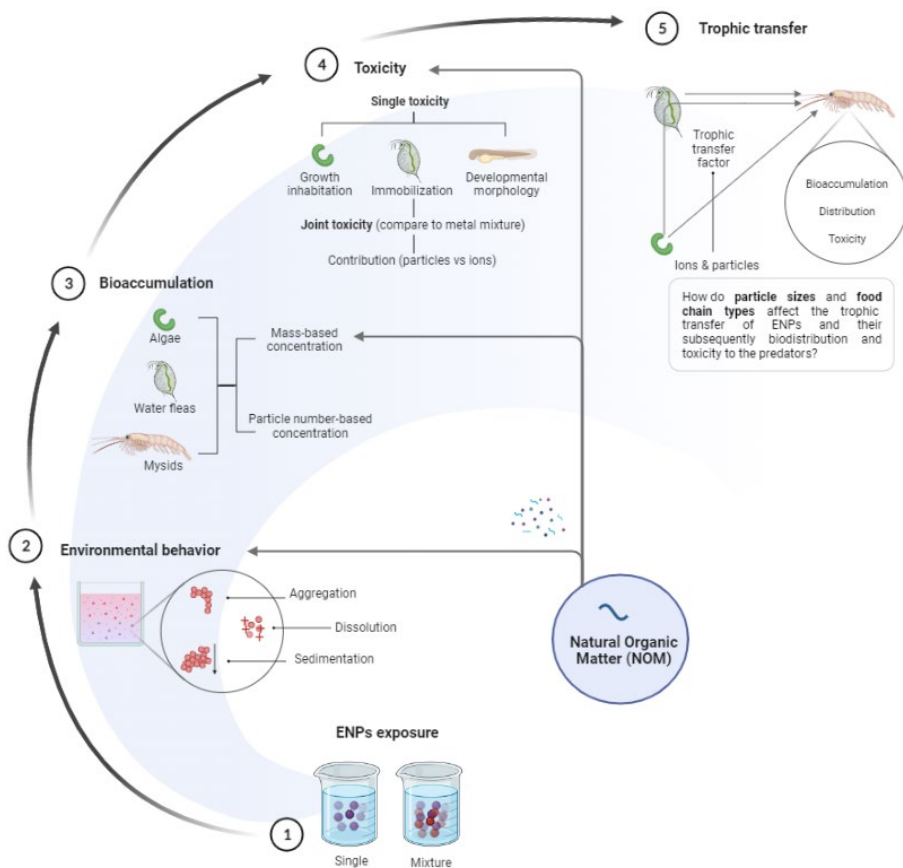
Figure 1.3 Scheme of investigating the toxicity, bioaccumulation and trophic transfer of engineered nanoparticles (ENPs) in the aquatic environment in this thesis.

1.7 Thesis outline

Chapter 1 General introduction on the application and release of ENPs and their fate, toxicity, accumulation and trophic transfer in the aquatic environment, as well as the test organisms used for

nanotoxicity testing. The objectives and research questions of this thesis were proposed.

Chapter 2 The impacts of humic substances (HS) on the aquatic stability and toxicity of cerium dioxide nanoparticles (CeO_2NPs) to three aquatic organisms with different exposure characteristics were investigated.

Chapter 3 The assessment of the joint toxicity and accumulation of copper nanoparticles (CuNPs) and zinc oxide nanoparticles (ZnONPs) in *D. magna* in the absence and presence of Suwannee River natural organic matter (SR-NOM), compared to the joint toxicity and accumulation of corresponding metal salts.

Chapter 4 This work investigated the uptake and transfer of different sized polystyrene particles (PSPs) in *Daphnia magna* to mysid *Limnomysis benedeni*, explicitly PSPs' fate in the aquatic system as a function of particle size (26, 500 and 4800 nm) was accounted. Moreover, the accumulation kinetics of particles in mysid fed by exposed daphnia were calculated.

Chapter 5 The trophic transfer of copper nanoparticles (CuNPs) was studied in a food chain consisting of the microalgae *Pseudokirchneriella subcapitata* as a representative of primary producers, the consumer waterflea *Daphnia magna,* and the omnivorous mysid *Limnomysis benedeni*. The impact of food chain types on the transfer extent of CuNPs, and the change of the profile of particulate Cu through food chains were investigated.

Chapter 6 Discussion on the research questions and main findings of the thesis. Single and mixture toxicity of ENPs towards aquatic organisms, and how the persistence of NOM affects the toxicity were understood. The extent of accumulation and trophic transfer of ENPs, the main driver of the transfer among particle sizes and food chain types were integrated. Future perspectives in terms of nanotoxicity, food chain transfer and risk assessment of ENPs were proposed.

References

Akaighe, N., Depner, S.W., Banerjee, S., Sharma, V.K., Sohn, M., 2012. The effects of monovalent and divalent cations on the stability of silver nanoparticles formed from direct reduction of silver ions by Suwannee River humic acid/natural organic matter. Sci. Total Environ. 441, 277–289.

Alstrup Jensen, K., Author Keld Alstrup Jensen, W., Kembouche, Y., Christiansen, E., Jacobsen, N.R., Wallin, H., Guiot, C., Spalla, O., Witschger, O., 2009. WP 4 : Physicochemical Characterisation of Manufactured Nanomaterials (MNs) and Exposure Media (EMs) Deliverable 3: Final protocol for producing suitable MN exposure media Deliverable leader: NRCWE.

Altenburger, R., Nendza, M., Schüürmann, G., 2003. Mixture toxicity and its modeling by quantitative structure-activity relationships. Environ. Toxicol. Chem.

Andrews, S., Walsh, K., 2007. Experiences merging two university websites. Proc. ACM SIGUCCS User Serv. Conf. 4–7.

Baalousha, M., Nur, Y., Römer, I., Tejamaya, M., Lead, J.R., 2013. Effect of monovalent and divalent cations, anions and fulvic acid on aggregation of citrate-coated silver nanoparticles. Sci. Total Environ. 454–455, 119–131.

Baccaro, M., Undas, A.K., De Vriendt, J., Van Den Berg, J.H.J., Peters, R.J.B., Van Den Brink, N.W., 2018. Ageing, dissolution and biogenic formation of nanoparticles: How do these factors affect the uptake kinetics of silver nanoparticles in earthworms? Environ. Sci. Nano 5, 1107–1116.

Balraadjsing, S., Peijnenburg, W.J.G.M., Vijver, M.G., 2022. Exploring the potential of in silico machine learning tools for the prediction of acute Daphnia magna nanotoxicity. Chemosphere 307, 135930.

Batley, G.E., Kirby, J.K., McLaughlin, M.J., 2013. Fate and Risks of Nanomaterials in Aquatic and Terrestrial Environments. Acc. Chem. Res. 46, 854–862.

Baun, A., Hartmann, N.B., Grieger, K., Kusk, K.O., 2008. Ecotoxicity of engineered nanoparticles to aquatic invertebrates: A brief review and recommendations for future toxicity testing. Ecotoxicology 17, 387–395.

Besseling, E., Redondo-Hasselerharm, P., Foekema, E.M., Koelmans, A.A., 2019. Quantifying ecological risks of aquatic micro- and nanoplastic. Crit. Rev. Environ. Sci. Technol. 49, 32–80.

Bhuvaneshwari, M., Kumar, D., Roy, R., Chakraborty, S., Parashar, A., Mukherjee, A.A., Chandrasekaran, N., Mukherjee, A.A., 2017. Toxicity, accumulation, and trophic transfer of chemically and biologically synthesized nano zero valent iron in a two species freshwater food chain. Aquat. Toxicol. 183, 63–75.

Bo, Z., Yorulmaz, S., Corliss, M.K., Chung, M., Cho, N., 2017. Influence of natural organic matter (NOM) coatings on nanoparticle adsorption onto supported lipid bilayers. J. Hazard. Mater. 339, 264–273.

Borm, P., Klaessig, F.C., Landry, T.D., Moudgil, B., Pauluhn, J., Thomas, K., Trottier, R., Wood, S., 2006. Research strategies for safety evaluation of nanomaterials, Part V: Role of dissolution in biological fate and effects of nanoscale particles. Toxicol. Sci. 90, 23–32.

Brunner, T.J., Wick, P., Manser, P., Spohn, P., Grass, R.N., Limbach, L.K., Bruinink, A., Stark, W.J., 2006. In vitro cytotoxicity of oxide nanoparticles: Comparison to asbestos, silica, and the effect of particle solubility. Environ. Sci. Technol. 40, 4374–4381.

Bundschuh, M., Seitz, F., Rosenfeldt, R.R., Schulz, R., 2016. Effects of nanoparticles in fresh waters : risks , mechanisms and interactions. Freshw. Biol. 61, 2185–2196.

Camboni, M., Hanlon, J., Pérez García, R., Floyd, P., 2019. A state of play study of the market for so called "next generation" nanomaterials. Helsinki.

Carapar, I., Jurkovi, L., Hamer, B., Lyons, D.M., 2022. Simultaneous Influence of Gradients in Natural Organic Matter and Abiotic Parameters on the Behavior of Silver Nanoparticles in the Transition Zone from Freshwater to Saltwater Environments. Nanomaterials 12, 296.

Carocci, A., Catalano, A., Lauria, G., Sinicropi, M.S., Genchi, G., 2015. Brief History of the Development of the Transfusion Service. How to Recruit Volunt. Donors Third World? 238, 22–28.

Central Michigan University, n.d. Zooplankton of the Great Lakes [WWW Document]. URL

http://people.se.cmich.edu/mcnau1as/zooplankton web/chydorus/chydorus.html

Cerrillo, C., Barandika, G., Igartua, A., Areitioaurtena, O., Mendoza, G., 2016. Towards the standardization of nanoecotoxicity testing: Natural organic matter "camouflages" the adverse effects of TiO2 and CeO$_2$ nanoparticles on green microalgae. Sci. Total Environ. 543, 95–104.

Chae, Y., An, Y.J., 2016. Toxicity and transfer of polyvinylpyrrolidone-coated silver nanowires in an aquatic food chain consisting of algae, water fleas, and zebrafish. Aquat. Toxicol. 173, 94–104.

Chang, S. IL, Reinfelder, J.R., 2000. Bioaccumulation , Subcellular Distribution , and Trophic Transfer of Copper in a Coastal Marine Diatom. Environ. Sci. Technol. 34, 4931–4935.

Chen, G., Vijver, M.G., Peijnenburg, W.J.G.M., 2015. Summary and analysis of the currently existing literature data on metal-based nanoparticles published for selected aquatic organisms: Applicability for toxicity prediction by (Q)SARs. ATLA Altern. to Lab. Anim. 43, 221–240.

Chen, J., Li, H., Han, X., Wei, X., 2015. Transmission and accumulation of nano-TiO$_2$ in a 2-Step Food Chain (*Scenedesmus obliquus* to *Daphnia magna*). Bull. Environ. Contam. Toxicol. 95, 145–149.

Chen, Q., Hu, X., Yin, D., Wang, R., 2016. Ecotoxicology and Environmental Safety Effect of subcellular distribution on n C 60 uptake and transfer ef fi ciency from Scenedesmus obliquus to Daphnia magna. Ecotoxicol. Environ. Saf. 128, 213–221.

Dalai, S., Iswarya, V., Bhuvaneshwari, M., Pakrashi, S., Chandrasekaran, N., Mukherjee, A., 2014. Different modes of TiO$_2$ uptake by *Ceriodaphnia dubia*: Relevance to toxicity and bioaccumulation. Aquat. Toxicol. 152, 139–146.

Dang, F., Huang, Y., Wang, Y., 2021. Transfer and toxicity of silver nanoparticles in the food chain. Environ. Sci. Nano 8, 1519–1535.

David P. Clark, Nanette J. Pazdernik, M.R.M., 2019. Cells and Organisms, in: David P. Clark, Nanette J. Pazdernik, M.R.M. (Ed.), Molecular Biology (Third Edition). pp. 2–37.

de los Ríos-Escalante, P., Hauenstein, E., Romero-Mieres, M., 2011. Microcrustacean assemblages composition and environmental

variables in lakes and ponds of the Andean region - South of Chile (37-39° S). Brazilian J. Biol. 71, 353–358.

Deng, R., Lin, D., Zhu, L., Majumdar, S., White, J.C., Gardea-Torresdey, J.L., Xing, B., 2017. Nanoparticle interactions with co-existing contaminants: joint toxicity, bioaccumulation and risk. Nanotoxicology 11, 591–612.

Dolez, P.I., 2015. Nanomaterials Definitions, Classifications, and Applications, Nanoengineering: Global Approaches to Health and Safety Issues.

Du, S., Wu, J., Alshareedah, O., Shi, X., 2019. Nanotechnology in cement-based materials: A review of durability, modeling, and advanced characterization. Nanomaterials.

Dunphy Guzman, K.A., Finnegan, M.P., Banfield, J.F., 2006. Influence of Surface Potential on Aggregation and Transport of Titania Nanoparticles. Environ. Sci. Technol. 40, 7688–7693.

Dwivedi, A.D., Dubey, S.P., Sillanpää, M., Kwon, Y.N., Lee, C., Varma, R.S., 2015. Fate of engineered nanoparticles: Implications in the environment. Coord. Chem. Rev. 287, 64–78.

European Commission, 2012. Internal Market, Industry, Entrepreneurship and SMEs - Nanomaterials [WWW Document]. URL https://ec.europa.eu/growth/sectors/chemicals/reach/nanomaterials_en

Fabrega, J., Fawcett, S.R., Renshaw, J.C., Lead, J.R., 2009. Silver nanoparticle impact on bacterial growth: Effect of pH, concentration, and organic matter. Environ. Sci. Technol. 43, 7285–7290.

Farkas, J., Christian, P., Urrea, J.A.G., Roos, N., Hassellöv, M., Tollefsen, K.E., Thomas, K. V., 2010. Effects of silver and gold nanoparticles on rainbow trout (Oncorhynchus mykiss) hepatocytes. Aquat. Toxicol. 96, 44–52.

Farner, J.M., Cheong, R.S., Mahé, E., Anand, H., Tufenkji, N., 2019. Comparing TiO 2 nanoparticle formulations: stability and photoreactivity are key factors in acute toxicity to Daphnia magna. Environ. Sci. Nano 6, 2532–2543.

Fryer. G, 1968. Evolution and Adaptive Radiation in the Chydoridae (Crustacea: Cladocera): A Study in Comparative Functional

Morphology and Ecology. Philos. Trans. R. Soc. London. Ser. B, Biol. Sci. 254, 226–384.

Gambardella, C., Gallus, L., Gatti, A.M., Faimali, M., Carbone, S., Antisari, L.V., Falugi, C., Ferrando, S., 2014. Toxicity and transfer of metal oxide nanoparticles from microalgae to sea urchin larvae. Chem. Ecol. 30, 308–316.

Garner, K.L., Keller, A.A., 2014. Emerging patterns for engineered nanomaterials in the environment: A review of fate and toxicity studies. J. Nanoparticle Res.

Geller, W., Müller, H., 1981. The filtration apparatus of Cladocera: Filter mesh-sizes and their implications on food selectivity. Oecologia 49, 316–321.

Gergs, R., Hanselmann, A.J., Eisele, I., Rothhaupt, K.O., 2008. Autecology of Limnomysis benedeni Czerniavsky, 1882 (Crustacea: Mysida) in Lake Constance, Southwestern Germany. Limnologica 38, 139–146.

Gray, E.P., Coleman, J.G., Bednar, A.J., Kennedy, A.J., Ranville, J.F., Higgins, C.P., 2013. Extraction and analysis of silver and gold nanoparticles from biological tissues using single particle inductively coupled plasma mass spectrometry-SI. Environ. Sci. Technol. 47, 14315–14323.

Griffitt, R.J., Luo, J., Gao, J., Bonzongo, J.C., Barber, D.S., 2008. Effects of particle composition and species on toxicity of metallic nanomaterials in aquatic organisms. Environ. Toxicol. Chem. 27, 1972–1978.

Grillo, R., Rosa, A.H., Fraceto, L.F., 2015. Chemosphere Engineered nanoparticles and organic matter : A review of the state-of-the-art. Chemosphere 119, 608–619.

Gupta, G.S., Kumar, A., Shanker, R., Dhawan, A., 2016. Assessment of agglomeration, co-sedimentation and trophic transfer of titanium dioxide nanoparticles in a laboratory-scale predator-prey model system. Sci. Rep. 6, 1–13.

Gupta, G.S., Shanker, R., Dhawan, A., Kumar, A., 2017. Impact of Nanomaterials on Food Functionality. Nanosci. Nanotechnol. Foods Beverages 27, 309–333.

Hernández-Moreno, D., Valdehita, A., Conde, E., Rucandio, I., Navas, J.M., Fernández-Cruz, M.L., 2019. Acute toxic effects caused by

the co-exposure of nanoparticles of ZnO and Cu in rainbow trout. Sci. Total Environ. 687, 24–33.

Holden, P.A., Gardea-Torresdey, J.L., Klaessig, F., Turco, R.F., Mortimer, M., Hund-Rinke, K., Cohen Hubal, E.A., Avery, D., Barceló, D., Behra, R., Cohen, Y., Deydier-Stephan, L., Ferguson, P.L., Fernandes, T.F., Herr Harthorn, B., Henderson, W.M., Hoke, R.A., Hristozov, D., Johnston, J.M., Kane, A.B., Kapustka, L., Keller, A.A., Lenihan, H.S., Lovell, W., Murphy, C.J., Nisbet, R.M., Petersen, E.J., Salinas, E.R., Scheringer, M., Sharma, M., Speed, D.E., Sultan, Y., Westerhoff, P., White, J.C., Wiesner, M.R., Wong, E.M., Xing, B., Steele Horan, M., Godwin, H.A., Nel, A.E., 2016. Considerations of environmentally relevant test conditions for improved evaluation of ecological hazards of engineered nanomaterials. Environ. Sci. Technol. 50, 6124–6145.

Huang, B., Wei, Z.B., Yang, L.Y., Pan, K., Miao, A.J., 2019. Combined Toxicity of Silver Nanoparticles with Hematite or Plastic Nanoparticles toward Two Freshwater Algae. Environ. Sci. Technol. 53, 3871–3879.

Internal Control Genes, 2017. Danio rerio [WWW Document]. URL http://icg.big.ac.cn/index.php/Danio_rerio

ISO, 2008. Nanotechnologies;Terminology and definitions for nano-objects;Nanoparticle, nanofibre and nanoplate. Geneva, Switzerland.

Jiang, C., Aiken, G.R., Hsu-Kim, H., 2015. Effects of Natural Organic Matter Properties on the Dissolution Kinetics of Zinc Oxide Nanoparticles. Environ. Sci. Technol. 49, 11476–11484.

Ju-Nam, Y., Lead, J.R., 2008. Manufactured nanoparticles: An overview of their chemistry, interactions and potential environmental implications. Sci. Total Environ. 400, 396–414.

Kalman, J., Paul, K.B., Khan, F.R., Stone, V., Fernandes, T.F., 2015. Characterisation of bioaccumulation dynamics of three differently coated silver nanoparticles and aqueous silver in a simple freshwater food chain. Environ. Chem. 12, 662–672.

Kelleher, B., van der Velde, G., Wittmann, K.J., Faasse, M.A., bij de Vaate, A., 1999. Current status of the freshwater Mysidae in The Netherlands, with records of Limnomysis benedeni Czerniavsky, 1882, a Pontocaspian species in Dutch Rhine branches. Bull. Zoölogisch Museum (Universiteit van Amsterdam) 16, 89–94.

Keller, A.A., Lazareva, A., 2013. Predicted releases of engineered nanomaterials: From global to regional to local. Environ. Sci. Technol. Lett. 1, 65–70.

Klaine, S.J., Alvarez, P.J.J., Batley, G.E., Fernandes, T.F., Handy, R.D., Lyon, D.Y., Mahendra, S., McLaughlin, M.J., Lead, J.R., 2008. Nanomaterials in the environment: Behavior, fate, bioavailability, and effects. Environ. Toxicol. Chem. 27, 1825–1851.

Ko, K.S., Koh, D.C., Kong, I.C., 2018. Toxicity evaluation of individual and mixtures of nanoparticles based on algal chlorophyll content and cell count. Materials (Basel). 11.

Kotov, A.A., Karabanov, D.P., Bekker, E.I., Neretina, T. V., Taylor, D.J., 2016. Phylogeography of the chydorus sphaericus group (Cladocera: Chydoridae) in the northern Palearctic. PLoS One 11, 1–20.

Lammel, T., Thit, A., Mouneyrac, C., Baun, A., Sturve, J., Selck, H., Tobias Lammel, ‡*ab Amalie Thit,‡*a Catherine Mouneyrac, c Anders Baun, d J.S. and H.S., 2014. Trophic transfer of CuO NPs and dissolved Cu from sediment to worms to fish - a proof-of-concept study. Environ. Sci. Nano 6, 1–2.

Lead, J.R., Batley, G.E., Alvarez, P.J.J., Handy, R.D., Mclaughlin, M.J., 2018. Nanomaterials in the Environment : Behavior , Fate , Bioavailability , and Effects — An Updated Review. Environ. Toxicol. Chem. 37, 2029–2063.

Lee, W.M., Yoon, S.J., Shin, Y.J., An, Y.J., 2015. Trophic transfer of gold nanoparticles from *Euglena gracilis* or *Chlamydomonas reinhardtii* to *Daphnia magna*. Environ. Pollut. 201, 10–16.

Levard, C., Hotze, E.M., Lowry, G. V, Brown, G.E., 2012. Environmental Transformations of Silver Nanoparticles : Impact on Stability and Toxicity Cle m. Environ. Sci. Technol. 46, 6900–6914.

Li, C., Hassan, A., Palmai, M., Snee, P., Baveye, P.C., Darnault, C.J.G., 2022. Colloidal stability and aggregation kinetics of nanocrystal CdSe / ZnS quantum dots in aqueous systems : Effects of ionic strength , electrolyte type , and natural organic matter. SN Appl. Sci. 4, 101.

Libralato, G., Galdiero, E., Falanga, A., Carotenuto, R., De Alteriis, E., Guida, M., 2017. Toxicity Effects of Functionalized Quantum

Dots, Gold and Polystyrene Nanoparticles on Target Aquatic Biological Models: A Review. Molecules 22.

Limbach, L.K., Li, Y., Grass, R.N., Hintermann, M.A., Muller, M., Gunther, D., Stark, W.J., 2005. Oxide Nanoparticle Uptake in Human Lung Fibroblasts : Effects of Particle Size , Agglomeration , and Diffusion at Low Concentrations. Environ. Sci. Technol. 39, 9370−9376.

Liu, H.H., Cohen, Y., 2014. Multimedia Environmental Distribution of Engineered Nanomaterials. Environ. Sci. Technol. 48, 3281–3292.

Lowry, G. V., Gregory, K.B., Apte, S.C., Lead, J.R., 2012. Transformations of Nanomaterials in the Environment. Environ. Sci. Technol. 46, 6893–6899.

Lu, G., Yang, H., Xia, J., Zong, Y., Liu, J., 2017. Toxicity of Cu and Cr Nanoparticles to Daphnia magna. Water. Air. Soil Pollut. 228.

Ma, H., Williams, P.L., Diamond, S.A., 2013. Ecotoxicity of manufactured ZnO nanoparticles e A review. Environ. Pollut. 172, 76−85.

Machado, M.D., Soares, E. V., 2014. Modification of cell volume and proliferative capacity of Pseudokirchneriella subcapitata cells exposed to metal stress. Aquat. Toxicol. 147, 1–6.

Maji, T.K., Sarkar, P.K., Kar, P., Liu, B., Lemmens, P., Karmakar, D., Pal, S.K., 2019. A combined experimental and computational study on a nanohybrid material for potential application in NIR photocatalysis. Appl. Catal. A Gen. 583.

Malhotra, N., Ger, T.R., Uapipatanakul, B., Huang, J.C., Chen, K.H.C., Hsiao, C. Der, 2020. Review of copper and copper nanoparticle toxicity in fish. Nanomaterials 10, 1–28.

Mateos-Cárdenas, A., van Pelt, F.N.A.M., O'Halloran, J., Jansen, M.A.K., 2021. Adsorption, uptake and toxicity of micro- and nanoplastics: Effects on terrestrial plants and aquatic macrophytes. Environ. Pollut. 284.

Merrifield, R.C., Arkill, K.P., Palmer, R.E., Lead, J.R., 2017. A high resolution study of dynamic changes of Ce2O3 and CeO2 nanoparticles in complex environmental media. Environ. Sci. Technol. 51, 8010–8016.

Mohd Omar, F., Abdul Aziz, H., Stoll, S., 2014. Aggregation and disaggregation of ZnO nanoparticles: influence of pH and adsorption of Suwannee River humic acid. Sci. Total Environ. 468–469, 195–201.

Monikh, F.A., Chupani, L., Arenas-Lago, D., Guo, Z., Zhang, P., Darbha, G.K., Valsami-Jones, E., Lynch, I., Vijver, M.G., van Bodegom, P.M., Peijnenburg, W.J.G.M., 2021. Particle number-based trophic transfer of gold nanomaterials in an aquatic food chain. Nat. Commun. 12, 1–12.

Moore, M.N., 2006. Do nanoparticles present ecotoxicological risks for the health of the aquatic environment? Environ. Int. 32, 967–976.

Mordor Intelligence, 2022. Nanomaterials Market - Growth, Trends, COVID-19 Ipact, And Forecasts (2022 - 2027).

Nam, D., Lee, B., Eom, I., Kim, P., Yeo, M., 2014. Uptake and bioaccumulation of titanium- and silver-nanoparticles in aquatic ecosystems. Mol Cell Toxicol 10, 9–17.

Nowack, B., Bucheli, T.D., 2007. Occurrence , behavior and effects of nanoparticles in the environment. Environ. Pollut. 150, 5–22.

OECD, 2004. Oecd Guideline for testing of chemicals Daohnia sp., Acute Immobilisation Test, OECD.

Ogunsuyi, O.I., Fadoju, O.M., Akanni, O.O., Alabi, O.A., Alimba, C.G., Cambier, S., Eswara, S., Gutleb, A.C., Adaramoye, O.A., Bakare, A.A., 2019. Genetic and systemic toxicity induced by silver and copper oxide nanoparticles, and their mixture in Clarias gariepinus (Burchell, 1822). Environ. Sci. Pollut. Res. 26, 27470–27481.

Pacheco, A., Martins, A., Guilhermino, L., 2018. Toxicological interactions induced by chronic exposure to gold nanoparticles and microplastics mixtures in Daphnia magna. Sci. Total Environ. 628–629, 474–483.

Pakrashi, S., Dalai, S., Chandrasekaran, N., Mukherjee, A., 2014. Trophic transfer potential of aluminium oxide nanoparticles using representative primary producer (Chlorella ellipsoides) and a primary consumer (Ceriodaphnia dubia). Aquat. Toxicol. 152, 74–81.

Pan, J., Buffet, P., Poirier, L., Amiard-triquet, C., Gilliland, D., Joubert, Y., Pilet, P., Guibbolini, M., Risso, C., Faverney, D.,

Roméo, M., Valsami-jones, E., Mouneyrac, C., 2012. Size dependent bioaccumulation and ecotoxicity of gold nanoparticles in an endobenthic invertebrate : The Tellinid clam Scrobicularia plana. Environ. Pollut. 168, 37–43.

Peijnenburg, W.J.G.M., Baalousha, M., Chen, J., Chaudry, Q., Von Der Kammer, F., Kuhlbusch, T.A.J., Lead, J., Nickel, C., Quik, J.T.K., Renker, M., Wang, Z., Koelmans, A.A., 2015. A Review of the Properties and Processes Determining the Fate of Engineered Nanomaterials in the Aquatic Environment. Crit. Rev. Environ. Sci. Technol. 45, 2084–2134.

PEN, 2013. The Project on Emerging Nanotechnologies.

Peng, C., Zhang, W., Gao, H., Li, Y., Tong, X., Li, K., 2017. Behavior and Potential Impacts of Metal-Based Engineered Nanoparticles in Aquatic Environments. Nanomaterials 7, 21.

Peralta-Videa, J.R., Zhao, L., Lopez-Moreno, M.L., de la Rosa, G., Hong, J., Gardea-Torresdey, J.L., 2011. Nanomaterials and the environment: A review for the biennium 2008-2010. J. Hazard. Mater. 186, 1–15.

Phenrat, T., Saleh, N., Sirk, K., Tilton, R.D., Lowry, G. V, 2007. Aggregation and Sedimentation of Aqueous Nanoscale Zerovalent Iron Dispersions. Environ. Sci. Technol. 41, 284–290.

Quik, J.T.K., Arie, J., Foss, S., Baun, A., Meent, D. Van De, 2011. How to assess exposure of aquatic organisms to manufactured nanoparticles ? Environ. Int. 37, 1068–1077.

Rai, P.K., Kumar, V., Lee, S.S., Raza, N., Kim, K.H., Ok, Y.S., Tsang, D.C.W., 2018. Nanoparticle-plant interaction: Implications in energy, environment, and agriculture. Environ. Int. 119, 1–19.

Reinsch, B.C., Levard, C., Li, Z., Ma, R., Wise, A., Gregory, K.B., Brown, G.E., Lowry, G. V., 2012. Sulfidation of silver nanoparticles decreases Escherichia coli growth inhibition. Environ. Sci. Technol. Technol. 46, 6992–7000.

Ribeiro, F., Van Gestel, C.A.M., Pavlaki, M.D., Azevedo, S., Soares, A.M.V.M., Loureiro, S., 2017. Bioaccumulation of silver in *Daphnia magna*: Waterborne and dietary exposure to nanoparticles and dissolved silver. Sci. Total Environ. 574, 1633–1639.

Rocha, T.L., Mestre, N.C., Sabóia-Morais, S.M.T., Bebianno, M.J., 2016. Environmental behaviour and ecotoxicity of quantum dots at various trophic levels: A review. Environ. Int. 98, 1–17.

Saleh, N.B., Nabiul Afrooz, A.R.M., Bisesi, J.H., Aich, N., Plazas-Tuttle, J., Sabo-Attwood, T., 2014. Emergent properties and toxicological considerations for nanohybrid materials in aquatic systems. Nanomaterials 4, 372–407.

Santschi, C., Moos, N., Koman, V.B., Slaveykova, V.I., Bowen, P., Martin, O.J.F., 2017. Non-invasive continuous monitoring of pro-oxidant effects of engineered nanoparticles on aquatic microorganisms. J. Nanobiotechnology 15, 1–18.

Science for Environment Policy, 2017. *Assessing the environmental safety of manufactured nanomaterials*. In-depth Report 14 produced for the European Commission, DG Environment by the Science Communication Unit,. UWE, Bristol.

Sharma, V.K., Sayes, C.M., Guo, B., Pillai, S., Parsons, J.G., Wang, C., Yan, B., Ma, X., 2019. Interactions between silver nanoparticles and other metal nanoparticles under environmentally relevant conditions: A review. Sci. Total Environ. 653, 1042–1051.

Shi, Q., Wang, C.L., Zhang, H., Chen, C., Zhang, X., Chang, X., 2020. Environmental Science Nano nanoparticles in an aquatic food chain †. Environ. Sci. Nano 7, 1240–1251.

Suzuki, S., Yamaguchi, H., Nakajima, N., Kawachi, M., 2018. Raphidocelis subcapitata (=Pseudokirchneriella subcapitata) provides an insight into genome evolution and environmental adaptations in the Sphaeropleales. Sci. Rep. 8, 1–13.

Tangaa, S.R., Selck, H., Winther-Nielsen, M., Khan, F.R., 2016. Trophic transfer of metal-based nanoparticles in aquatic environments: A review and recommendations for future research focus. Environ. Sci. Nano 3, 966–981.

Terminology for nanoma- terials, 2007. . London, UK.

The European Commission recommendations, 2010. Commission recommendations, Nursing Standard.

Thomas, S.P., Al-Mutairi, E.M., De, S.K., 2013. Impact of Nanomaterials on Health and Environment. Arab. J. Sci. Eng. 38, 457–477.

Tortella, G.R., Rubilar, O., Durán, N., Diez, M.C., Martínez, M., Parada, J., Seabra, A.B., 2020. Silver nanoparticles : Toxicity in model organisms as an overview of its hazard for human health and the environment. J. Hazard. Mater. 390, 121974.

Van Koetsem, F., Verstraete, S., Van der Meeren, P., Du Laing, G., 2015. Stability of engineered nanomaterials in complex aqueous matrices: Settling behaviour of CeO2 nanoparticles in natural surface waters. Environ. Res. 142, 207–214.

van Pomeren, M., Brun, N.R., Peijnenburg, W.J.G.M., Vijver, M.G., 2017. Exploring uptake and biodistribution of polystyrene (nano)particles in zebrafish embryos at different developmental stages. Aquat. Toxicol. 190, 40–45.

Velzeboer, I., Hendriks, A.J., Ragas, A.M.J., Van De Meent, D., 2008. Aquatic ecotoxicity tests of some nanomaterials. Environ. Toxicol. Chem. 27, 1942–1947.

Wallace, W.G., Lopez, G.R., Levinton, J.S., 1998. Cadmium resistance in an oligochaete and its effect on cadmium trophic transfer to an omnivorous shrimp. Mar. Ecol. Prog. Ser. 172, 225–237.

Wang, J., Wang, W.X., 2014. Significance of physicochemical and uptake kinetics in controlling the toxicity of metallic nanomaterials to aquatic organisms. J. Zhejiang Univ. Sci. A 15, 573–592.

Wang, Z., Li, J., Zhao, J., Xing, B., 2011. Toxicity and internalization of CuO nanoparticles to prokaryotic alga microcystis aeruginosa as affected by dissolved organic matter. Environ. Sci. Technol. 45, 6032–6040.

Wang, Z., Quik, J.T.K., Song, L., Wouterse, M., Peijnenburg, W.J.G.M., 2018. Dissipative particle dynamic simulation and experimental assessment of the impacts of humic substances on aqueous aggregation and dispersion of engineered nanoparticles. Environ. Toxicol. Chem. 37, 1024–1031.

Wang, Z., Xia, B., Chen, B., Sun, X., Zhu, L., Zhao, J., Du, P., Xing, B., 2017. Trophic transfer of TiO_2 nanoparticles from marine microalga (*Nitzschia closterium*) to scallop (*Chlamys farreri*) and related toxicity. Environ. Sci. Nano 4, 415–424.

Wang, Z., Zhang, L., Zhao, J., Xing, B., 2016. Environmental processes and toxicity of metallic nanoparticles in aquatic

systems as affected by natural organic matter. Environ. Sci. Nano 3, 240–255.

Williams, R.J., Harrison, S., Keller, V., Kuenen, J., Lofts, S., Praetorius, A., Svendsen, C., Vermeulen, L.C., van Wijnen, J., 2019. Models for assessing engineered nanomaterial fate and behaviour in the aquatic environment. Curr. Opin. Environ. Sustain. 36, 105–115.

Wolf, S., Zwickel, H., Hartmann, W., Lauermann, M., Clemens, K., Altenhain, L., Schmid, R., Luo, J., Jen, A.K., Randel, S., Freude, W., Koos, C., 2018. Silicon-Organic Hybrid (SOH) Mach-Zehnder Modulators for 100 Gbit / s on-off Keying. Sci. Rep. 8, 2598.

Wu, F., Bortvedt, A., Harper, B.J., Crandon, L.E., Harper, S.L., 2017. Uptake and toxicity of CuO nanoparticles to *Daphnia magna* varies between indirect dietary and direct waterborne exposures. Aquat. Toxicol. 190, 78–86.

Xiao, Y., Vijver, M.G., Chen, G., Peijnenburg, W.J.G.M., 2015. Toxicity and accumulation of Cu and ZnO nanoparticles in *Daphnia magna*. Environ. Sci. Technol. 49, 4657–4664.

Xu, H., Li, C., Zeng, Q., Agrawal, I., Zhu, X., Gong, Z., 2016. Genome-wide identification of suitable zebrafish Danio rerio reference genes for normalization of gene expression data by RT-qPCR. J. Fish Biol. 88, 2095–2110.

Yamagishi, T., Yamaguchi, H., Suzuki, S., Horie, Y., Tatarazako, N., 2017. Cell reproductive patterns in the green alga Pseudokirchneriella subcapitata (=Selenastrum capricornutum) and their variations under exposure to the typical toxicants potassium dichromate and 3,5-DCP. PLoS One 12, 1–12.

Yan, N., Wang, W.X., 2021. Novel imaging of silver nanoparticle uptake by a unicellular alga and trophic transfer to *Daphnia magna*. Environ. Sci. Technol. 55, 5143–5151.

Yang, R.S.H., Thomas, R.S., Gustafson, D.L., Campain, J., Benjamin, S.A., Verhaar, H.J.M., Mumtaz, M.M., 1998. Approaches to developing alternative and predictive toxicology based on PBPK/PD and QSAR modeling, in: Environmental Health Perspectives. Public Health Services, US Dept of Health and Human Services, pp. 1385–1393.

Ye, N., Wang, Z., Wang, S., Peijnenburg, W.J.G.M., 2018. Toxicity of mixtures of zinc oxide and graphene oxide nanoparticles to aquatic organisms of different trophic level: particles outperform dissolved ions. Nanotoxicology 12, 423–438.

Yohannes, E., Rothhaupt, K.O., 2017. Dual-tracer-based isotope turnover rates in a highly invasive mysid Limnomysis benedeni from Lake Constance. Ecol. Evol. 7, 4173–4178.

Zhang, H., Chen, B., Banfield, J.F., 2010. Particle Size and pH Effects on Nanoparticle Dissolution. J. Phys. Chem. C 114, 14876–14884.

Zhao, X., Yu, M., Xu, D., Liu, A., Hou, X., Hao, F., Long, Y., Zhou, Q., Jiang, G., 2017. Distribution, Bioaccumulation, Trophic Transfer, and Influences of CeO2 Nanoparticles in a Constructed Aquatic Food Web. Environ. Sci. Technol. 51, 5205–5214.

Zhu, X., Wang, J., Zhang, X., Chang, Y., Chen, Y., 2010. Trophic transfer of TiO2 nanoparticles from daphnia to zebrafish in a simplified freshwater food chain. Chemosphere 79, 928–933.

Chapter 2

Effects of humic substances on the aqueous stability of cerium dioxide nanoparticles and their toxicity to aquatic organisms

Qi Yu, Zhuang Wang, Yujia Zhai, Fan Zhang, Martina G. Vijver, Willie J.G.M. Peijnenburg

Abstract

The impacts of humic substances (HS) on the aquatic stability and toxicity of cerium dioxide nanoparticles (CeO_2NPs) to three organisms with different exposure characteristics were investigated. Addition of HS to suspensions of CeO_2NPs lowered the surface zeta potential of the particles, reduced their hydrodynamic size, and increased the energy barrier as indicated by the total potential energy profile. This resulted in a more stable suspension compared to suspensions without HS added. Moreover, a higher concentration of HS further stabilized CeO_2NPs in the suspension. Acute toxicity of the suspensions to the unicellular green alga *Raphidocelis subcapitata* and to the crustacean *Chydorus sphaericus* was lower as compared to exposure without HS added. The acute toxicity of CeO_2NPs suspensions to the zebrafish (*Danio rerio*) eleutheroembryo was on the other hand significantly enhanced (additive and synergistic) upon increasing HS concentration. Our findings emphasize that HS is important to stabilize the nano-suspensions and that its impact on CeO_2NPs toxicity differs across different aquatic organisms. Emphasizing the exposure characteristics of each of the organisms selected from the trophic levels can explain how particle stability impacts particle toxicity.

Keywords: CeO_2NPs; Stability; Toxicity; Humic substances; Aquatic test species

2.1 Introduction

The prospects of engineered nanoparticles (ENPs) of different sizes, shapes, and material properties in a number of applications have progressed rapidly (Guinée et al., 2017; Martínez et al., 2020), although the market benefits brought about by ENPs have also created some concerns of their possible effects on human health and environmental safety (Savolainen et al., 2013; Baun et al., 2017; Deng et al., 2017). Many studies emphasized the challenging relationship between typical ENPs features such as shape, size, modifications and the abiotic factors of the environment such as pH, divalent cation ions, dissolved organic carbon (Lu et al., 2017; Liu et al., 2018; Yu et al., 2018; Singh et al., 2021). Understanding how ENPs interact with the environment can assist in predicting the fate and effect of ENPs and may provide a basis for their ecological risk assessment.

Cerium dioxide nanoparticles (CeO_2NPs) is increasingly being applied in fuel additives and polishing agents (Collin et al., 2014). To date, the estimated production of CeO_2NPs is around 1000 tons/year and it has become one of the most produced ENPs in the world (Piccino et al., 2012). Upon their release into the aquatic environment, CeO_2NPs may provoke adverse effects to various organisms (Rundle et al., 2016; Taylor et al., 2016; Kosak et al., 2018; Wang and Nowack 2018; Correia et al., 2020).

Natural organic matter (NOM) is ubiquitous in every water and is known to affect the fate and toxicity of ENPs by modifying the surface properties (e.g., charge and hydrophobicity), subsequently affecting their stability as well as nanoparticle-cellular interactions (Van Hoecke et al., 2011; Loosli et al., 2013; Baalousha et al., 2018; Liu et al., 2020). Evidence was found that the presence of Suwannee River

and Bihain NOM can stabilize CeO_2NPs in an algae growth medium (Quik et al., 2010). Moreover, Suwannee River NOM can alleviate the adverse effects of NPs on algal growth (Cerrillo et al., 2016). However, how the CeO_2NPs-NOM interaction alters the toxicity of CeO_2NPs to aquatic organisms is not completely understood.

This work aimed to explore the impact of humic substances (HS) on the aqueous stability and subsequent toxicity of CeO_2NPs to different organisms. The aqueous stability of CeO_2NPs in the presence of HS was determined by measuring the zeta potential of suspensions and the sizes of the agglomerates formed, whereas suspension concentrations were measured in simulated natural environmental conditions. Short-term experiments were performed with aquatic organisms with different exposure characteristics, namely the microalga *Raphidocelis subcapitata*, the microcrustacean *Chydorus sphaericus*, and the fish *Danio rerio*. The different exposure characteristics of the organisms assist in understanding the actual exposure of aquatic organisms to nanoparticles and the effective interactions with nanoparticles. The starting hypotheses were:

Ho_1 = Algal cells and HS will compete for binding with the nanoparticles. Thus, it is expected that the addition of HS to CeO_2NPs suspensions will diminish the toxicity of the suspensions to algae.

Ho_2 = The microcrustacean are bottom-feeders that graze on the bottom of the vessels. Stabilization of CeO_2NPs suspensions by HS decreases the toxicity to Chydoridae compared to relative instable CeO_2NPs suspensions without HS addition.

Ho_3 = Nanoparticle sedimentation increases the particle concentration at the bottom of the test well and that is where the zebrafish embryos reside. Accordingly, the embryos are exposed to CeO_2NPs at a higher extent when the CeO_2NPs is not stabilized. When

hatched, the larvae swim around and mix the CeO_2NPs and thus higher toxicity is expected without HS added.

2.2 Materials and Methods

2.2.1 Test materials and medium

CeO_2 nanoparticles were supplied by Umicore Ltd as powders. The particles were redispersed and stocked by milling into Milli-Q water as 10 wt% suspensions at pH 4 containing nitric acid, as well as stored at 4 °C for later use. Moreover, the test suspensions were characterized immediately after their preparation. The primary particle size of CeO_2NPs was 20 nm and the specific surface area was 42 m^2/g as determined by the manufacturer. The model HS purchased from J&K Chemical, a humic acid sodium salt (50–60% as humic acid, CAS: 68131-04-4), was selected to mimic natural organic matter (NOM). The humic acid sodium salt acts as a proxy for humic-like substances that were also identified as a major component of NOM. The exposure medium was defined to be the Dutch standard (DSW) (Hermsen et al., 2011) consisting of $NaHCO_3$ (1.19 mM), $KHCO_3$ (0.20 mM), $CaCl_2$ (1.36 mM), and $MgSO_4$ (0.73 mM) with a pH adjustment of 8.0 ± 0.2.

2.2.2 Treatments and concentrations tested

Drop-wise addition of the CeO_2NPs stock suspensions into the DSW was carried out to prepare the different test dosages of the nanoparticles, which were 0.5, 1, 5, 10, 25, 50, 100 mg/L. Moreover, the test suspensions of the CeO_2NPs were stirred for 24 h in the dark.

A HS stock solution was prepared by dissolving 100 mg/L by stirring for 24 h at room temperature and filtering over a 0.20 μm nylon membrane filter prior to use. The actual HS concentrations of suspensions of nominal 0.5, 10, and 40 mg C/L in the DSW were measured by using a Thermo Hiper TOC analyzer. The CeO_2NPs suspensions in the presence of HS were prepared by adding the CeO_2NPs stock suspensions into the HS solutions. The suspensions of CeO_2NPs with HS were further stirred for 24 h in the dark. The pH values of all samples were adjusted to 8.0 ± 0.2 using a 1 mol/L HCl or NaOH solution.

2.2.3 Physical and chemical analysis

The physical and chemical measurements were performed on the 10 mg/L CeO_2NPs suspension in glass flasks (5 cm in diameter and 10 cm in height) with 100 mL under the same conditions as the toxicity testing for 0, 24, 48, 72, and 96 h. Zeta potentials, mean (the average of all particles) particle diameters, and particle concentrations of suspensions in the absence and presence of HS were determined at the end of different intervals. The zeta potential was measured by a ZetaSizer (Nano series, Malvern Instruments) in triplicate. The particle size distribution of CeO_2NPs in the DSW was measured by a Nanosight LM20 system (NanoSight Ltd., Salisbury, UK) using Nanoparticle Tracking Analysis (NTA) (software version 1.5). From the classical Derjaguin-Landau-Verwey-Overbeek (DLVO) theory (Cosgrove 2005), the stability of a particle in the test medium was determined by simulating the total potential energy for interactions between the CeO_2 particles in the absence and presence of HS. The detailed process and parameter settings of the DLVO calculations are

described in the Supplementary Information. The total Ce concentration was determined by high resolution inductively coupled plasma mass spectroscopy (Element 2 HR-ICP-MS, Thermo, Bremen, Germany) after a 2 h hot open destruction treatment with 1 mL hydrogen peroxide (9.8 mol/L) and 7 mL nitric acid (14.4 mol/L) at 103°C.

2.2.4 Bioassays

Toxicity of the CeO_2NPs in the absence and presence of HS to the test organisms was assessed by concentration–response experiments. For each batch of toxicity tests, a control consisting of the test medium was included to ensure that the observed effects were associated with exposure to the test compounds.

Microalga *R. subcapitata* from a continuous culture were suspended in DSW to a total volume of 3 mL in glass vials, to obtain a final density of 1×10^6 cells/mL. The inhibition of 4.5 h photosynthetic efficiency was determined for the algae using a pulse-amplitude modulation fluorometer (Wang et al., 2012). The algae were exposed to various initial concentrations (0.5, 1, 5, 10, 25, 50, and 100 mg/L) of the CeO_2NPs suspensions in the absence and presence of HS (0.5, 10, and 40 mg C/L), as well as the HS alone (0.5, 10, and 40 mg C/L).

The 48 h acute immobilization tests with *C. sphaericus* followed the protocol of the Chydotox toxicity test developed in the National Institute of Public Health and the Environment (Netherlands) (Verweij et al., 2009). Twenty neonates (< 24 h) at each exposure concentration, divided into four batches of five animals each, were added to a single droplet of DSW with a diameter of approximately 5 mm in the glass vial. 250 μL test solution was added into each vial.

The vials were covered with a crimp cap to prevent evaporation and incubated for 48 h in a climate room at 20 °C and a light : dark regime of 16 : 8 h.

Crustaceans *C. sphaericus* were exposed to various initial concentrations (0.5, 1, 5, 10, 25, 50, and 100 mg/L) of the CeO_2NPs suspensions in the absence and presence of HS (0.5, 10, and 40 mg C/L), as well as the HS alone (0.5, 10, and 40 mg C/L). After 48 h, the vials were placed under a reverse dissecting microscope and the immobility was determined by activation of *C. sphaericus* by slightly shaking the vial and monitoring them for 30 sec.

An early life stage test with zebrafish (*D. rerio*) embryos was performed in accordance with the procedure described by Lammer et al. (2009). Each exposure concentration and control in 3 independent experiments was tested with 10 eggs/embryos (4-64 cell stage) from 20 vital and fertilized eggs, and the selected eggs were transferred into 24-well cell culture plates with 2 mL freshly prepared control medium or test suspensions. Embryos were incubated at 26 ± 1 °C for 96 h and were exposed to three CeO_2NPs exposure concentrations (1, 10, and 100 mg/L) in the absence and presence of HS (10 and 40 mg C/L), as well as the HS alone (10 and 40 mg C/L). The development of zebrafish embryos was microscopically screened daily. Lethality as well as sub-lethal developmental morphology and teratogenicity toxicological endpoints (Hermsen et al., 2011) were scored after 96 h (Supplementary Information, Table S2.1). Embryos were scored according to the classifications given by King-Heiden et al. (2009) as (0) no toxic response, (1) one or two toxic endpoints, (2) two or three toxic endpoints, (3) more than three toxic endpoints, and (4) dead. The choice of the scores depends on the severity of the toxicity endpoint. In order to avoid overestimating the toxicity of the test

materials, a lower score was selected if a certain toxicity endpoint of an embryo was slightly damaged.

2.2.5 Toxicity evaluating of CeO_2NPs in the presence of HS

CeO_2NPs with the addition of HS can be regarded as a binary mixture system. The observed mixture toxicity effect, ME_{obs}, determined in the toxicity testing was compared with the theoretically predicted mixture toxicity effect, ME_{pre}, calculated using a probability theory based model (Hadjispyrou et al. 2001):

$$ME_{pre} = E_{nCeO_2} + E_{HS} - (E_{nCeO_2} \cdot E_{HS}/100) \tag{1}$$

where E_{nCeO_2} is the single toxicity effect of CeO_2NPs and E_{HS} is the single toxicity effect of HS.

The result was applied to reflect a synergistic or antagonistic effect if ME_{obs} was significantly higher or lower than ME_{pre}, respectively. On the contrary, the interaction of the binary mixture was considered as an additive effect only if there was no significant difference between ME_{obs} and ME_{pre}. The presented method was applied to predict the toxicity of the studied systems to *D. rerio*, which is due to the fact that there was no observed toxicity to the algae and to the cladoceran induced by the HS studied.

All values were reported as mean ± standard deviation (SD). SD of the mean was calculated from parallel experiments. Statistically significant differences between test treatments in the present study were determined by the Student's *t*-test. The significance levels $p < 0.05$, $p < 0.01$, and $p < 0.001$ were used.

2.3 Results and Discussion

2.3.1 Effects of HS on aqueous stability of CeO_2NPs

The variation of the zeta potential values of CeO_2NPs with the HS concentrations and with the time of incubation is shown in Figure 2.1A. The zeta potential values of the CeO_2NPs were found to be negative and changed slightly over time. Furthermore, the zeta potential values were more negative when the HS were present compared with the zeta potential values when the HS were absent, implying that the HS can influence electrokinetic properties, causing an increased nanoparticle surface charge. The HS effect on the particle zeta potential depended on the HS concentrations, irrespectively of the time of incubation.

Observed changes in the mean particle diameters with the HS concentrations over the experimental duration in the absence and presence of HS are presented in Figure 2.1B. The CeO_2NPs particles immediately agglomerated in DSW-medium at an initial mean particle diameters size of 218 nm, which is a tenfold higher than the primary size (20 nm). This implies that the CeO_2NPs particles were agglomerated. Upon increasing HS concentrations, the mean particle diameters of the CeO_2NPs agglomerates decreased. This may be explained because the HS acts as a polyelectrolyte or surfactant, thus providing electrostatic repulsive forces of the particles (Baalousha et al., 2008; Domingos et al., 2009). This stabilization of the particles by HS and subsequent decrease of the mean particle diameters of the agglomerates, was detectable regardless of exposure time.
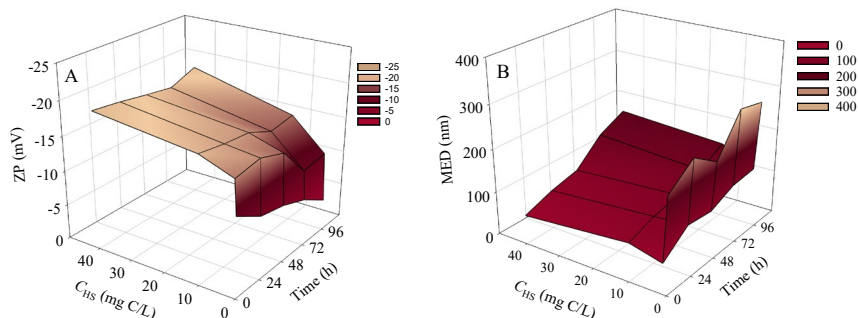
Figure 2.1 Zeta potential (ZP) (A) and mean particle diameter (MED) (B) of the CeO₂NPs suspensions with particle concentration of 10 mg/L in the absence and presence of different concentrations of HS (C_{HS}) (0.5, 10, and 40 mg C/L) (pH = 8.0). Results are expressed as mean (n = 3)

On the basis of the DLVO theory (Cosgrove 2005), the total potential energy profiles for the CeO₂NPs colloids with nanoparticle concentrations of 10 mg/L were calculated (Figure 2.2). The magnitudes of the primary maximum of the CeO₂NPs colloids in the presence of the different concentrations of the HS follow the order: CeO₂NPs + 10 mg C/L HS (19.1 K_BT) is approximately equal to CeO₂NPs + 40 mg C/L HS (18.9 K_BT) > CeO₂NPs + 0.5 mg C/L HS (9.8 K_BT) > CeO₂NPs (6.6 K_BT), implying that the stability of the colloids studied follows the order: CeO₂NPs + 10 mg C/L HS is approximately equal to CeO₂NPs + 40 mg C/L HS > CeO₂NPs + 0.5 mg C/L HS > CeO₂NPs. It is the primary maximum in the total energy which provides the mechanism for the stability of the charged colloidal particles. As two particles approach each other, they must collide with sufficient energy to overcome a barrier provided by the primary maximum. Thus, the larger the barrier, the longer the system will remain stable. In the present study, we also observed that the

stability of the binary systems of CeO$_2$NPs + 10 mg C/L HS is approximately equal to the stability of the combination of CeO$_2$NPs + 40 mg C/L HS. This also implies that only a part of the HS at the highest concentrations (40 mg C/L HS) could be actually adsorbed.
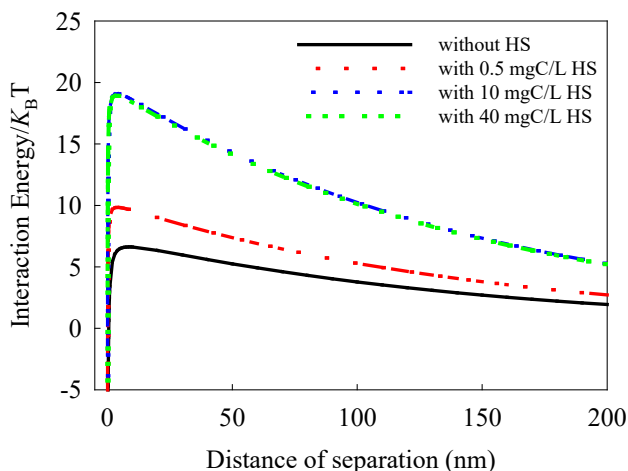

Figure 2.2 Total potential energy curves for the CeO$_2$NPs with particle concentration of 10 mg/L in the presence of HS of 0.5, 10, and 40 mg C/L

The stability of CeO$_2$NPs in suspensions depends on the total potential energy of interaction between colloidal particles according to the DLVO theory. In the present study, the steric stabilization induced by HS was not considered in calculating the interaction energy between the colloidal particles as the thickness of the surface coating layer was found to be very small (≤ 0.8 nm) (Baalousha et al., 2008). Moreover, the studied HS analogue is a small molecule (MW: 226.14 g/mol) without any significant spatial extent and CeO$_2$NPs is thus considered to be a hard sphere. Although these assumptions and DLVO calculations are simplistic, they are indicative of the interaction

forces between the nanoparticles and therefore the aggregation mechanisms (Baalousha 2009).

Figure 2.3A shows the variation of the ratios of the particle concentrations of suspensions to the initial particle concentration of CeO_2NPs in the absence and presence of HS over time. In the first 24 h this decline was steep and similar for all treatments. In the time span of 24 h to 96 h this steep decline could only be observed in the treatment without HS addition. The treatments with HS addition showed a dose-dependent stabilization of the CeO_2NPs suspensions. As shown in Figure 2.3B, the CeO_2NPs-HS interaction resulted in a co-sedimentation behavior of HS and CeO_2NPs. This evidence supports the adsorption of HS upon the surface of the particles. Over 96 h, the amount of HS adsorbed on the particles was estimated to be approximately 0.1, 1.2, and 1.8 mg C/L corresponding to the initial HS concentration of 0.5, 10, and 40 mg C/L, respectively.
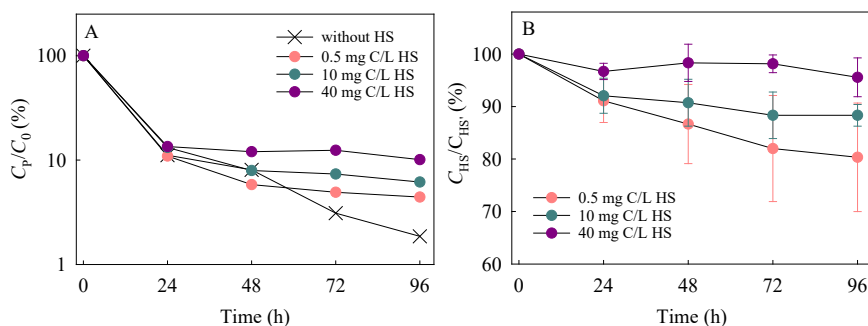

Figure 2.3 Ratios of the suspended particle concentrations (C_P) to the initial particle concentration (C_0, 10 mg/L) of CeO_2NPs in the absence and presence of HS (A, results are expressed as a single value) and ratios of the concentration of HS in the suspensions of CeO_2NPs in the presence of HS (C_{HS}) to the concentration of only HS (C_{HS}') (B, results are expressed as mean ± SD ($n = 3$))

2.3.2 Effects of HS on aquatic toxicity of CeO$_2$NPs

Concentration-dependent effects obtained for CeO$_2$NPs in the presence of different initial HS concentrations for the algae and cladoceran are given in Figure 2.4, and for the zebrafish embryos in Figure 2.5A. Throughout the test duration the *R. subcapitata* cells are gentle shaken continuously on a shaking table, hence the algal exposure was mainly within the water column where the nanoparticles were as well, representing relative high chances for exposure. As shown in Figure 2.4A, the addition of 10 and 40 mg C/L HS to the CeO$_2$NPs suspensions significantly inhibited the acute toxicity measured as photosynthetic activity to *R. subcapitata* ($p <$ 0.05). Note that no toxic effects on the algae were observed for the HS. This means that the presence of 10 or 40 mg C/L HS interfered with the interaction of CeO$_2$NPs with the algal cells and weakened the toxic effect. This interference might also be explained by the fact that the physicochemical analysis indicated adsorption of HS to the CeO$_2$NPs particles, which subsequently hinders the particles from directly interacting with algal cells. Van Hoecke et al. (2011) also concluded that decrease in algal toxicity might be due to a reduction in bioavailability of the particles when NOM is present. Cerrillo et al. (2016) found that NOM alleviated the adverse effects of CeO$_2$NPs on algal growth to some extent and suggested a 'camouflage' effect of CeO$_2$NPs.

The Chydoridae species is commonly grazing on the bottom of a vessel and sedimentation would increase exposure in case of particle agglomeration and subsequently sedimentation. These processes were largely affected by the addition of HS, with treatments without HS addition yielding relative instable nanoparticle suspensions. The

acute toxicity of the CeO$_2$NPs to *C. sphaericus* (Figure 2.4B) was mitigated when HS was present, particular for the concentration of 40 mg C/L HS. The physicochemical analysis here also showed that HS stabilized the CeO$_2$NPs suspensions. Taking into account that *C. sphaericus* is a benthic cladoceran species and is likely to ingest sediment particles into the gut and adsorb them on to carapaces, the reduced toxicity to *C. sphaericus* might be explained by the fact that a lower amount of NPs were allowed to sediment and subsequently, a lower amount of particles was accumulated in the cladoceran when HS was present as compared to the situation in which HS were absent. The analysis for the variation of the initial particle concentration of CeO$_2$NPs in the absence and presence of HS over time (Figure 2.3A) also supports the conclusion that relatively more particles were stabilized when HS were present during the exposure.
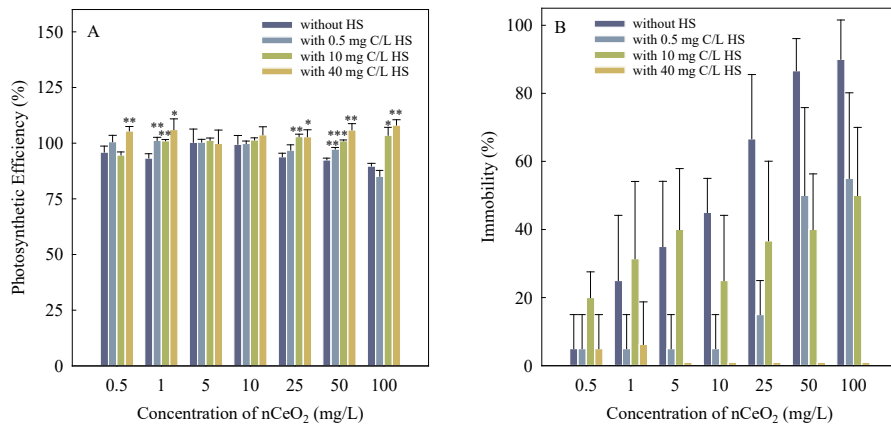

Figure 2.4 Concentration-dependent effects for *Raphidocelis subcapitata* (A) and *Chydorus sphaericus* (B) exposed to CeO$_2$NPs suspensions in the presence and absence of humic substances (HS) (*t*-test *$p < 0.05$ when comparing the treatments of CeO$_2$NPs without HS to CeO$_2$NPs with HS). Results are expressed as mean ± SD (*n* = 3

for *R. subcapitata* and *n* = 4 for *C. sphaericus*)

As shown in Figure 2.5A, the toxicity of CeO_2NPs to the larvae of *D. rerio* in the presence of 40 mg C/L HS was significantly enhanced in comparison with the toxicity of CeO_2NPs to the larvae in the absence of HS. In addition, the toxicity of 10 mg C/L HS alone treatment was equivalent to the toxicity of 1 and 10 mg/L CeO_2NPs and significantly lower than 100 mg/L CeO_2NPs. Thus, it can be concluded that concomitant exposure of the HS and CeO_2NPs caused the toxicity to *D. rerio*. The observed toxicity effects of the binary mixtures of the HS and CeO_2NPs were compared with their predicted toxicity (Figure 2.5B), calculated using the result of individual toxic effects based on the equation 1. No significant differences were observed for the cases 1 and 10 mg/L CeO_2 + 10 mg C/L HS between the results of the observation and prediction ($p < 0.05$), implying that these combinations showed additive action (observed toxicity similar to expected toxicity). The predicted mixture toxicity of the treatments 100 mg/L CeO_2 + 10 mg C/L HS and 1 and 10 mg/L CeO_2 + 40 mg C/L HS was significantly greater than their observed mixture toxicity, indicating that these combinations had synergistic effects. In addition, the average value of the predicted toxicity of the binary mixture of 100 mg/L CeO_2 and 40 mg C/L HS was higher than the observed toxicity, although there was no significant difference between the observation and prediction.

The images of zebrafish larvae exposed to different concentrations of CeO_2NPs in the absence and presence of HS at 96 h depict the concentration-dependent malformations during development. Compared to the control (Figure 2.5C), to the HS alone (Figure 2.5D, no obvious anomalies), and to the individual CeO_2NPs (Figure 2.5E,

only scoliosis), the combination of CeO_2NPs and 40 mg C/L HS induced more morphology and teratogenicity toxicity endpoints including pericardial oedema, yolk sac oedema, and scoliosis (Figure 2.5F). Here again, the presence of HS stabilized the particles of suspensions by decreasing their agglomerated MED size, implying that the zebrafish embryo would be exposed to the particles with lower size. This also means that the particles in suspensions with lower size induced more toxicity to the zebrafish larvae.

Thereupon, the zebrafish eggs with a chorion lie at the bottom of the test well. The chorion is considered as an effective barrier to protect the embryo from uptake of nanoparticles (Brun et al., 2018; Brinkmann et al., 2020). Due to the sedimentation of CeO_2NPs, the zebrafish embryos were exposed to a higher extent to the nanoparticles. However, the chorion protected the zebrafish larvae against CeO_2NPs toxicity. After the hatching, the zebrafish larvae actively swam around in the water column and mixed with the nanoparticles. As aforementioned, the HS stabilized more nanoparticles than when the HS was absent. Consequently, the direct exposure of the zebrafish larvae to CeO_2NPs in the presence of HS was relatively higher than the direct exposure of the zebrafish larvae to CeO_2NPs in the absence of HS, which could lead to a higher toxicity induced by CeO_2NPs when the HS was present. Furthermore, increasing the amount of the HS increased the severity of toxicity. Taken together, comparison analysis on the toxicity testing results suggests that the studied HS had a dual impact on the aquatic toxicity of CeO_2NPs, depending on the exposure characteristics of the test species. Moreover, the HS concentration modulates its degree of influence on the toxicity.
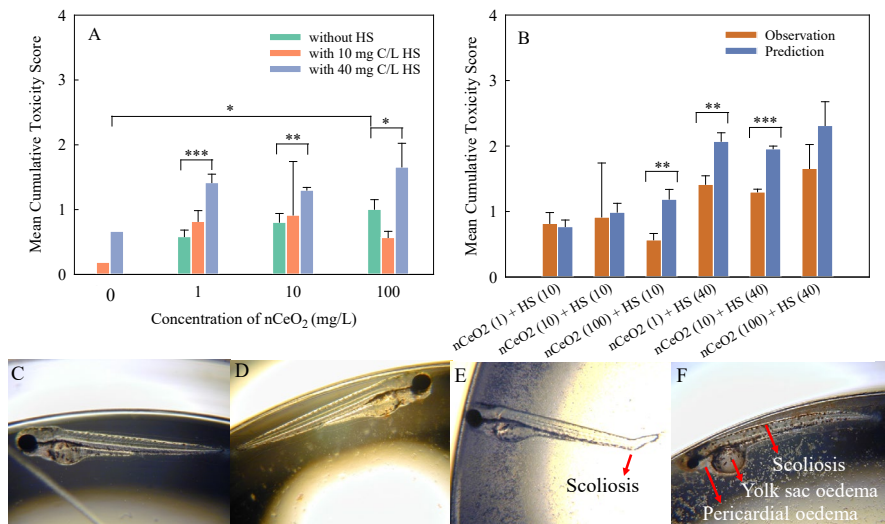
Figure 2.5 Concentration-dependent effects (A) for *Danio rerio* exposed to the CeO$_2$NPs suspensions in the presence and absence of HS, summary of the observed and expected toxic effects (B) of the binary mixtures of the CeO$_2$NPs (1, 10, 100 mg/L) and HS (10 and 40 mg C/L). *$p < 0.05$, **$p < 0.01$, ***$p < 0.001$ when comparing the treatments, results are expressed as mean $\pm$ SD ($n = 3$). Photos of zebrafish larvae exposed to different concentrations of CeO$_2$NPs in the absence and presence of HS at 96 h (C: control; D: 40 mg C/L HS; E: 10 mg/L CeO$_2$; F: 10 mg/L CeO$_2$ + 40 mg C/L HS)

2.4 Conclusions

Our results reveal how and to what extend the stability of CeO$_2$NPs was enhanced when HS was present in the aquatic medium at concentrations exceeding 0.5 mg C/L. Like expected by means of hypothesis H0$_1$, the addition of HS mitigated the CeO$_2$NPs suspensions toxicity to algae *R. subcapitata*. The H0$_2$ for the *C.*

sphaericus species was accepted; CeO_2NPs suspensions stabilized by HS were less toxic as compared to relative instable suspensions of CeO_2NPs without HS added. Suspension of CeO_2NPs without HS added were more toxic to zebrafish larvae, which made us reject the Ho_3.

The extent and the effects of HS on the toxicity were associated with the concentration (ranging from 0.5 to 40 mg C/L) of HS added. Furthermore, the aqueous stability of CeO_2NPs and the aquatic species influenced the toxicity of the particles in the presence of HS. Our results are stepping stones towards improving the understanding the processes that determine the actual exposure of a suite of aquatic organisms to exposure media of different composition, mimicking to an increasing extend natural aquatic systems. Understanding the exposure characteristics of the organisms selected – explicitly considering where in the water column of the experimental test the organisms is most present will explain if stabilization of nanomaterials with HS or any other type of NOM will affect the toxicity of the nanomaterials.

References

Baalousha, M., Afshinnia, K., Guo, L., 2018. Natural organic matter composition determines the molecular nature of silver nanomaterial NOM-corona. Environ. Sci: Nano 5, 868-881.

Baalousha, M., Manciulea, A., Cumberland, S., Kendall, K., Lead, J.R., 2008. Aggregation and surface properties of iron oxide nanoparticles: Influence of pH and natural organic matter. Environ. Toxicol. Chem. 27, 1875-1882.

Baalousha, M., 2009. Aggregation and disaggregation of iron oxide nanoparticles: Influence of particle concentration, pH and natural organic matter. Sci. Total Environ. 407, 2093-2101.

Baun, A., Sayre, P., Steinhäuser, K.G., Rose, J., 2017. Regulatory relevant and reliable methods and data for determining the environmental fate of manufactured nanomaterials. NanoImpact 8, 1-10.

Brinkmann, B.W., Koch, B.E.V., Spaink, H.P., Peijnenburg, W.J.G.M., Vijver, M.G., 2020. Colonizing microbiota protect zebrafish larvae against silver nanoparticle toxicity. Nanotoxicology 14(6), 725-739.

Brun, N.R., Koch, B.E.V., Varela, M., Peijnenburg, W.J.G.M., Spaink, H.P., Vijver, M.G., 2018. Nanoparticles induce dermal and intestinal innate immune system responses in zebrafish embryos. Environ Sci: Nano 5(4), 904-916.

Cerrillo, C., Barandika, G., Igartua, A., Areitioaurtena, O., Mendoza, G., 2016. Towards the standardization of nanoecotoxicity testing: Natural organic matter 'camouflages' the adverse effects of TiO_2 and CeO_2 nanoparticles on green microalgae. Sci. Total Environ. 543 (Pt A), 95-104.

Collin, B., Auffan, M., Johnson, A.C., Kaur, I., Keller, A.A., Lazareva, A., Lead, J.R., Ma, X., Merrifield, R.C., Svendsen, C., White, J.C., Unrine, J.M., 2014. Environmental release, fate and ecotoxicological effects of manufactured ceria nanomaterials. Environ Sci: Nano 1, 533-548.

Correia, A.T., Rodrigues, S., Ferreira-Martins, D., Nunes, A.C., Ribeiro, M.I., Antunes, S.C., 2020. Multi-biomarker approach to assess the acute effects of cerium dioxide nanoparticles in gills,

liver and kidney of *Oncorhynchus mykiss*. Comp. Biochem. Physiol. C Toxicol. Pharmacol. 238, 108842.

Cosgrove, T., 2005. Colloid science: Principles, methods and applications. Blackwell Publishing Ltd.

Deng, R., Lin, D., Zhu, L., Majumdar, S., White, J.C., Gardea-Torresdey, J.L., Xing, B., 2017. Nanoparticle interactions with co-existing contaminants: joint toxicity, bioaccumulation and risk. Nanotoxicology 11(5), 591-612.

Domingos, R.F., Tufenkji, N., Wilkinson, K.J., 2009. Aggregation of titanium dioxide nanoparticles: Role of a fulvic acid. Environ. Sci. Technol. 43, 1282-1286.

Guinée, J.B., Heijungs, R., Vijver, M.G., Peijnenburg, W.J.G.M., 2017. Setting the stage for debating the roles of risk assessment and life-cycle assessment of engineered nanomaterials. Nat. Nanotechnol. 12, 727-733.

Hadjispyrou, S., Kungolos, A., Anagnostopoulos, A., 2001. Toxicity, bioaccumulation and interactive effects of organotin, cadmium and chromium on *Artemia franciscana*. Ecotoxicol. Environ. Saf. 49, 179-186.

Hermsen, S.A.B., van den Brandhof, E.-J., van der Ven, L.T.M., Piersma, A.H., 2011. Relative embryotoxicity of two classes of chemicals in a modified zebrafish embryotoxicity test and comparison with their *in vivo* potencies. *Toxicol In Vitro* 25, 745-753.

King-Heiden, T.C., Wiecinski, P.N., Mangham, A.N., Metz, K.M., Nesbit, D., Pedersen, J.A., Hamers, R.J., Heideman, W., Peterson, R.E., 2009. Quantum dot nanotoxicity assessment using the zebrafish embryo. Environ. Sci. Technol. 43, 1605-1611.

Kosak Née Röhder, L.A., Brandt, T., Sigg, L., Behra, R., 2018. Uptake and effects of cerium (III) and cerium oxide nanoparticles to *Chlamydomonas reinhardtii*. Aquat. Toxicol. 197, 41-46.

Lammer, E., Carr, G.J., Wendler, K., Rawlings, J.M., Belanger, S.E., Braunbeck, T., 2009. Is the fish embryo toxicity test (FET) with the zebrafish (*Danio rerio*) a potential alternative for the fish acute toxicity test? Comp. Biochem. Physiol. Part C Toxicol. Pharmcol. 149, 196-209.

Loosli, F., Le Coustumer, P., Stoll, S., 2013. TiO$_2$ nanoparticles aggregation and disaggregation in presence of alginate and Suwannee River humic acids, pH and concentration effects on nanoparticle stability. Water Res. 47, 6052-6063.

Liu, J., Dai, C., Hu, Y., 2018. Aqueous aggregation behavior of citric acid coated magnetite nanoparticles: Effects of pH, cations, anions, and humic acid. Environ. Res. 161, 49-60.

Liu, Y., Huang, Z., Zhou, J., Tang, J., Yang, C., Chen, C., Huang, W., Dang, Z., 2020. Influence of environmental and biological macromolecules on aggregation kinetics of nanoplastics in aquatic systems. Water Res. 186, 116316.

Lu, K., Dong, S., Petersen, E.J., Niu, J., Chang, X., Wang, P., Lin, S., Gao, S., Mao, L., 2017. Biological uptake, distribution, and depuration of radio-labeled graphene in adult zebrafish: Effects of graphene size and natural organic matter. ACS Nano 11, 2872-2885.

Martínez, G., Merinero, M., Pérez-Aranda, M., Pérez-Soriano, E.M., Ortiz, T., Begines, B., Alcudia, A., 2020. Environmental impact of nanoparticles' application as an emerging technology: A review. Materials (Basel) 14(1), E166.

Piccino, F., Gottschalk, F., Seeger, S., Nowack, B., 2012. Industrial production quantities and uses of ten engineered nanomaterials in Europe and the world. J. Nanopart. Res. 14, 1109.

Quik, J.T., Lynch, I., Van Hoecke, K., Miermans, C.J., De Schamphelaere, K.A., Janssen, C.R., Dawson, K.A., Stuart, M.A., Van De Meent, D., 2010. Effect of natural organic matter on cerium dioxide nanoparticles settling in model fresh water. Chemosphere 81, 711-715.

Rundle, A., Robertson, A.B., Blay, A.M., Butler, K.M., Callaghan, N.I., Dieni, C.A., MacCormack, T.J., 2016. Cerium oxide nanoparticles exhibit minimal cardiac and cytotoxicity in the freshwater fish *Catostomus commersonii*. Comp. Biochem. Physiol. C Toxicol. Pharmacol. 181-182, 19-26.

Savolainen, K., Backman, U., Brouwer, D., Fadeel, B., Fernandes, T., Kuhlbusch, T., Landsiedel, R., Lynch, I., Pylkkänen, L., 2013. Nanosafety in Europe 2015-2025: Towards safe and sustainable nanomaterials and nanotechnology innovations. Helsinki, Finnish

Inst.   Occup.   Heal.
http://www.eu-vri.eu/filehandler.ashx?file=12392.

Singh, N., Khandelwal, N., Tiwari, E., Naskar, N., Lahiri, S., Lützenkirchen, J., Darbha, G.K., 2021. Interaction of metal oxide nanoparticles with microplastics: Impact of weathering under riverine conditions. Water Res. 189, 116622.

Taylor, N.S., Merrifield, R., Williams, T.D., Chipman, J.K., Lead, J.R., Viant, M.R., 2016. Molecular toxicity of cerium oxide nanoparticles to the freshwater alga *Chlamydomonas reinhardtii* is associated with supra-environmental exposure concentrations. Nanotoxicology 10, 32-41.

Van Hoecke, K., De Schamphelaere, K.A., Van der Meeren, P., Smagghe, G., Janssen, C.R., 2011. Aggregation and ecotoxicity of CeO_2 nanoparticles in synthetic and natural waters with variable pH, organic matter concentration and ionic strength. Environ. Pollut. 159, 970-976.

Verweij, W., Durand, A.M., Maas, J.L., van der Grinten, E., 2009. Chydotox toxicity test in toxicity measurements in concentrated water samples. RIVM report 607013011/2009. National Institute of Public Health and the Environment, Bilthoven, the Netherlands.

Wang, Y., Nowack, B., 2018. Environmental risk assessment of engineered nano-SiO_2, nano iron oxides, nano-CeO_2, nano-Al_2O_3, and quantum dots. Environ. Toxicol. Chem. 37, 1387-1395.

Wang, Z., Chen, J., Li, X., Shao, J., Peijnenburg, W.J.G.M., 2012. Aquatic toxicity of nanosilver colloids to different trophic organisms: Contributions of particles and free silver ion. Environ. Toxicol. Chem. 31, 2408-2413.

Yu, S., Liu, J., Yin, Y., Shen, M., 2018. Interactions between engineered nanoparticles and dissolved organic matter: A review on mechanisms and environmental effects. J. Environ. Sci. (China). 63, 198-217.

Supplementary Information

The classical DLVO calculation

Based on the classical DLVO theory (Cosgrove et al., 2005), the stability of a particle in solution is dependent upon the total potential energy of interaction between colloidal particles (V_T). V_T is the balance of two competing contributions:

$$V_T = V_A + V_R \tag{S1}$$

where V_A is the attractive potential energy; V_R stands for the repulsive potential energy. The V_A between two identical spherical particles can be written as:

$$V_A = -\frac{A}{12}\left[\frac{1}{x(x+2)} + \frac{1}{(x+1)^2} + 2\ln\frac{x(x+2)}{(x+1)^2}\right], x = \frac{h}{2r} \tag{S2}$$

where r is a particle radius; h is the distance of separation; A is the Hamaker constant. In this study, A was estimated as the geometric mean of the Hamaker constants of the particle (A_{CeO_2}) and of the medium (A_{water}) with respect to their values in vacuum, i.e.

$$A = (\sqrt{A_{CeO_2}} - \sqrt{A_{water}})^2 \tag{S3}$$

Where the values of A_{CeO_2} (5.56×10^{-20} J) (Song et al., 2011) and A_{water} (3.7×10^{-20} J) (Karimian and Babaluo, 2007) were adopted. The electrostatic repulsion is expressed as:

$$V_R = 2\pi\varepsilon r\zeta^2 \exp(-\kappa h) \tag{S4}$$

where ε is the dielectric constant for water (81 F/m); ζ represents the zeta potential; κ stands for the Debye constant. The value of κ for CeO$_2$NPs in the test media can be estimated by the expression:

$$\kappa = \sqrt{\frac{2e^2 \, \mathrm{N_A} \, I}{\varepsilon \varepsilon_0 \, \mathrm{K_B} \, T}} \tag{S5}$$

where e is the formal charge on an electron (1.60×10^{-19} C); $\mathrm{N_A}$ is Avogadro's constant (6.02×10^{23} mol^{-1}); I is the ionic strength of the test media (8.39 mM); ε_0 is the vacuum permittivity (8.85×10^{-12} C$^2 \cdot$N$^{-1} \cdot$m^{-2}); $\mathrm{K_B}$ is the Boltzman's constant (1.38×10^{-23} C$^2 \cdot$J$\cdot$K^{-1}); T is temperature (K).

Table S2.1 Developmental morphology and teratogenicity endpoints in the zebrafish (*Danio rerio*) test (*adopted from* Hermsen et al. (2011))

Toxicological endpoints
Morphology
Tail detachment
Formation of somite
Eye development
Spontaneous movement
Beating heart
Reductions in blood circulation or loss of circulation
Pigmentation head-body
Pigmentation tail
Pectoral fin
Protruding mouth
Teratogenicity
Pericardial oedema
Yolk sac oedema
Eye oedema
Head malformation
Absence/malformation of sacculi/otoliths
Malformation of tail
Malformation of heart
Modified chorda structure
Scoliosis
Rachischisis
Yolk deformation

References

Cosgrove, T. Colloid science: Principles, methods and applications. Blackwell Publishing Ltd, 2005.

Hermsen, S.A.B., van den Brandhof, E.-J., van der Ven, L.T.M., Piersma, A.H. Relative embryotoxicity of two classes of chemicals in a modified zebrafish embryotoxicity test and comparison with their *in vivo* potencies. Toxicol. In Vitro 2011, 25, 745-753.

Karimian, H., Babaluo, A.A. Halos mechanism in stabilizing of colloidal suspensions: Nanoparticle weight fraction and pH effects. J. Eur. Ceram. Soc. 2007, 27 (1), 19-25.

Song, J.E., Phenrat, T., Marinakos, S., Xiao, Y., Liu, J., Wiesner, M.R., Tilton, R.D., Lowry, G.V. Hydrophobic interactions increase attachment of gum Arabic- and PVP-coated Ag nanoparticles to hydrophobic surfaces. Environ. Sci. Technol. 2011, 45 (14), 5988-5995.

Chapter 3

Effects of natural organic matter on the joint toxicity and accumulation of Cu nanoparticles and ZnO nanoparticles in *Daphnia magna*

Qi Yu, Zhuang Wang, Guiyin Wang, Willie J. G. M. Peijnenburg, Martina G. Vijver

Abstract

Various modern products have metallic nanoparticles (MNPs) embedded to enhance products performance. Technological advances enable nowadays even multiple hybrid nanoparticles. Consequently, the future co-release of multiple MNPs will inevitably result in the presence of MNP mixtures in the environment. An important question is if the responses of mixtures of MNPs can be dealt with in a similar way as with the responses of biota to mixtures of metal salts. Moreover, natural organic matter (NOM) is an important parameter affecting the behavior and effect of MNPs. Herein, we determined the joint toxicity and accumulation of copper nanoparticles (CuNPs) and zinc oxide nanoparticles (ZnONPs) in *Daphnia magna* in the absence and presence of Suwannee River natural organic matter (SR-NOM), compared to the joint toxicity and accumulation of corresponding metal salts. The results of toxicity testing showed that the joint toxicity of CuNPs + ZnONPs was greater than the single toxicity of CuNPs or ZnONPs. The joint toxic action of CuNPs + ZnONPs was additive or more-than-additive for *D. magna*. A similar pattern was found in the toxicity of the mixtures of Cu- and Zn-salts from the literature data. The presence of SR-NOM had no significant impact on the joint toxicity of CuNPs + ZnONPs. The calculated component-specific contribution to overall toxicity indicated that SR-NOM increased the relative contribution of dissolved ions released from the MNPs to the toxicity of the binary mixtures at high-effect concentrations of individual MNPs. Moreover, dissolved Zn-ions released from the ZnONPs were found to dominate the joint toxicity of CuNPs + ZnONPs in the presence of SR-NOM. Furthermore, the results of the accumulation experiment displayed that the presence of SR-NOM significantly

enhanced the accumulation of either CuNPs or ZnONPs in *D. magna* exposed to the MNP mixtures.

3.1 Introduction

With the rapid progress in nanotechnology, various metallic nanoparticles (MNPs) are embedded in industrial and domestic products (Guinée et al., 2017; Mitrano et al., 2015). Nowadays, hybrid nanoparticles are constantly emerging to achieve multiple functionalities for single-component nanoparticles (Ma, 2019). Consequently, the potential co-release of multiple-component MNPs will inevitably bring out the presence of MNP mixtures in the environment. Nanotoxicological studies on multiple MNPs are gradually becoming a topic of interest. Current studies indicated that the toxic potential of multiple MNP mixtures is likely to be distinct from the summed toxicity of the individual MNPs. For instance, synergistic effects were found after exposure of *Escherichia coli* to a mixture of AgNPs + TiO$_2$NPs (Wilke et al., 2018), and for *Nitrosomonas europaea* after exposure to a mixture of CeO$_2$NPs + ZnONPs (Yu et al., 2016). On the other hand, some binary mixtures such as TiO$_2$NPs + CeO$_2$NPs (Yu et al., 2016), and AgNPs + CuONPs (Ogunsuyi et al., 2019) induced antagonistic toxicity to *N. europaea* and *Clarias gariepinus*, respectively.

Many MNPs undergo dissolution, namely the shedding of metal ions from MNPs, in an aqueous medium. Thus, particles (MNP$_{particle}$), dissolved ions released from MNPs (MNP$_{ion}$), or both MNP$_{particle}$ and MNP$_{ion}$, may contribute to the overall toxicity of MNPs (MNP$_{overall}$) (Wang et al., 2012; Cronholm et al., 2013; Adam et al., 2014; Xiao et al., 2015; Ye et al., 2018). It is also realized that the assessment of the ecotoxicological effects of mixtures of MNPs is more complicated because of the coexistence of different MNP$_{particle}$ and different MNP$_{ion}$

in suspensions. Given that total MNP_{ion} in the mixtures of MNPs contributes to the joint toxicity of multiple MNPs mainly, it is necessary to unravel if the responses of mixtures of MNPs can be dealt with in a similar way as with the responses of biota to mixtures of metal salts.

Natural organic matter (NOM) plays an important role in modulating the ecotoxicological effects of metals (Nogueira et al., 2017) and nanoparticles (Wang et al., 2011). Previous studies have shown that the addition of NOM reduced the toxicity of metals such as Cu and Zn to aquatic organisms, due to the complexation of metal ions with NOM and thereby decreasing the bioavailability of the metals (Hyne et al., 2005; Nadella et al., 2009; Clifford et al., 2009). Moreover, NOM is known to have a significant impact on the dissolution and toxicity of individual MNPs in the aquatic environment (Zhang et al., 2009; Wang et al., 2016; Sani-Kast et al., 2017; Sharma et al., 2019). The impacts of NOM on the toxicity of nanoparticles depend on several mechanisms, including altered electrostatic repulsion between nanoparticles and/or between nanoparticles and cells, scavenging of nanoparticles-induced reactive oxidative species, and the formation of complexes with MNPs-released ions (Deng et al., 2017). In addition, NOM can show different influences on the aquatic toxicity of MNPs with different types. For example, in the presence of NOM, the mitigation of the mortality of CuNPs on *Daphnia magna* occurred by reducing the contribution of dissolved Cu^{2+} to the toxicity of the suspension (Xiao et al., 2018). However, the addition of NOM stabilized ZnONP suspensions and did not decrease toxicity (Cupi et al., 2015). It is interesting to reveal whether there is an alteration of mixture toxicity due to the changes in bioavailability of MNPs when the amount of the ions versus particle fraction changed in the presence of NOM.

CuNPs and ZnONPs are not only widely applied in numerous products, but they are also reported to be toxic to a wide range of aquatic organisms (Bondarenko et al., 2013; Xiao et al., 2015; Ho et al., 2018). The objectives of the present study are to: (1) determine the joint toxicity of binary mixtures of CuNPs and ZnONPs to the zooplankton species *Daphnia magna*; (2) evaluate the contribution of each mixture constituent to the overall toxicity of the binary mixtures; (3) elucidate the differences in toxicity and accumulation between mixed metal-salt exposures and mixed MNP exposures; (4) use a surrogate for NOM which provides binding sites to modulate the fate, toxicity, contribution to toxicity of the individual constituents present in the mixture, and metal accumulation following exposure to binary MNP mixtures. Our starting hypothesis is that the toxicity and accumulation are associated with the dissolved fraction of the MNPs, as dependent on the type of MNPs, the number of nanoparticle constituents (individual or multiple MNPs), and the properties of the exposure medium such as in the presence of NOM.

3.2 Materials and Method

3.2.1 Test materials

CuNPs (reported specific surface area of 30-50 m^2/g; purity > 99.5%) and ZnONPs (reported specific surface area of 19 ± 5 m^2/g; purity > 99.5%) purchased from IoLiTecGmbh (Heibronn, Germany) and Plasmachem GmbH (Berlin, Germany) were selected in this study. The two MNPs have the same primary size of 25 nm and they are both spherically shaped. $Cu(NO_3)_2$ and $Zn(NO_3)_2$ obtained from Sigma-Aldrich (Zwijndrecht, The Netherlands) were used as reference materials, which have previously been reported to be an effective

approach of assessing the impacts of dissolved ions released from MNPs (Xiao et al., 2015). Suwannee River NOM (SR-NOM, 2R101N) as the surrogate for NOM was supplied by the International Humic Substances Society (IHSS). The selected SR-NOM was acquired from filtered river water, which was concentrated using two portable reverse osmosis systems (Green et al., 2015). The preparation procedures of the MNP and SR-NOM stocks are described in the Supplementary data.

3.2.2 Physicochemical characterizations

The morphology, size distribution (Z-average hydrodynamic diameter), and zeta-potential of MNPs in suspensions were determined to characterize their physicochemical properties in the test medium. Details for all of these characterizations are given in the Supplementary data. The actual concentrations of Zn- and Cu-ions released from ZnONPs, CuNPs, $Cu(NO_3)_2$, and $Zn(NO_3)_2$ were measured using Atomic Absorption Spectroscopy (AAS; Perkin Elmer 1100B).

For modeling dissolved Cu and Zn speciation, a geochemical code, Visual MINTEQ (version 3.1) (Gustafsson, 2013) was used. The NICA-Donnan model was applied for describing the binding of metals to humic substances (Minteq and Agency, 2000). The NICA-Donnan model uses a bimodal, continuous distribution of affinities for protons and metal ions (Unsworth et al., 2006). This model has been successfully used for evaluating Cu and Zn complexation to dissolved organic matter in a previous study (Baker et al., 2012). The modeling of metal ions, metal-inorganic complexes, and NOM-bound complexes (Metal-NOM complexes) could be performed at the same time. Hence, a direct comparison of each species of dissolved ions in the suspensions was possible.

3.2.3 Experimental outline

Figure 3.1 depicts the outline of toxicity and accumulation testing. The cultures (Supplementary data) and 48 h acute toxicity assays with *D. magna* were performed following the OECD Guideline 202 (OECD, 2004).

3.2.3.1 Single and joint toxicity tests

Neonates (< 24 h) were used in the test after cleaning their guts for around 2 h in ElendtM7 medium. Ten individuals were randomly placed in each beaker, containing either 100 mL of a suspension of the MNPs or a control. Daphnids were exposed to increasing initial concentrations of CuNPs (ranging from 0.01 to 7 mg L^{-1}), ZnONPs (from 0.5 to 100 mg L^{-1}), $Cu(NO_3)_2$ (from 0.1 to 0.88 mg L^{-1}), and $Zn(NO_3)_2$ (from 1 to 8 mg L^{-1}). Three replicates were included for each treatment. Each acute toxicity test was repeated with different batches of *D. magna* at three different times and the data presented are the mean of the runs ($n = 3$). The tests were maintained under a 16:8 h light/dark photoperiod (22 ± 1 °C) without feeding during the 48 h exposure period. The actual exposure concentrations of particles and ions in each treatment were measured by AAS after incubation in the test medium without daphnids. The detailed sampling procedures for the determination of the actual exposure concentrations of particles and ions were described in the Supplementary data.

The concentration–response curves (CRCs) were constructed via GraphPad Prism 8.0 for each of the single toxicants (CuNPs, ZnONPs, Cu^{2+}, and Zn^{2+}). From the CRCs, the estimated LC_{10} and LC_{50}

(concentrations at which 10% and 50% of mortality of test species are observed) of CuNPs and ZnONPs were selected as exposure concentrations used in tests for single and mixture toxicity in the presence of SR-NOM (1, 10 and 20 mg L^{-1}). The LC_{10} and LC_{50} values of each MNP were employed to give the fixed concentration ratios that were used in the toxicity tests performed on the binary mixtures of CuNPs and ZnONPs.
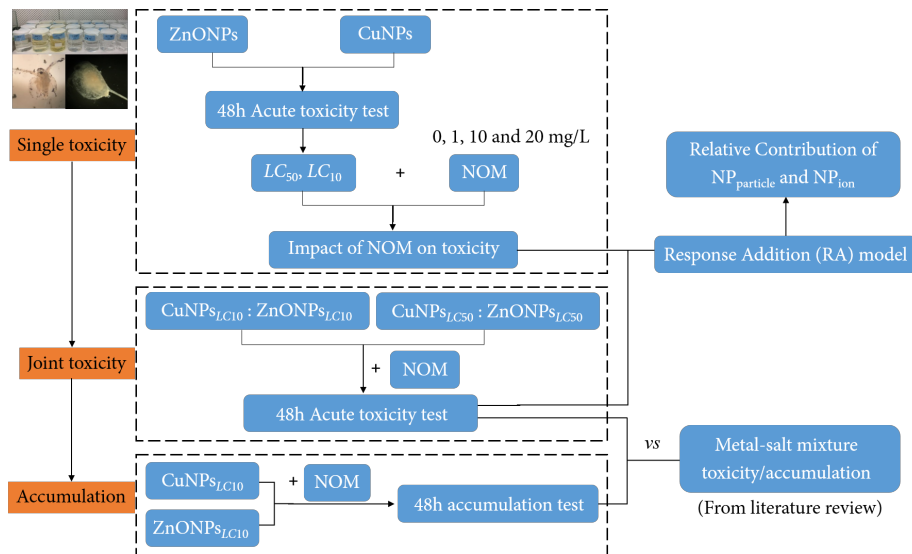

Figure 3.1. Scheme of the experimental outline.

3.2.3.2 Relative contributions to toxicity of MNP$_{particle}$ and MNP$_{ion}$

It is widely believed that the modes of actions of MNP$_{particle}$ and MNP$_{ion}$ are likely to be independent (Xiao et al., 2015; Liu et al., 2016), which is in line with the assumption of the response addition (RA) model (Bliss, 1939). Thus, the RA model is selected as a simplified way of estimating the toxicity of MNP$_{particle}$ from the experimentally

determined overall toxicity of MNP suspensions (MNP$_{overall}$) to evaluate the relative contribution of MNP$_{particle}$ and MNP$_{ion}$ to toxicity (Xiao et al., 2015; Wu et al., 2020). The RA model is defined as follows:

$$E_{overall} = 1 - (1 - E_{ion})(1 - E_{particle}) \qquad (1)$$

where $E_{overall}$ and E_{ion} represent the toxic effects caused by the MNP suspensions and their corresponding released ions (scaled from 0 to 1), respectively. $E_{overall}$ was quantified by the mixture toxicity testing. The combined effect (E_{ion}) of the two dissolved ions released from the MNPs present in the binary MNP mixtures was calculated as follows:

$$E_{ion(Cu^{2+}+Zn^{2+})} = 1 - (1 - E_{Cu^{2+}})(1 - E_{Zn^{2+}}) \qquad (2)$$

Then, the effects caused by the particles ($E_{particle}$) were directly calculated by the RA model.

3.2.3.3 Accumulation tests

The accumulation profile of the MNPs by *D. magna* was measured through a 48 h accumulation test. Following the acute toxicity test, the concentrations of CuNPs and ZnONPs used in the accumulation experiments were the actual particle concentrations of MNPs at the LC_{10} level for the exposure to both single and binary MNPs. For the accumulation test, the exposure time and all other conditions were the same as in the toxicity test. The pre-treatment of daphnid accumulation was based on the procedure described by Bossuyt and Janssen (2005) with slight modification. Briefly, after the 48 h exposure period, healthy *D. magna* (150-200 daphnids for each replicate) were selected and transferred to 5% EDTA solution for around 15 mins. They were then washed two times with 5% EDTA and then two times with fresh Milli-Q water to remove the absorbed

particles and ions upon the surface of the daphnids. After absorbing the water left behind on the organisms using tissue paper, the animals were dried at 80 °C overnight in pre-weighed glass containers before weighing on a microbalance and then digested in 65% HNO_3 at 80 °C overnight. The Cu and Zn concentrations in the digested samples were subsequently determined by AAS. The statistical analyses were listed in the Supplementary data.

3.3 Results and discussion

3.3.1 Characterization of CuNPs and ZnONPs in the absence and presence of SR-NOM

The morphology of the CuNPs and ZnONPs in the single and binary mixtures and the impact of SR-NOM in the test medium are presented in Figure S3.1 (Supplementary data). Analysis of the TEM images indicates that the CuNPs (Figure S3.1A) or ZnONPs (Figure S3.1B) agglomerated intensely and formed irregular shapes in the test medium. However, in the presence of SR-NOM, the CuNPs (Figure S3.1D) or ZnONPs (Figure S3.1E) showed a greater tendency to disagglomerate. In addition, the CuNPs or ZnONPs co-agglomerated regardless of the absence (Figure S3.1C) or presence (Figure S3.1F) of SR-NOM.

The hydrodynamic diameter (D_H in nm) and zeta potential (ZP in mV) of CuNPs and ZnONPs and their binary mixtures in the absence and presence of 1, 10, and 20 mg L^{-1} SR-NOM in the test medium are depicted in Figure 3.2 and Figure S3.2 (Supplementary data). After 48 h of exposure, the degree of agglomeration of individual and binary mixtures of CuNPs and ZnONPs in the absence of SR-NOM increased

in the order of CuNPs > ZnONPs ≈ mixture of CuNPs and ZnONPs (Figure 3.2A). For the individual CuNPs and ZnONPs, the addition of SR-NOM reduced the extent of agglomeration remarkably, corresponding to the results shown in the TEM images (Figs. S1D and S1E). The inhibition of agglomeration implied that SR-NOM stabilized the individual MNPs, which facilitated their dispersion. The stabilization effect arising from SR-NOM depended upon the exposure concentration of SR-NOM. The co-agglomeration behavior of the binary mixtures was significantly modified only after adding 20 mg L^{-1} SR-NOM. Meanwhile, no significant change in the ZP values of MNPs was observed in the absence and presence of SR-NOM. The only exception was the case of 20 mg L^{-1} SR-NOM as this concentration of SR-NOM reduced the absolute ZP value of CuNPs over 48 h of incubation (Figure 3.2B), which might be due to the reduction of electrical double layer repulsion between particles.
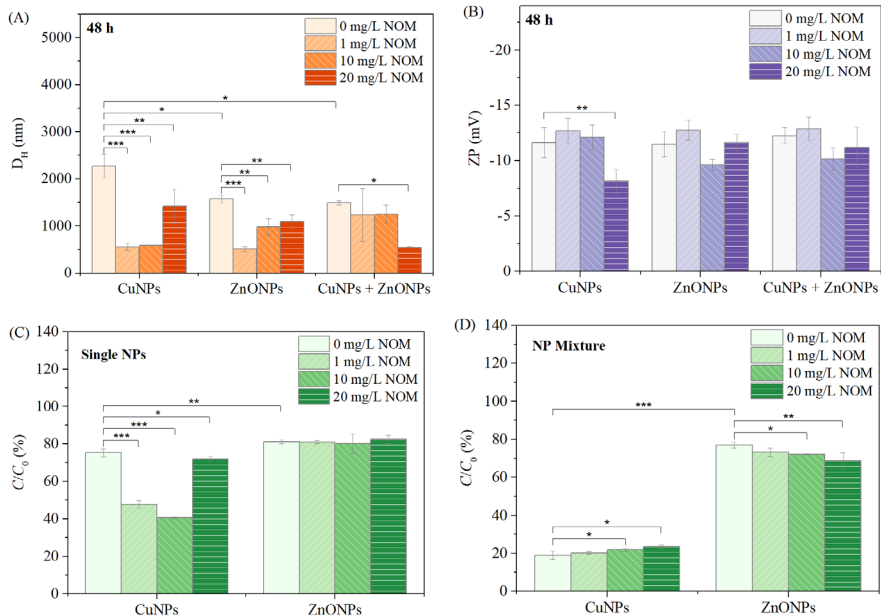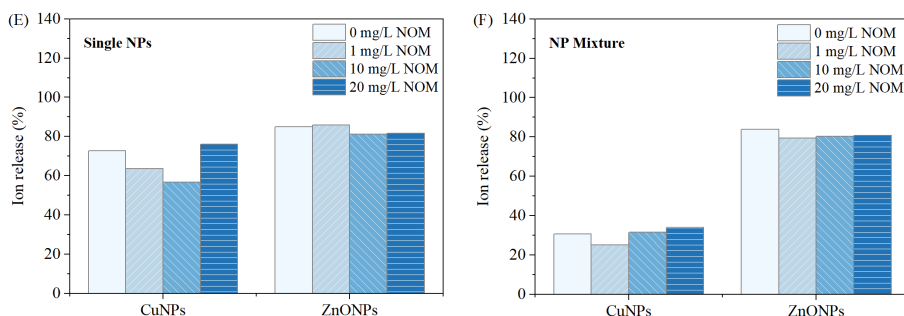
Figure 3.2. Variation in D_{H} (A) and ZP (B) of CuNPs and ZnONPs and their binary mixtures in the absence and presence of SR-NOM after 48 hours of exposure; ratios (%) of actual concentrations (C) of CuNPs and ZnONPs (based on total metal) at 48 h (C) and of their mixture (D) to initial exposure concentrations (C_{o}) of the nanoparticle suspensions in the test medium; the ion release (%, based on C_{TWA}, the average value expressed as a single value calculated based on concentrations at 0, 24 and 48h) released from CuNPs and ZnONPs (E) and from the binary mixture (F). Values shown in A-D are expressed as mean ± standard deviation (n=3). *$p < 0.05$, **$p < 0.01$, and ***$p < 0.001$ indicating significant differences between the treatments.

The sedimentation of the particles was evaluated by relating the actual concentrations (C) of the MNPs (based on total metal) after 48h of exposure in the suspensions to the initial concentrations (C_{o}) of the MNP suspensions. According to Figure 3.2C, the actual concentrations of CuNPs and ZnONPs decreased by around 20-25% after 48 h of settling in the absence of SR-NOM. Upon the addition of 1 and 10 mg L^{-1} SR-NOM, the actual concentration of CuNPs dropped by 28-35% in the test medium due to the sedimentation of particles. This is in good agreement with the change of D_{H} values of CuNPs as aforementioned, suggesting that the reduction of aggregation of CuNPs by SR-NOM (1

and 10 mg L^{-1}) was mainly caused by the increased sedimentation of the particles. The actual concentration of ZnONPs after 48 h of incubation in the absence and presence of SR-NOM did not differ significantly, irrespective of the concentration of SR-NOM. In the binary system, the actual concentration of CuNPs after 48 h of exposure in the mixture suspensions dropped dramatically by 54% compared to the concentration of the individual CuNPs suspension, while the actual concentration of ZnONPs after 48 h settling did not change significantly when comparing the concentrations of single MNPs and mixtures.

The profiles of ion release shedded from the individual and binary MNPs in the absence and presence of SR-NOM are shown in Figure 3.2E and Figure 3.2F, where it is expressed based on the concentration of the time-weighted average C_{TWA}. The high percentage (>70%) of dissolved ions in the individual MNPs suspensions demonstrated that ions from both CuNPs and ZnONPs to a high degree dissolved (Figure 3.2E). The concentration of Zn-ions was not influenced by the addition of SR-NOM, and the concentration of Cu-ions only decreased by about 9 and 16% when 1 and 10 mg L^{-1} SR-NOM were added into the suspensions, respectively. The dissolution of ZnONPs in the mixture suspensions was similar to the dissolution in the individual exposure system, as shown in Figure 3.2F. However, the ion release of CuNPs shifted from 73% to 31% when they were incubated in the mixture suspensions. The presence of SR-NOM only slightly influenced the degree of dissolution of both CuNPs and ZnONPs in the mixtures. In addition, the prediction of the SR-NOM-dependent speciation as obtained using Visual MINTEQ 3.1 is shown in Figure S3.5. It is found that the ratio of ions (Cu^{2+} and Zn^{2+}) to the total dissolved metal (Cu and Zn) hugely decreased in the presence of SR-NOM in both

individual MNP suspensions and mixture suspensions. Note that the Cu-NOM complex accounted for almost all of the dissolved Cu-ions with the addition of any concentration of SR-NOM, confirming that Cu^{2+} was easily bound to SR-NOM through weak electrostatically binding and chemical complexation, as previously suggested (Field et al., 2014). The ratio of the concentration of Zn^{2+} to the concentration of total dissolved Zn-ions shifted from 84% to 67% after adding 1 mg L^{-1} SR-NOM and to 0% after adding 10 and 20 mg L^{-1} SR-NOM, respectively. Similar interactions between SR-NOM and dissolved ions were observed in the mixture suspensions.

3.3.2 Single and joint acute toxicity of CuNPs and ZnONPs to *D. magna* in the absence and presence of SR-NOM

3.3.2.1 Single and joint toxic effects

CRCs of CuNPs, ZnONPs, $Cu(NO_3)_2$, and $Zn(NO_3)_2$ are presented in Figure S3.3. The LC_{50} and LC_{10} values of single compounds calculated from the CRCs are provided in Table 3.1. Based on the LC_{50} and LC_{10} values, the toxicity decreased in the order of $Cu(NO_3)_2$ > CuNPs > $Zn(NO_3)_2$ > ZnONPs. Xiao et al. (2015) also found that the acute toxicity of CuNPs was greater than that of ZnONPs. Furthermore, *D. magna* was more sensitive to metal ions than to the corresponding MNPs, with Cu^{2+} being the most toxic to daphnids. The difference in the sensitivity of *D. magna* to Cu/Zn-ions and Cu/ZnNPs was also observed by Xiao et al. (2015).

Table 3.1 Lethal concentrations (mgCu L^{-1} or mgZn L^{-1}) of suspensions of Cu and Zn NPs, and of solutions of $Cu(NO_3)_2$ and $Zn(NO_3)_2$ towards *D. magna*, expressed based on time-weighted average concentrations of Cu and Zn after 48 h of exposure.

Test materials	LC_{50} (95% confidence limits)	LC_{10} (95% confidence limits)
CuNPs	0.40 (0.26 – 0.57)	0.11 (0.02 – 0.22)
$Cu(NO_3)_2$	0.04 (0.03 – 0.06)	0.02 (0.01 – 0.03)
ZnONPs	4.01 (2.90 – 54.35)	1.29 (0.12 – 2.61)
$Zn(NO_3)_2$	0.75 (0.58 – 0.96)	0.27 (0.17 – 0.41)

In the presence of SR-NOM, a significant reduction in the mortality of *D. magna* exposed to CuNPs was observed (Figure 3.3A). It is obvious that different concentrations of SR-NOM significantly reduced the mortality of CuNPs to a similar degree. Xiao et al. (2018) also found that the toxicity of CuNPs to *D. magna* decreased with increasing the concentrations of humic acid. The decrease in toxicity for CuNPs with the addition of SR-NOM may be due to the complexation of released ions with NOM and the passivation of the particle surface by NOM adsorption (Fabrega et al., 2009). Noteworthy, the opposite, hence, an increase in the mortality of daphnids exposed to ZnONPs (Figure 3.3B) was observed. These results are in line with Cupi et al. (2015) who found a similar effect of SR-NOM on the toxicity towards daphnids, namely that the presence of SR-NOM significantly enhanced the toxicity (in terms of 48h-EC_{50} values) of ZnONPs test suspensions prepared from nanoparticle Stock I to *D. magna*. The enhancement of the toxicity might be explained by the fact that the stabilization of the ZnONP suspensions in the presence of SR-NOM is significant.

Organisms can take in stabilized nanoparticles in the aqueous medium, and the bioaccumulation/biological effects are likely enhanced (Deng et al., 2017).

As can be seen in Figure S3.4, the mortality of the binary mixtures of CuNPs and ZnONPs at the LC_{10} and LC_{50} ratios was 45% and 98%, respectively. This means that the co-exposure of CuNPs and ZnONPs exerted more-than-additive or additive toxic effects on *D. magna*. To investigate the differences in the modes of joint toxic action between the co-exposure of CuNPs and ZnONPs and their corresponding metal-ion counterparts, we summarized literature data on the joint toxicity of Cu- and Zn-salts to freshwater organisms in Table S3.1. As shown in Table S3.1, additive or more-than-additive effects on *D. magna* were found in most studies on the joint toxicity of Cu- and Zn-salts (Komjarova and Blust, 2008; Cooper et al., 2009; Meyer et al., 2015; Lari et al., 2017). This indicated that the two studied MNPs in the mixtures interacted in a manner similar to their corresponding metal salts.

The impact of SR-NOM on the mortality of the binary mixtures of CuNPs and ZnONPs at the LC_{10} and LC_{50} ratios is presented in Figure 3.3C. Generally, no significant impact ($p < 0.05$) on the joint toxicity of CuNPs and ZnONPs was found in the presence of SR-NOM, regardless of the mixture ratios and the SR-NOM concentration.
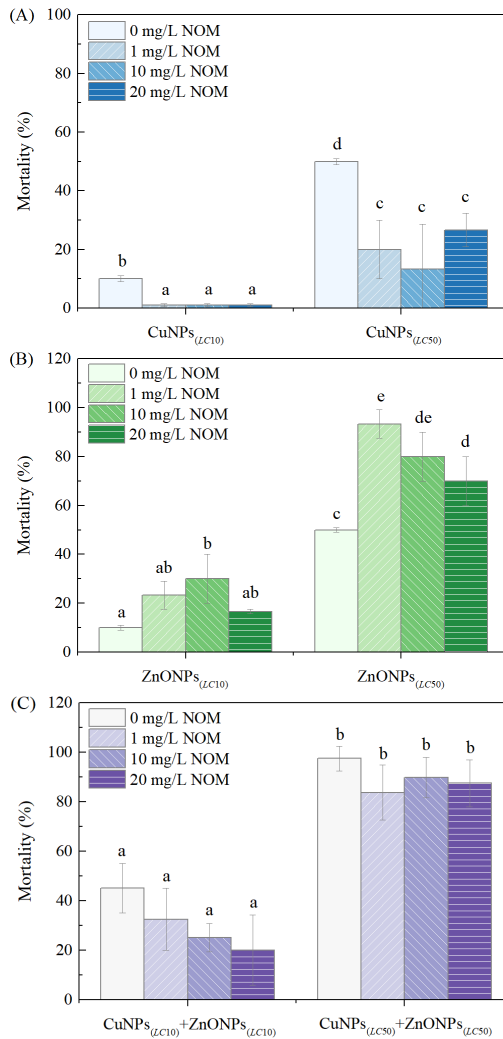
Figure 3.3. Mortality (%) of *D. magna* exposed to individual CuNPs (A) and ZnONPs (B) in the presence of 0, 1, 10, and 20 mg L^{-1} SR-NOM; and the impact of SR-NOM (0, 1, 10 and 20 mg L^{-1}) on mixture toxicity of CuNPs and ZnONPs, based on the LC_{10} and LC_{50} ratios (C) at their individual LC_{10} and LC_{50} concentration. Values are expressed as mean ± standard deviation (*n*=3). Letters indicate statistically significant (*p* < 0.05) differences between the treatments.

3.3.2.2 Relative contribution of MNP_{ion} and $MNP_{particle}$ to overall toxicity

Figure 3.4 depicts the relative contribution of MNP_{ion} and $MNP_{particle}$ to the overall toxicity of the individual and binary mixtures of CuNPs and ZnONPs. As shown in Figure 3.4A, $CuNPs_{particle}$ and $CuNPs_{ion}$ accounted for 82% and 18% of the toxicity of $CuNPs_{overall}$ at the LC_{50} level, respectively, while $CuNPs_{particle}$ and $CuNPs_{ion}$ accounted for 0% and 100% of the toxicity of $CuNPs_{overall}$ at the LC_{10} level. The high contribution of dissolved Cu-ions to the toxicity of $CuNPs_{overall}$ at the LC_{10} level is due to the relative high ion release as mentioned above. Note that in the presence of SR-NOM no data were obtained for the relative contribution of $CuNPs_{particle}$ and $CuNPs_{ion}$ to the toxicity of $CuNPs_{overall}$ at the LC_{10} level, which is due to the fact that no mortality was observed for the $CuNPs_{overall}$ in the presence of SR-NOM (Figure 3.4A). Upon the addition of SR-NOM, the relative contribution of $CuNPs_{ion}$ to the toxicity of $CuNPs_{overall}$ at the LC_{50} level decreased owing to the reduction of dissolved Cu^{2+}-concentrations by SR-NOM. As shown in Figure 3.4B, $ZnONPs_{ion}$ accounted for 100% of the relative contribution to the toxicity of $ZnONPs_{overall}$ in the absence of SR-NOM, implying that the single toxicity of ZnONPs was to be fully ascribed to the dissolved Zn-ions. In contrast, some previous studies found that the particles of ZnONPs were the main source of toxicity (Xiao et al., 2015; Ye et al., 2018). This difference might be explained by a difference in dissolution rates due to the studied MNPs' characteristics and the exposure conditions (Lopes et al., 2014). It was found that SR-NOM had no impact on the relative contribution of $ZnONPs_{ion}$ to the toxicity of $ZnONPs_{overall}$ at the LC_{10} level, whereas SR-NOM had different impacts on the relative contribution of $ZnONPs_{ion}$ to the

toxicity of $ZnONPs_{overall}$ at the LC_{50} level. Generally, decreasing the concentration of SR-NOM increased the relative contribution of $ZnONPs_{particle}$ to the toxicity of $ZnONPs_{overall}$ at the LC_{50} level.

Figure 3.4C presents the relative contribution of MNP_{ion} and $MNP_{particle}$ to the toxicity of the binary mixtures of CuNPs and ZnONPs at the LC_{10} and LC_{50} ratios to *D. magna* in the absence and presence of SR-NOM. The contribution of MNP_{ion} to the joint toxicity of the binary mixtures at the LC_{10} ratio was 100%, irrespective of whether SR-NOM was present. This implies that dissolved ions play an absolute role in the joint toxicity of CuNPs + ZnONPs, which can be regarded as a mixture of Cu^{2+} and Zn^{2+}. For the toxicity of the binary mixtures at the LC_{50} ratio, the relative contribution of MNP_{ion} (47%) to the joint toxicity of the binary mixtures was lower than that of $MNP_{particle}$ (53%). However, a contribution of MNP_{ion} of more than 50% was observed in the presence of SR-NOM, implying that the contribution of dissolved ions to the joint toxicity of the binary mixtures was enhanced by SR-NOM.
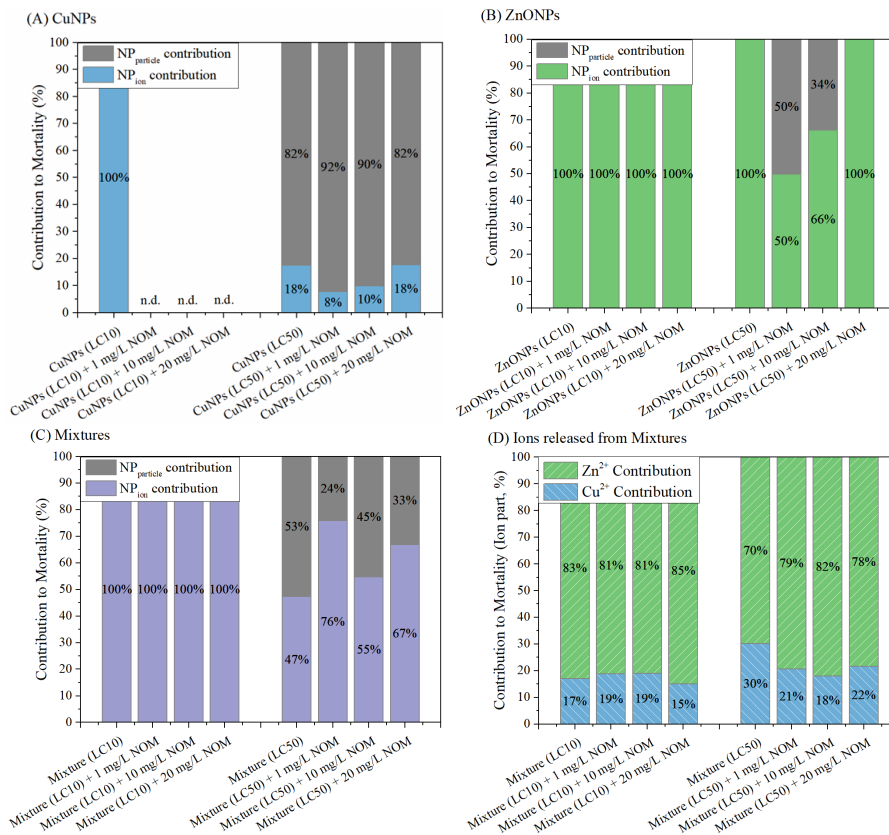
Figure 3.4. Relative contribution to toxicity of $MNP_{particle}$ and MNP_{ion} of the individual CuNPs (A) and ZnONPs (B), and the binary mixtures (C) at the LC_{10} and LC_{50} ratios in the absence and presence of 1, 10 and 20 mg L^{-1} SR-NOM. (D) depicts the relative contribution of Cu-ions and Zn-ions released from the MNPs to the toxicity caused by the total dissolved ions. n.d. = not determined.

The specific contribution of Cu-ions and Zn-ions to the toxicity induced by total dissolved ions was further separated, as shown in Figure 3.4D. Generally, the contribution of Zn-ions to the overall toxicity induced by MNP_{ion} in the binary mixtures in the absence and presence of SR-NOM was markedly greater than Cu-ions. This means

that Zn-ions dictated the toxicity of MNP_{ion} in the binary mixtures no matter whether SR-NOM was present or absent. It can be concluded that the concentration of SR-NOM used was inadequate to counteract the impacts of ions on the overall toxicity of the binary mixtures of CuNPs and ZnONPs.

3.3.3 Single and joint accumulation of CuNPs and ZnONPs in *D. magna* in the absence and presence of SR-NOM

The accumulation of MNPs (based on ingested and internalized metal) in *D. magna* exposed to the individual CuNPs and ZnONPs and the binary mixtures at the LC_{10} ratio in the absence and presence of 20 mg L^{-1} SR-NOM is shown in Figure 3.5. After 48 h of exposure, the amounts of Cu and Zn accumulated in the daphnids were 0.79 ± 0.04 and 1.09 ± 0.01 mg g^{-1} dry weight for CuNPs and ZnONPs, respectively. It is obvious that the total Zn accumulation was higher than the total Cu accumulation. This is consistent with the experimental results of Xiao et al. (2015).

The accumulated amount of Zn in the binary mixtures of CuNPs and ZnONPs increased by a factor of 2.5 compared to the accumulated amount of Zn in the individual ZnONPs, as shown in Figure 3.5. A similar phenomenon in which the accumulated amount of Zn increased in the presence of Cu was also found for the case of exposure of daphnids to Cu- and Zn-salts (Komjarova and Blust, 2008). This also means that CuNPs and ZnONPs acted in an interaction mode similar to Cu-salts and Zn-salts. However, there is no significant change in the amounts of CuNPs (in terms of total Cu) accumulated in daphnids after the addition of ZnONPs.
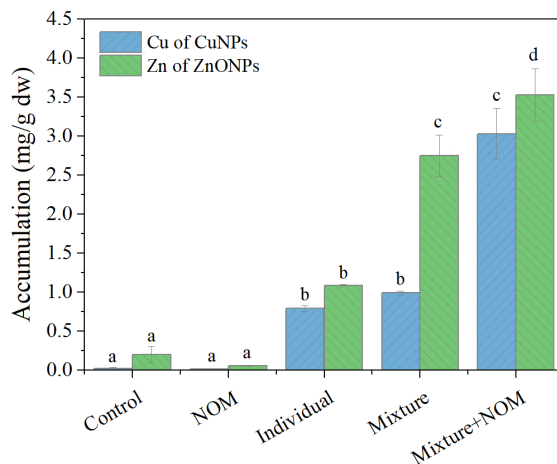
Figure 3.5. Accumulation (mg g^{-1} dry weight) of total Cu and Zn in *D. magna* after 48 h exposed to the single and binary mixtures of CuNPs and ZnONPs in the presence of 20 mg L^{-1} SR-NOM. Values are expressed as mean ± standard deviation (n=3). Different letters indicate significant differences between the treatments for the accumulation of the same elementary ($p < 0.05$).

The amounts of Cu and Zn in the binary mixtures of CuNPs and ZnONPs accumulated in *D. magna* were 3.1 and 1.3 times higher in the presence of SR-NOM than when SR-NOM was not present. This means that the addition of SR-NOM increased the accumulation of the MNPs. In particular, in the presence of SR-NOM the accumulation of Cu increased more obviously. NOM was previously shown to reduce metal bioavailability via chelating and sequestering metal cations (Gheorghiu et al., 2010; Al-Reasi et al., 2011; DePalma et al., 2011; Nogueira et al., 2017; Qiao et al., 2019). Nevertheless, it cannot be excluded that metal ions bound with NOM are available accumulation by aquatic organisms (Wang et al., 2016), especially for *D. magna* which can ingest suspended and sediment particles smaller than the reported size limit

of 70 µm (Geller and Müller, 1981; Tervonen et al., 2010; Lee and Ranville, 2012). The maximum size of detected metal-NOM complexes and agglomerates of MNP mixtures was smaller than 2 µm in this work, hence the complexes, agglomerates, or their sediments, could be taken up by *D. magna*. Moreover, similar results suggested that some organisms could provide indirect routes for the uptake of Cu-NOM complexes (Lorenzo et al., 2005), or some active biological processes in organisms could counteract the chelation of Cu by NOM (Lores et al., 1999), thus increasing the accumulation of Cu in presence of NOM. Consequently, an analogous mechanism might be responsible for the enhancement of accumulation of either Cu or Zn in the binary mixtures of CuNPs and ZnONPs when NOM was present. In addition, the increase in bioavailability and accumulation of mixed MNPs in the presence of SR-NOM are in good agreement with a deduction that the competition of Cu-Zn binding with NOM will enhance the accumulation of Cu or Zn ions (Meyer et al., 2015; Crémazy et al., 2019).

3.4 Conclusions

The joint toxicity effects of CuNPs and ZnONPs were determined to be additive or more-than-additive in *D. magna*, which is similar to the joint toxicity effects of Cu- and Zn-ions reported in the literature. SR-NOM had no significant impact on the apparent toxicity of the binary mixtures of CuNPs and ZnONPs. However, the addition of SR-NOM increased the relative contribution of total dissolved ions released from the MNPs compared to the particles to the toxicity of the binary mixtures at high-effect concentrations of individual MNPs. Moreover, the Zn-ions released from the ZnONPs had a dominant role in the

binary mixtures of CuNPs and ZnONPs as a result of the agglomeration and sedimentation of CuNPs and the complexation of the CuNPs released Cu-ions with SR-NOM. Furthermore, SR-NOM remarkably enhanced the bioaccumulation of both Cu and Zn in the binary mixtures of CuNPs and ZnONPs. Overall the results corroborate the importance of natural environmental factors in determining the ecotoxicity of multiple MNPs in the aquatic environment.

References

Adam, N.; Schmitt, C.; Galceran, J.; Companys, E.; Vakurov, A.; Wallace, R.; Knapen, D.; Blust, R. The chronic toxicity of ZnO nanoparticles and ZnCl$_2$ to *Daphnia magna* and the use of different methods to assess nanoparticle aggregation and dissolution. Nanotoxicology 2014, 8, 709-717.

Al-Reasi, H. A.; Wood, C. M.; Smith, D. S. Physicochemical and spectroscopic properties of natural organic matter (NOM) from various sources and implications for ameliorative effects on metal toxicity to aquatic biota. Aquat. Toxicol. 2011, 179-190.

Baker, B. J. Investigation of the competitive effects of copper and zinc on fulvic acid complexation: Modeling analytical approaches, Colorado School of Mines, 2012.

Bliss, C. I. The toxicity of poisons applied jointly. Ann. Appl. Biol. 1939, 26, 585-615.

Bondarenko, O.; Juganson, K.; Ivask, A.; Kasemets, K.; Mortimer, M.; Kahru, A. Toxicity of Ag, CuO and ZnO nanoparticles to selected environmentally relevant test organisms and mammalian cells *in vitro*: A critical review. Arch. Toxicol. 2013, 1181-1200.

Bossuyt, B. T.; Janssen, C. R. Copper regulation and homeostasis of *Daphnia magna* and *Pseudokirchneriella subcapitata*: Influence of acclimation. Environ. Pollut. 2005, 136: 135-144.

Clifford, M.; McGeer, J. C. Development of a biotic ligand model for the acute toxicity of zinc to *Daphnia pulex* in soft waters. Aquat. Toxicol. 2009, 91, 26-32.

Cooper, N. L.; Bidwell, J. R.; Kumar, A. Toxicity of copper, lead, and zinc mixtures to *Ceriodaphnia dubia* and *Daphnia carinata*. Ecotoxicol. Environ. Saf. 2009, 72, 1523-1528.

Crémazy, A.; Brix, K. V.; Wood, C. M. Using the biotic ligand model framework to investigate binary metal interactions on the uptake of Ag, Cd, Cu, Ni, Pb and Zn in the freshwater snail *Lymnaea Stagnalis*. Sci. Total Environ. 2019, 647, 1611-1625.

Cronholm, P.; Karlsson, H.L.; Hedberg, J.; Lowe, T.A.; Winnberg, L.; Elihn, K.; Wallinder, I.O.; Möller, L. Intracellular uptake and toxicity of Ag and CuO nanoparticles: a comparison between nanoparticles and their corresponding metal ions. Small. 2013, 9: 970-982.

Cupi, D.; Hartmann, N. B.; Baun, A. The influence of natural organic matter and aging on suspension stability in guideline toxicity testing of silver, zinc oxide, and titanium dioxide nanoparticles with *Daphnia magna*. Environ. Toxicol. Chem. 2015, 34, 497-506.

Deng, R.; Lin, D.; Zhu, L.; Majumdar, S.; White, J. C.; Gardea-Torresdey, J. L.; Xing, B. Nanoparticle interactions with co-existing contaminants: Joint toxicity, bioaccumulation and risk. Nanotoxicology. 2017, 11, 591-612.

DePalma, S. G. S.; Ray Arnold, W.; McGeer, J. C.; George Dixon, D.; Scott Smith, D. Effects of dissolved organic matter and reduced sulphur on copper bioavailability in coastal marine environments. Ecotoxicol. Environ. Saf. 2011, 74, 230-237.

Fabrega, J.; Fawcett, S. R.; Renshaw, J. C.; Lead, J. R. Silver nanoparticle impact on bacterial growth: effect of pH, concentration, and organic matter. Environ. Sci. Technol. 2009, 43, 7285-7290.

Field, S.; Sea, S. W. B. Stabilization of Metals and Shooting Range Soils - the Metalloids in Contaminated Effect of Iron-Based Amendments, University of Oslo, 2014.

Geller, W.; Müller, H. The filtration apparatus of cladocera: Filter mesh-sizes and their implications on food selectivity. Oecologia 1981, 49, 316-321.

Gheorghiu, C.; Smith, D. S.; Al-Reasi, H. A.; McGeer, J. C.; Wilkie, M. P. Influence of natural organic matter (NOM) quality on Cu-gill binding in the rainbow trout (*Oncorhynchus mykiss*). Aquat. Toxicol. 2010, 97, 343-352.

Green, N. W.; Mcinnis, D.; Hertkorn, N.; Maurice, P. A.; Perdue, E. M. Suwannee River Natural Organic Matter: Isolation of the 2R101N Reference Sample by Reverse Osmosis.

Guinée, J. B.; Heijungs, R.; Vijver, M. G.; Peijnenburg, W. J. G. M. Setting the stage for debating the roles of risk assessment and life-cycle assessment of engineered nanomaterials. Nat. Nanotechnol. 2017, 12, 727-733.

Gustafsson, J. P. Visual MINTEQ 3.1. https://vminteq.lwr.kth.se/: KTH, Sweden.

Ho, K. T.; Portis, L.; Chariton, A. A.; Pelletier, M.; Cantwell, M.; Katz, D.; Cashman, M.; Parks, A.; Baguley, J. G.; Conrad-Forrest, N.;

Boothman, W.; Luxton, T.; Simpson, S. L.; Fogg, S.; Burgess, R. M. Effects of micronized and nano-copper azole on marine benthic communities. Environ. Toxicol. Chem. 2018, 37, 362-375.

Hyne, R. V.; Pablo, F.; Julli, M.; Markich, S. J. Influence of water chemistry on the acute toxicity of copper and zinc to the cladoceran *Ceriodaphnia cf dubia*. Environ. Toxicol. Chem. 2005, 24, 1667-1675.

Liu, Y.; Baas, J.; Peijnenburg, W. J. G. M.; Vijver, M. G. Evaluating the combined toxicity of Cu and ZnO nanoparticles: Utility of the concept of additivity and a nested experimental design. Environ. Sci. Technol. 2016, 50, 5328-5337.

Komjarova, I.; Blust, R. Multi-metal interactions between Cd, Cu, Ni, Pb and Zn in water flea Daphnia magna, a stable isotope experiment. Aquat. Toxicol. 2008, 90, 138-144.

Lee, B. T.; Ranville, J. F. The effect of hardness on the stability of citrate-stabilized gold nanoparticles and their uptake by *Daphnia magna*. J. Hazard. Mater. 2012, 213-214, 434-439.

Lopes, S.; Ribeiro, F.; Wojnarowicz, J.; Lojkowski, W.; Jurkschat, K.; Crossley, A.; Soares, A. M. V. M.; Loureiro, S. Zinc oxide nanoparticles toxicity to *Daphnia magna*: Size-dependent effects and dissolution. Environ. Toxicol. Chem. 2014, 33, 190-198.

Lorenzo, J. I.; Beiras, R.; Mubiana, V. K.; Blust, R. Copper uptake by Mytilus edulis in the presence of humic acids. Environ. Toxicol. Chem. 2005, 24, 973-980.

Lores, E. M.; Snyder, R. A.; Pennock, J. R. The effect of humic acid on uptake/adsorption of copper by a marine bacterium and two marine ciliates. Chemosphere 1999, 38, 293-310.

Ma, D. Hybrid nanoparticles: An introduction - ScienceDirect. 2019.

Meyer, J. S.; Ranville, J. F.; Pontasch, M.; Gorsuch, J. W.; Adams, W. J. Acute toxicity of binary and ternary mixtures of Cd, Cu, and Zn to *Daphnia magna*. Environ. Toxicol. Chem. 2015, 34, 799-808.

Minteq, V.; Agency, E. P. Visual MINTEQ - a Brief Tutorial. 2000, 1-5.

Mitrano, D. M.; Motellier, S.; Clavaguera, S.; Nowack, B. Review of nanomaterial aging and transformations through the life cycle of nano-enhanced products. Environ. Int. 2015, 77: 132-147.

Nadella, S. R.; Fitzpatrick, J. L.; Franklin, N.; Bucking, C.; Smith, S.; Wood, C. M. Toxicity of dissolved Cu, Zn, Ni and Cd to developing embryos of the blue mussel (*Mytilus trossolus*) and the protective effect of dissolved organic carbon. Comp. Biochem. Physiol. - C Toxicol. Pharmacol. 2009, 149, 340-348.

Nogueira, L. S.; Bianchini, A.; Smith, S.; Jorge, M. B.; Diamond, R. L.; Wood, C. M. Physiological effects of five different marine natural organic matters (NOMs) and three different metals (Cu, Pb, Zn) on early life stages of the blue mussel (*Mytilus galloprovincialis*). PeerJ 2017, 5: e3141.

OECD. Guideline for Testing of Chemicals. Daphnia sp., Acute Immobilization Test. OECD 202. Paris, 2004.

Ogunsuyi, O. I.; Fadoju, O. M.; Akanni, O. O.; Alabi, O. A.; Alimba, C. G.; Cambier, S.; Eswara, S.; Gutleb, A. C.; Adaramoye, O. A.; Bakare, A. A. Genetic and systemic toxicity induced by silver and copper oxide nanoparticles, and their mixture in Clarias gariepinus (Burchell, 1822). Environ. Sci. Pollut. Res. 2019, 26, 27470-27481.

Qiao, R.; Lu, K.; Deng, Y.; Ren, H.; Zhang, Y. Combined effects of polystyrene microplastics and natural organic matter on the accumulation and toxicity of copper in zebrafish. Sci. Total Environ. 2019, 682, 128-137.

Sani-Kast, N.; Labille, J.; Ollivier, P.; Slomberg, D.; Hungerbühler, K.; Scheringer, M. A network perspective reveals decreasing material diversity in studies on nanoparticle interactions with dissolved organic matter. Proc. Natl. Acad. Sci. U. S. A. 2017, 114, E1756-E1765.

Sharma, V. K.; Sayes, C. M.; Guo, B.; Pillai, S.; Parsons, J. G.; Wang, C.; Yan, B.; Ma, X. Interactions between silver nanoparticles and other metal nanoparticles under environmentally relevant conditions: A review. Sci. Total Environ. 2019, 653, 1042-1051.

Tervonen, K.; Waissi, G.; Petersen, E. J.; Akkanen, J.; Kukkonen, J. V. K. Analysis of fullerene-C60 and kinetic measurements for its accumulation and depuration in *Daphnia magna*. Environ. Toxicol. Chem. 2010, 29, 1072-1078.

Unsworth, E. R.; Warnken, K. W.; Zhang, H.; Davison, W.; Black, F.; Buffle, J.; Cao, J.; Cleven, R.; Galceran, J.; Gunkel, P.; et al. Model predictions of metal speciation in freshwaters compared to measurements by in situ techniques. Environ. Sci. Technol. 2006, 40, 1942-1949.

Wang, Z.; Chen, J.; Li, X.; Shao, J.; Peijnenburg, W. J. G. M. Aquatic toxicity of nanosilver colloids to different trophic organisms: contributions of particles and free silver ion. Environ. Toxicol. Chem. 2012, 31, 2408-2413.

Wang, Z.; Li, J.; Zhao, J.; Xing, B. Toxicity and internalization of CuO nanoparticles to prokaryotic alga *Microcystis aeruginosa* as affected by dissolved organic matter. Environ. Sci. Technol. 2011, 45, 6032-6040.

Wang, Z.; Zhang, L.; Zhao, J.; Xing, B. Environmental processes and toxicity of metallic nanoparticles in aquatic systems as affected by natural organic matter. Environ. Sci. Nano 2016, 3, 240-255.

Wilke, C. M.; Wunderlich, B.; Gaillard, J. F.; Gray, K. A. Synergistic bacterial stress results from exposure to nano-Ag and nano-TiO₂ mixtures under light in environmental media. Environ. Sci. Technol. 2018, 52, 3185-3194.

Wu, J., Wang, G., Vijver, M.G., Bosker, T., Peijnenburg, W.J.G.M. Foliar versus root exposure of AgNPs to lettuce: Phytotoxicity, antioxidant responses and internal translocation. Environ. Pollut. 2020, 261, 114117.

Xiao, Y.; Peijnenburg, W. J. G. M.; Chen, G.; Vijver, M. G. Impact of water chemistry on the particle-specific toxicity of copper nanoparticles to *Daphnia magna*. Sci. Total Environ. 2018, 610-611, 1329-1335.

Xiao, Y.; Vijver, M. G.; Chen, G.; Peijnenburg, W. J. G. M. Toxicity and accumulation of Cu and ZnO nanoparticles in *Daphnia magna*. Environ. Sci. Technol. 2015, 49, 4657-4664.

Ye, N.; Wang, Z.; Wang, S.; Peijnenburg, W. J. G. M. Toxicity of mixtures of zinc oxide and graphene oxide nanoparticles to aquatic organisms of different trophic level: particles outperform dissolved ions. Nanotoxicology 2018, 12, 423-438.

Yu, R.; Wu, J.; Liu, M.; Zhu, G.; Chen, L.; Chang, Y.; Lu, H. Toxicity of binary mixtures of metal oxide nanoparticles to *Nitrosomonas Europaea*. Chemosphere 2016, 153, 187-197.

Zhang, Y.; Chen, Y.; Westerhoff, P.; Crittenden, J. Impact of natural organic matter and divalent cations on the stability of aqueous nanoparticles. Water Res. 2009, 43, 4249-4257.

Supplementary Information

Preparation of test suspensions

Stock suspensions containing 100 mg L^{-1} MNPs or metal salts were freshly prepared in ElendtM7 medium (OECD 202(OECD, 2004)). To disperse the nanoparticles in the medium, each suspension was sonicated for 15 min at 50 Hz in a water bath sonicator (USC200T, VWR, Amsterdam, The Netherlands). A SR-NOM stock solution was prepared by dissolving the SR-NOM in Milli-Q water. After stirring for 24 h at 22 °C in a dark room and filtration through a 0.45 μm cellulose acetate membrane, the stock solution was covered with aluminum-foil and stored at 4 °C prior to use. The SR-NOM contained 43.7% organic carbon[2].

Physicochemical characterization

The morphology and size of suspensions of 1 mg L^{-1} of ZnONPs and CuNPs were determined using transmission electron microscopy (TEM, JEOL 1010, JEOL Ltd., Japan). The size distribution (Z-average hydrodynamic diameter), and zeta-potential of suspensions of 1 mg L^{-1} MNPs with different nominal concentrations of SR-NOM (1, 10, and 20 mg L^{-1}) were analyzed by dynamic light scattering (DLS) using a zetasizer Nano-ZS instrument (Malvern, Instruments Ltd., UK).

The stock solutions were diluted to the appropriate test concentrations in ElendtM7 medium. The pH values of all test suspensions were adjusted by the addition of either 0.1 M NaOH or 0.1 M HCl to maintain a fixed value of around 8.4. During the 48 h of incubation, these suspensions were stored in a climate room under a

16:8 h light-dark cycle (22 ± 1 °C, RH: 80.0%). The samples were collected at the top 0.5 to 1 cm layer of the dispersion after 0, 24, and 48 h. Samples for analysis of the concentration of dissolved ions shedding from the MNPs were firstly centrifuged at 30392 g for 30 min at 4 °C (Sorvall RC5Bplus centrifuge, Fiberlite F21-8 × 50y rotor). Eight mL supernatant (in full) was then decanted into another tube and were digested by the addition of 2 drops of 65% nitric acid for at least 1 d.

Cultures of *Daphnia magna*

Daphnia magna cultures originate from Leiden University. Sensitivity of the organisms is verified every 6 months using potassium dichromate ($K_2Cr_2O_7$), as described within OECD Guideline 202(OECD, 2004). The daphnia culture medium, ElendtM7 medium, was prepared at pH 8.4 ± 0.4 according to OECD Guideline 202(OECD, 2004). *D. magna* was cultured at 22 ± 1 °C with a 16:8 light-dark cycle. Groups of 50-60 adult females were kept in 11 L glass aquariums filled with 5 L of culture medium. Cultures were renewed every week and daphnids were fed with *Pseudokirchneriella subcapitata* every 2 days.

Sampling procedure for the determination of the actual exposure concentrations of particles and ions

The actual exposure concentrations of particles and ions in each treatment were measured by AAS after incubation in the test medium without daphnids. The treatments were digested in 65% HNO_3 for at least 24 h. To obtain the ions released from the nanoparticles, the nanoparticle suspensions firstly were centrifuged at 30392 g for 30 min at 4°C (Sorvall 114 RC5Bplus centrifuge, Fiberlite F21-8 × 50y rotor) to

obtain the supernatants, which were then filtered through a syringe filter with 0.02 µm pore diameter (Antop 25, Whatman).

Calculation of simplified time weighted average concentrations

To express the actual exposure concentrations over time, a simplified time weighted average (TWA) concentration was calculated based on the measured actual concentrations at 0, 24 and 48 h of exposure. As in our previous study, the TWA concentrations were calculated according to the following formula[3,4]:

$$C_{TWA} = \frac{\sum_{n=1}^{N}(\Delta t_n \frac{C_{n-1} + C_n}{2})}{\sum_{n-1}^{N} \Delta t_n}$$

Where Δt is the time interval, n is the time interval number, N is the total number of intervals, C is the concentration at the end of the time interval. The simulated TWA concentrations were used for all calculations expressing the exposure.

Statistical analyses

A linear model with a Tukey's post Hoc test was developed to analyze the significance level and the contribution (%) of each treatment using SPSS 16.0 (IBM SPSS Statistics for Windows, Ver. 19.0, IBM Corp., Armonk, NY). Data were checked for normality and homogeneity before analysis of variance (ANOVA). The significance level in all calculations was set at $p < 0.05$.

Table S3.1 List of published studies (to date) conducted on joint toxicity of Cu- and Zn-salts to organisms in freshwater

Organism	Species	Cu:Zn ratio	Exposure conditions	Endpoint	Joint effect	References
Fish	*Gobiocypris rarus*	1:1	pH: 7.8 ± 0.2 25 ± 1°C 16:8 h light:dark photoperiod	75 h Embryo–larval toxicity bioassays (including hatching, lethality,etc.)	synergistic	Zhu et al., 2011[5]
Fish	*Pimephales promelas*	1:2	22.8 – 25.8°C	96 h lethality tests	more-than-additive	Lynch et al., 2016[6]
Fish	*Danio rerio*	series of combination	pH: 7.0 26 ± 0.5 °C 12:12 h light:dark photoperiod	24 h lethality tests Accumulation	antagonistic	Gao et al., 2017[7]
Freshwater snail	*Lymnaea stagnalis*	series of combination	pH: 7.9 ± 0.2 25 ± 1 °C 16:8 h light:dark photoperiod	Short-term accumulation	antagonistic	Crémazy et al., 2019[8]
Freshwater Alga	*Chlorella sp.*	EC_{50} ratio	27°C 12:12 h light:dark photoperiod	72 h growth inhibition Accumulation	less-than-additive or antagonistic	Franklin et al., 2002[9]
Water flea	***Daphnia magna***	series of combination	pH: 7.4–7.8 20 ± 1°C 16:8 h light:dark photoperiod 3mg/L DOC	48 h lethality tests	additive or more-than-additive	Meyer et al., 2014[10]

Water flea	*Daphnia magna*	EC_{20} ratio (1:10)	20 ± 1 ∘C DOC <1 mg/L	Feeding behaviour 48 h lethality	more-than-additive	Lari et al., 2017(Lari et al., 2017)[1]
Water flea	*Daphnia magna*	series of combination	pH: 7.0 21 ± 1 ∘C 16:8 h light:dark photoperiod	96 h accumulation test Bioavailability	additive or less-than-additive	Komjarova and Blust, 2008[12]
Water flea	*Ceriodaphnia dubia* and *Daphnia carinata*	1:10	pH: 7.5 ± 0.3 25 ± 1 ∘C 16:8 h light:dark photoperiod	48 h lethality tests 7 d lethality tests	additive or more-than-additive	Cooper et al., 2009[13]
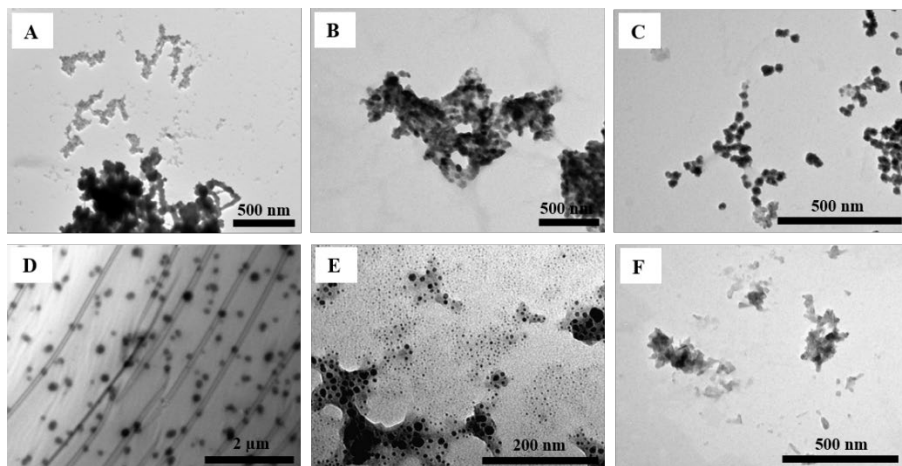
Figure S3.1 TEM images of the MNPs in the absence and presence of SR-NOM (A: CuNPs; B: ZnONPs; C: CuNPs and ZnONPs; D: CuNPs with SR-NOM; E: ZnONPs with SR-NOM; F: CuNPs and ZnONPs with SR-NOM) in the ElendtM7 medium.
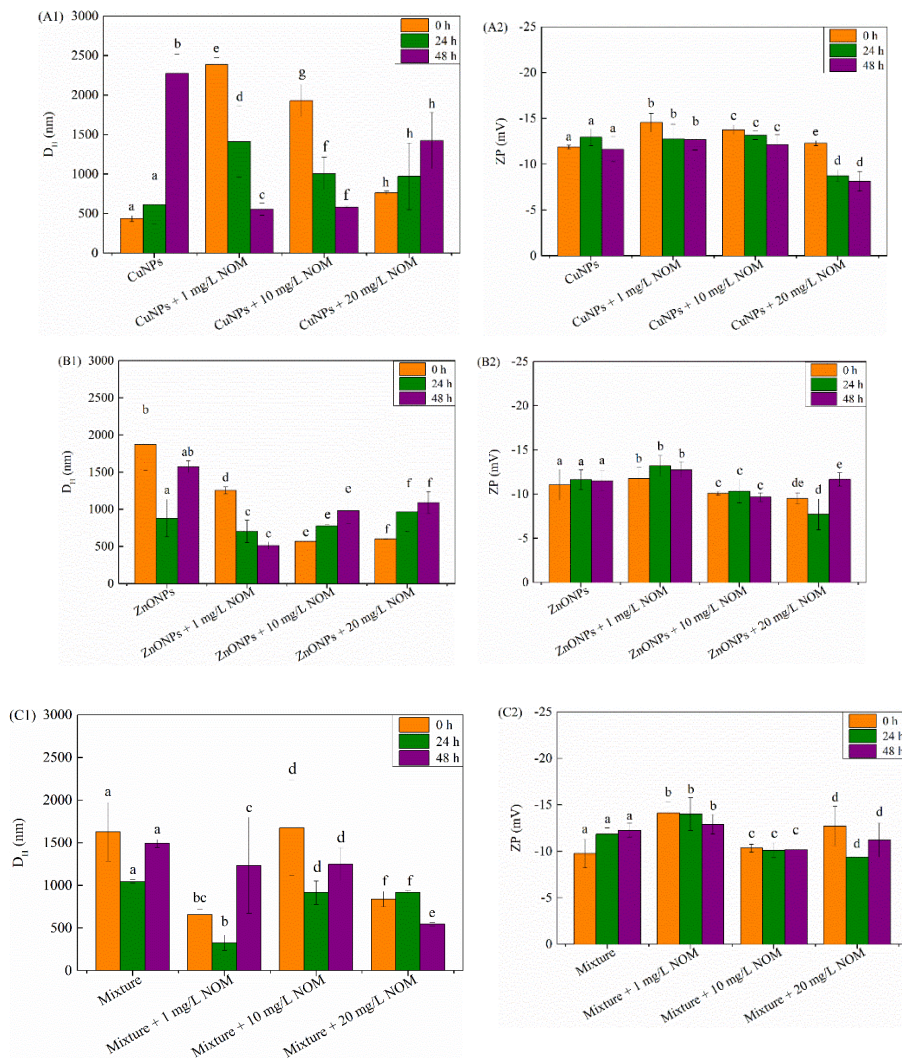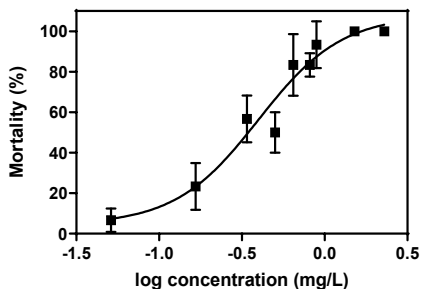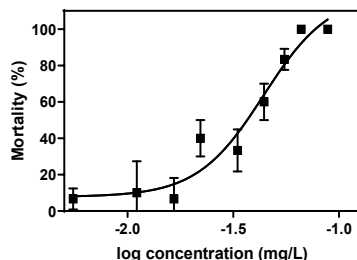
Figure S3.2 Variation in hydrodynamic diameter (D_H in nanometer) and zeta potential (ZP in mVolt) of CuNPs and ZnONPs and their binary mixture in the presence of 0, 1, 10, and 20 mg/L SR-NOM as a function of time (0, 24, and 48 hours). Values are expressed as mean ± standard deviation (n = 3). Letters indicate statistically significant (p < 0.05) differences between the treatments.
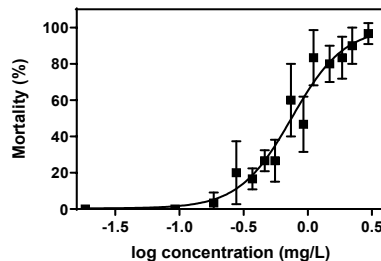
CuNPs   Cu(NO$_3$)$_2$
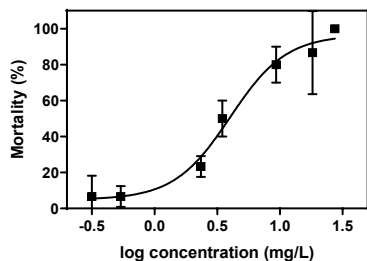
ZnONPs   Zn(NO$_3$)$_2$

Figure S3.3 Concentration−response curves of mortality (%) of *D. magna* exposed to individual CuNPs, ZnONPs, Cu(NO$_3$)$_2$, and Zn(NO$_3$)$_2$. The actual exposure concentration is expressed as the time weighted concentration (C_{TWA}). Actual log-transformed Cu or Zn concentrations are plotted on the *x*-axis. Data are mean ± standard deviation (SD) (n = 3).
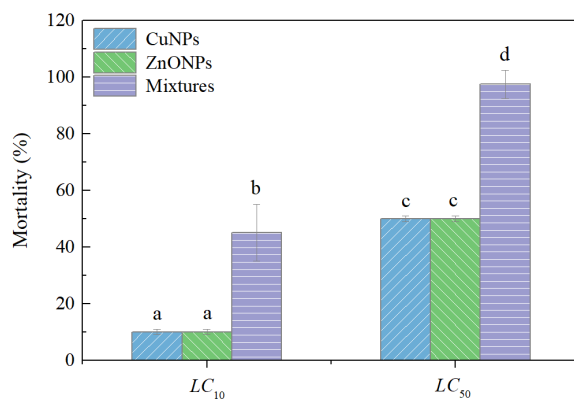
Figure S3.4 Comparison in mortality (%) between the individual and mixtures of CuNPs and ZnONPs. Values are expressed as mean ± standard deviation ($n = 3$). Letters indicate statistically significant ($p < 0.05$) differences between the treatments.

(A) Single NPs

ZnONPs + 20 mg/L NOM — 100.0%
ZnONPs + 10 mg/L NOM — 100.0%
ZnONPs + 1 mg/L NOM — 67.0% | 6.7% | 26.3%
ZnONPs — 84.2% | 15.8%

CuNPs + 20 mg/L NOM — 100.0%
CuNPs + 10 mg/L NOM — 100.0%
CuNPs + 1 mg/L NOM — 100.0%
CuNPs — 34.2% | 65.8%

Percentage of total dissolved ion concentration (%)

Free metal ions   Metal-Inorganic complexes   Metal-NOM complexes

(B) NP mixture

ZnONPs + 20 mg/L NOM — 100.0%
ZnONPs + 10 mg/L NOM — 100.0%
ZnONPs + 1 mg/L NOM — 63.4% | 6.3% | 30.2%
ZnONPs — 90.9% | 9.1%

CuNPs + 20 mg/L NOM — 100.0%
CuNPs + 10 mg/L NOM — 100.0%
CuNPs + 1 mg/L NOM — 0.7% | 1.3% | 98.0%
CuNPs — 34.8% | 65.2%

Percentage of total dissolved ion concentration (%)

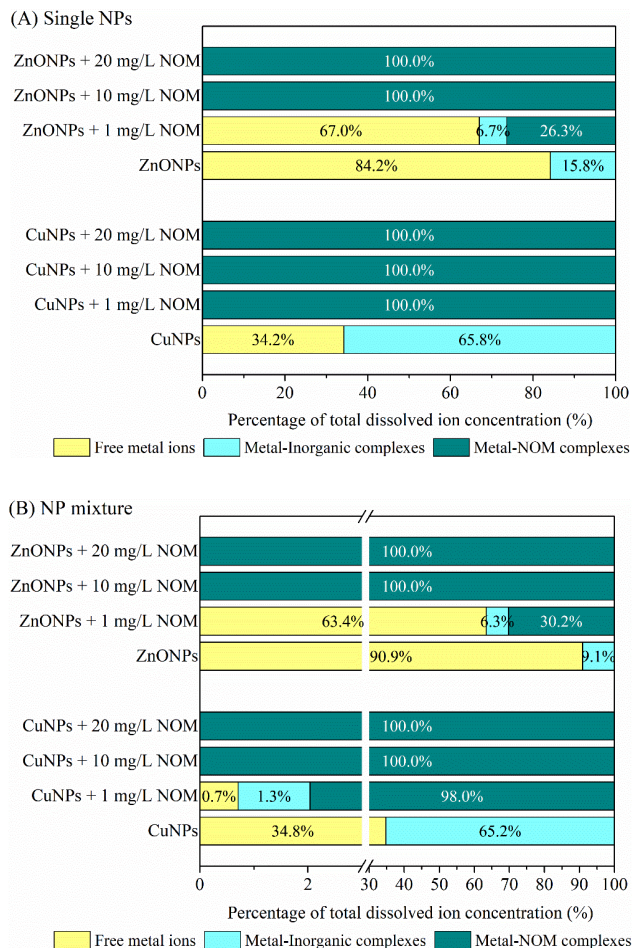Free metal ions   Metal-Inorganic complexes   Metal-NOM complexes

Figure S3.5 Percentage of free metal ions (yellow), metal-inorganic complexes (blue) and metal-NOM complexes (green) calculated with Visual MINTEQ3.1 for dissolved ions in suspensions of CuNPs and ZnONPs(Gustafsson, n.d.)[4]. Complexation to natural organic matter was simulated with state-of-the-art models (NICA-Donnan)(Baker, 2012; Gustafsson, 2001, n.d.; Gustafsson and Berggren Kleja, 2005)[7].

References

Baker, B.J., 2012. Investigation of the competitive effects of copper and zinc on fulvic acid complexation: modeling analytical approaches. Colorado School of Mines.

Gustafsson, J.P., 2001. Modeling the acid-base properties and metal complexation of humic substances with the Stockholm Humic Model. J. Colloid Interface Sci. 244, 102–112.

Gustafsson, J.P., n.d. Visual MINTEQ 3.1.

Gustafsson, J.P., Berggren Kleja, D., 2005. Modeling Salt-Dependent Proton Binding by Organic Soils with the NICA-Donnan and Stockholm Humic Models. Environ. Sci. Technol. 39, 5372–5377.

Lari, E., Gauthier, P., Mohaddes, E., Pyle, G.G., 2017. Interactive toxicity of Ni, Zn, Cu, and Cd on Daphnia magna at lethal and sub-lethal concentrations. J. Hazard. Mater. 334, 21–28.

OECD, 2004. Oecd Guideline for testing of chemicals Daohnia sp., Acute Immobilisation Test, OECD.

Chapter 4

Accumulation kinetics of polystyrene nano- and micro-plastics in the waterflea *Daphnia magna* and trophic transfer to the mysid *Limnomysis benedeni*

Qi Yu, Tom A.P. Nederstigt, Zhuang Wang, Juan Wu, Aranka Kolmas, Thijs Bosker, Zuzanna Filipiak, Willie J. G. M. Peijnenburg, Martina G. Vijver

Abstract

Trophic transfer of nano-and micro-plastics (NMPs) has attracted the attention of scientists. Here we investigated the accumulation of differently sized polystyrene particles (PSPs) in *Daphnia magna* and their subsequent transfer to *Limnomysis benedeni*, explicitly accounting for the fate of the PSPs in the aquatic system as a function of particle size (26, 500 and 4800 nm). *L. benedeni* were fed with *D. magna* exposed to 8 mg/L PSPs (8.3×10^{11} particles mL^{-1} 26 nm PSPs, 1.2×10^8 particles mL^{-1} 500 nm PSPs, 1.3×10^5 particles mL^{-1} 4800 nm PSPs) for 16 h and were subsequently depurated for 48 h (in the absence of food). On the basis of mass of particles accumulated in the organisms, the internal concentration of 4800 nm PSPs was found to be 4-10 times higher than that of 26 and 500 nm PSPs in *D. magna*. Uptake rate constants in daphnids for 26 nm (1.7 ± 0.4 L/g·h) and 4800 nm (1.7 ± 0.4 L/g·h) were significantly ($p < 0.05$) higher than uptake rate constants for the 500 nm (0.7 ± 0.1 L/g·h) PSPs. It was estimated that a small fraction (1 to 5 %) of the PSPs ingested by *D. magna* was transferred to *L. benedeni*. Moreover, the larger the particle size, the higher the extent of transfer in the food chain. Elimination rate constants in *L. benedeni* were found to be 0.03 ± 0.03, 0.1 ± 0.2 and 0.2 ± 0.8 per hour for 26, 500 and 4800 nm PSPs respectively, and were not significantly different from one another. Visual observations of fluorescence showed that PSPs were mainly accumulated in the stomach and intestine of *L. benedeni*. Furthermore, the calculated trophic transfer factor on the basis of mass of particles accumulated in the organisms was < 1 for all PSP treatments, implying that no biomagnification was observed in the predator. These findings indicated that NMPs can be transferred along the daphnia-mysids food

chain, but that biomagnification does not occur. It also highlights that particle size affects accumulation and trophic transfer.

4.1 Introduction

Pollution of aquatic environments by nano- (1 - 100 nm) (Bouwmeester et al., 2015) and microplastics (100 nm - 5 mm) (Waring et al., 2018) originates from the release of primary manufactured particles employed in many industrial and consumer products (Imhof et al., 2016; Mattsson et al., 2018; Napper et al., 2015; van Wezel et al., 2016; Wang et al., 2019), as well as from the degradation of larger plastic items into nano- or micro-sized fragments (Andrady, 2017; Botterell et al., 2019; Carbery et al., 2018; Franzellitti et al., 2019). As a result there are significant quantities of nano- and microplastics (NMPs) present in the aquatic environment (Botterell et al., 2019; Jambeck et al., 2015; Wang et al., 2019). Furthermore, the concentrations of NMPs in the environment are measured and estimated to be between 1 pg/L and 1 g/L, and they are expected to rise exponentially as their particle size decreases (Lenz et al., 2016). These particles can be ingested by organisms and subsequently be transferred across trophic levels (Chae et al., 2019, 2018; Crooks et al., 2019; Elizalde-Velázquez and Gómez-Oliván, 2021).

Particle size is an important factor affecting the accumulation and trophic transfer of NMPs (Markic et al., 2020; Monikh et al., 2021; Provencher et al., 2019). Van Pomeren et al. (2017) found that nanoplastics with particle sizes of 25 and 50 nm migrate through the body of zebrafish embryos and eventually accumulate in specific organs and tissues, whereas nanoplastics larger than 50 nm were predominantly adsorbed onto the intestinal tract and outer epidermis of zebrafish embryos. Similarly, 5 μm microplastics were found to accumulate in the gills, gut and liver of zebrafish (*Danio rerio*), whilst accumulation of 20 μm particles was restricted to the gills and gut (Lu

et al., 2016). In addition, Monikh et al. (2021) found that the uptake and trophic transfer of microplastics with a particle size of 270 nm along an algae-daphnids food chain were higher than the uptake and transfer of 640 nm particles. However, to date the kinetics of the accumulation of NMPs as a function of particle size have been poorly quantified.

In aquatic environments, actual exposure of organisms to NMPs is dependent on the environmental fate of NMPs. One key characteristic which determines the fate of NMPs is considered to be their density (Ding et al., 2021). Plastics with a low density (ρ < 1.0 g/cm^3) will primarily remain in the top/surface layers of the water phase and can be ingested by organisms feeding from the water phase (Devriese et al., 2015; Pegado et al., 2018; Zhang et al., 2017). In contrast, plastics where ρ > 1.0 g/cm^3 likely settle to the sediment layer, where they can be ingested by zoobenthos (Zhang et al., 2017). When the density of plastics is similar to 1.0 g/cm^3, their spatial distribution is additionally affected by particle size and shape and mediated by turbulent mixing and biofouling rates (Shamskhany et al., 2021).

Within the current study, we hypothesized that trophic transfer increases with decreasing particle size of PSPs, and a smaller particle has a higher likelihood of penetration and translocation in/within a predator. Moreover, the fate of PSPs in the aqueous phase is, apart from their density, hypothesized to be associated with their particle size in the aqueous phase. To test the hypotheses, we selected fluorescently labeled polystyrene particles (PSPs) (ρ = 1.05 g/cm^3) with particle sizes of 26, 500 and 4800 nm as model NMPs. A food chain experiment was conducted using the waterflea *Daphnia magna* and the predatory mysid *Limnomysis benedeni*. *D. magna* neonates were exposed to PSPs for 7 hours, and subsequently fed to *L. benedeni* over

the course of 16 hours, followed by 48 hours of depuration. Biota samples were collected at several timepoints to determine uptake and elimination kinetics, and water and sediment samples were collected to explore the spatial distribution of PSPs in the simulated aquatic system.

4.2 Materials and Method

4.2.1 Test materials and medium

Three fluorescent-dye-labeled and spherical PSPs (diameter 26 nm with an excitation/emission at 505/515 nm and diameters 500 and 4800 nm with an excitation/emission at 468/508 nm) were purchased from ThermoFisher Scientific (Waltham, USA). The 500 and 4800 nm PSPs were unmodified, whilst the 26 nm PSPs contained carboxyl groups bound to the particle surface. Stock suspensions of PSPs (100 mg/L) were freshly prepared in ElendtM7 medium according to OECD 202 (OECD, 2004) and subsequently dispersed by sonicating for 10 min at 50 Hz in a water bath sonicator (USC200T, VWR, Amsterdam, The Netherlands).

4.2.2 Quantitative analysis of mass concentration and particle number concentration

The exposure concentrations (mass-based) of PSPs were determined after measuring their fluorescence intensity (FI) using a Sparks Multimode Microplate reader (TECAN, Switzerland). The particle number concentration (particles/mL) converted from the mass concentration (mg/L) was used as a reference dose metric for the PSPs.

This conversion was performed according to following equation (Facts, 2005):

$$\text{Number of PSPs/ mL} = \frac{6C \times 10^{12}}{\rho \times \pi \times \varnothing^3} \tag{1}$$

Where, C is the concentration of suspended PSPs in g/mL, ϕ is the diameter of PSPs in μm, and ρ is the density of polystyrene (1.05 g/mL).

4.2.3 Cultures of test organisms

Daphnids were taken from the culture maintained at Leiden University which is kept according to OECD Guideline 202 (OECD, 2004). Elendt M7 medium (OECD, 2004) was used as the culture medium (pH 8.4 ± 0.4). *D. magna* were maintained at a temperature of 22 ± 1 °C with a 16:8 light-dark cycle and fed with the algae *Pseudokirchneriella subcapitata* every two days.

L. benedeni were collected in spring from a pond in the Netherlands. All collected individuals were acclimated for several weeks and fed cultured daphnids. *L. benedeni* was cultured according to the following acclimatization steps in the climate room (22 ± 1 °C, 6:8 light-dark cycle). 1) Day 1: *L. benedeni* were kept in a mixture of water collected from the original pond and Elendt M7 medium, including a small amount of sediment collected from the original pond. 2) Day 2: *L. benedeni* were transferred into ElendtM7 medium with sediment and were fed with cultured daphnia neonates. 3) Day 3: *L. benedeni* were cultured in ElendtM7 medium without sediment and food to clean their guts. *L. benedeni* were cultured under continuously aeration in the same conditions as *D. magna*. Only female *L. benedeni* (1.2 ± 0.1 cm length) were selected for the experiment for reasons of consistency.

4.2.4 Survival tests

To investigate PSPs-induced responses on the selected test organisms, the survival rates of the daphnids and mysids exposed to all PSP treatments for 24 and 72 h were recorded. *D. magna* neonates (< 24 h) were used in the test after cleaning their guts for around 2 h in Elendt M7 medium. Twenty five neonate daphnids (5 replicates) and 10 mysids (single replicate) were used in each treatment. The test organisms were exposed to increasing nominal concentrations of PSPs of 0, 0.5, 1, 2, 4 and 8 mg/L.

4.2.5 Food chain transfer from *D. magna* to *L. benedeni*

The feeding rate of *L. benedeni* was assessed via a pre-feeding test of 16 h (Supplementary data, Figure S4.1). After 2 h of gut cleaning, *D. magna* neonates were non-exposed (control group) and exposed to the PSP suspensions for 7 h accumulation period. Two exposed daphnids were introduced as food to each mysid (previously maintained without food for 24 h); the feeding session lasted for 16 h, and daphnids were washed 3 times with clean ElendtM7 medium to remove potentially adsorbed particles. After the feeding session, the exposed mysids ($n = 8$) were washed 3 times to remove the adsorbed PSPs. Subsequently, these mysids were transferred to uncontaminated medium without feeding for another 48 h in order to monitor the depuration of PSPs in the predator (*L. benedeni*). The control mysids ($n = 8$) were fed two non-exposed neonate daphnids during the feeding period. An initial exposure concentration of 8 mg/L of PSPs (i.e., 8.3×10^{11} particles/mL 26 nm PSPs, 1.2×10^8 particles/mL 500 nm PSPs, 1.3×10^5 particles/mL 4800 nm PSPs) was chosen in the trophic transfer test.

Daphnid samples were collected at 0, 0.25, 1, 2, 4 and 7 h and mysid samples were collected at 0, 16, 20, 40, 46 and 64 h. All samples were washed once with ElendtM7 medium and twice with MilliQ water (Milipore Milli-Q reference A+ system, Waters-Millipore Corporation, Milford, MA, USA), and afterwards homogenized at 30 rps for 1 minute (TissueLyzer II, QIAGEN, USA). The internal concentrations of PSPs in the test organisms were determined based on fluorescence using a Sparks Multimode Microplate reader. Concentrations of excreted PSPs from mysids into the aqueous medium were measured simultaneously. The aqueous samples were collected from the middle layer of the exposure suspensions. Also, a control group containing non-exposed organisms was included to ensure that the results of the fluorescence analysis of feeding and depuration were associated with exposure to the test materials.

4.2.6 Modelling kinetics of accumulation process

First-order kinetics were used to model the accumulation of PSPs in the test organisms. The uptake rate of PSPs in the organisms was calculated as follows:

$$\frac{dC_{org}}{dt} = k_w C_{external}$$

(2)

Where C_{org} is the concentration (mg/g) of PSPs in organisms, k_w is the uptake rate constant (L/g·h), and $C_{external}$ is the exposure concentration (mg/L) of PSPs.

The elimination rate of PSPs in the organisms was calculated with the following formula:

$$\frac{dC_{org}}{dt} = -k_e C_{org}$$

(3)

Where k_e is the elimination rate constant (1/h).

The accumulation process can be described as the sum of the rates of uptake and elimination, as presented in Equation 4:

$$\frac{dC_{org}}{dt} = k_w C_{external} - k_e C_{org}$$

(4)

4.2.7 Evaluation of the trophic transfer factor

The trophic transfer potential of PSPs from daphnids to the mysid was evaluated by calculating the trophic transfer factor (TTF). The TTF was evaluated by using the ratio of the PSP concentration in the mysid (C_{mysid}, mg/g wet mass) to the PSP concentration in the daphnids ($C_{daphnia}$, mg/g wet mass):

$$\text{TTF} = \frac{C_{mysid}}{C_{daphnia}}$$

(5)

If TTF > 1, biomagnification of PSPs occurs in the mysid; if TTF ≤ 1, the extent of transfer of PSPs from the daphnia to the mysid is limited.

4.2.8 Characterization and *in vivo* distribution

The biodistribution of PSPs in the test organisms was visualized using a Leica MZ 16FA fluorescent stereo microscope equipped with a digital camera (DFC 420) and image acquisition software of Leica. A GFP3 filter (excitation at 470/40 nm, barrier at 525/50 nm) was used and exposure was set at 2.5 s, gain at 2.0 and gamma at 0.6. Transmission

settings were set at exposure 146.4 ms, gain 1.0 and gamma 0.6. Daphnia samples were collected at 0 and 7 h. Mysid samples ($n = 3$, both control and exposure groups) were collected at 0, 16, 20, 40 and 64 h. These samples were rinsed with uncontaminated medium for 1 min before the characterization of the biodistribution of PSPs.

4.2.9 Statistical analyses

Statistically significant differences in the accumulation kinetic rate constants between the PSP treatments and in the mass concentrations between the exposure group and control group were determined by one-way analysis of variance (ANOVA) with the Tukey's HSD post hoc tests, at a significance level of $p < 0.05$ using SPSS 16.0 (IBM SPSS Statistics for Windows, Ver. 19.0, IBM Corp., Armonk, NY). Data were checked for normality and homogeneity before performing the relevant tests. Statistically significant differences in the observed fluorescence between the PSP treatments was analyzed by means of one way ANOVA followed by Tukey's HSD post hoc tests using the SPSS. Prior to analysis, fluorescence data were Log10 transformed to assure that the requirements for residual- and variance distributions were met. Values in all controls and treatments are expressed as mean ± standard deviation.

4.3 Results and discussion

4.3.1 Survival of *D. magna* and *L. benedeni* exposed to PSPs

Survival data for *D. magna* and *L. benedeni* are presented in Table S4.1 and Figure S4.2 (Supplementary data), respectively. As shown in Table S4.1, the survival rate of *D. magna* was close to 100% for all PSP treatments, independent of particle size and exposure concentration of the PSPs. This means that the PSPs showed no acute lethal toxicity to *D. magna* at all concentrations studied. As shown in Figure S4.2, *L. benedeni* exposed to all the PSP treatments showed a time-dependent decrease in survival rates in comparison to controls, implying that the PSPs exhibited time-dependent acute lethal toxicity.

4.3.2 Accumulation of PSPs in *D. magna*

The kinetics of the accumulation of different sizes of PSPs in *D. magna* directly from the aqueous phase over the exposure period of 7 h are depicted in Figure 4.1. The kinetic rate constants of PSPs in the daphnids were calculated as shown in Table 4.1. The background concentrations in daphnia were detected to be around 0.003 ± 0.006 mg PSPs/g daphnia wet mass during the whole experimental period. Moreover, three separate images in Figure S4.3 (Supplementary data) show overlapping curves (Figure 4.1) for the data of background auto-fluorescence. The ingestion of PSPs in *D. magna* was faster in the first hour of exposure and thus the internal concentrations of PSPs subsequently stabilized. During the exposure, the internal mass concentration (based on mg/g dry weight) of 4800 nm PSPs was 4-10 times higher than the mass concentration of 26 and 500 nm PSPs in *D. magna*. The order of the uptake rate constants (on the basis of mass

concentration) of PSPs in *D. magna* decreased as follows: 26 = 4800 > 500 nm (Table 4.1). These findings were not in line with expectations, as we hypothesized that uptake rates as determined on the basis of mass concentration would be inversely related to particle size. The filter apparatus of the *D. magna* acts like a net and thus allows particles to be ingested in certain size ranges related to the individual mesh sizes (Geller and Muller, 1981; Lee and Ranville, 2012; Tervonen et al., 2010). Thereupon, too small particles only will be ingested when they are aggregated, and too large particles will not be taken into the filter apparatus.
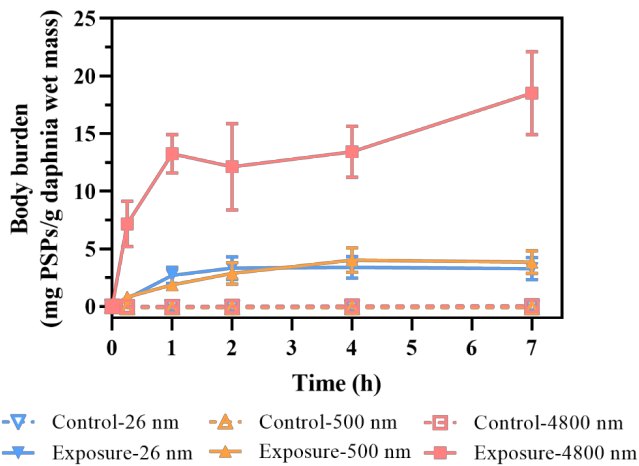
Figure 4.1. Accumulation of PSPs (26, 500 and 4800 nm) in *D. magna* neonates over 7 h exposure period

Table 4.1 Accumulation kinetic rate constants of PSPs in *D. magna* and *L. benedeni* [a] as determined on the basis of mass of particles accumulated in the organisms.

PSPs	k_w (L/g·h, *D. magna*)	k_e (1/h, *L. benedeni*)
26 nm	1.7 ± 0.4a	0.2 ± 0.8A
500 nm	0.7 ± 0.1b	0.1 ± 0.2A
4800 nm	1.7 ± 0.4a	0.03 ± 0.03A

[a] The different letters in a column indicate significant differences among different treatments at $p < 0.05$.

4.3.3 Fate of PSPs introduced by *D. magna* in simulated aquatic system

In the simulated aquatic system used for the food chain transfer, the fate of PSPs introduced by *D. magna* might be divided into three compartments including the predator (*L. benedeni*), the aqueous phase and the depositional phase (excretions of *L. benedeni*). The ratio of PSPs in each compartment (the mass concentration of PSPs in the predator-*L. benedeni*, the aqueous phase and the depositional phase, respectively) compared to the input (the mass concentration of PSPs accumulated in the prey-*D. magna*) as a function of time can be found in Fig 2. As shown in Figure 4.2, the ratios of the PSPs distributed in *L. benedeni* were only in the range of 1 to 5 % over the exposure and depuration periods, which implies that trophic transfer of PSPs was limited. Moreover, for 26 and 500 nm PSPs, the ratios of PSPs in the aqueous phase increased from 31 to 69 % and from 58 to 88 % over time, respectively. This means that 26 and 500 nm PSPs introduced by *D. magna* tended to distribute in the aqueous phase. In contrast, the

ratios of 4800 nm PSPs in the depositional phase reached 93 – 97 %, implying that 4800 nm PSPs introduced by *D. magna* fell sedimented into the depositional phase. It can be concluded that the particle size influenced the fate of PSPs introduced by the prey in the simulated aquatic system.
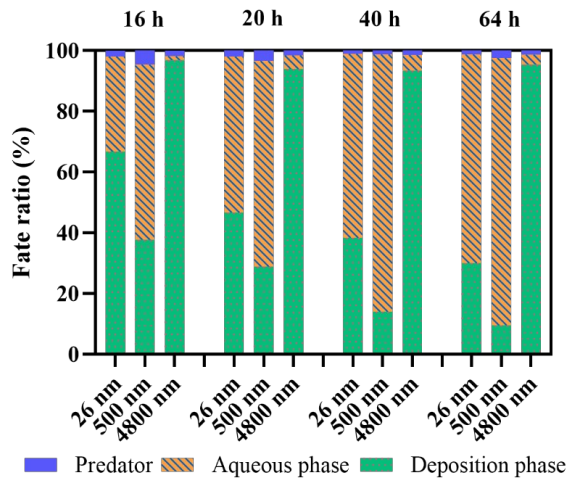

Figure 4.2 Fate ratio (%) of PSPs introduced from *D. magna* to *L. benedeni*, the aqueous phase and the depositional phase.

4.3.4 Trophic transfer of PSPs from *D. magna* to *L. benedeni*

The variation of the mass concentrations of PSPs with different sizes in the predator (*L. benedeni*) transferred from the prey (*D. magna*) over the feeding exposure and depuration periods is presented in Figure 4.3. Generally, the mass concentrations of all PSPs increased in *L. benedeni* after the feeding exposure of 16 h (Figure 4.3) and a significant

difference ($p < 0.05$) from the control group (Table S4.2) was observed, indicating transfer of PSPs from the prey to the predator. The variation in the average mass concentration between the exposure and control groups decreased in order of 4800 nm (4 µg PSPs/g mysid wet mass) > 26 nm (3 µg PSPs/g mysid wet mass) > 500 nm (2 µg PSPs/g mysid wet mass). This also means that the extent of trophic transfer of 4800 nm PSPs to *L. benedeni* was the highest among the studied PSPs based on the mass concentrations, which corresponded to the highest accumulation concentration of 4800 nm PSPs in *D. magna*. Moreover, the extent of trophic transfer of 26 nm PSPs was higher than for the 500 nm PSPs, although their extent of accumulation in *D. magna* was similar. During the 48 h depuration period (Figure 4.3), there was no significant difference in the mass concentration for the 26 nm PSP treatment between the exposure groups and control groups. Note that the average mass concentration of the 26 nm PSPs at 20 h was higher than in the control group. For the 500 nm PSP treatment, although no significant difference in the mass concentration was found between the exposure groups and control groups, the average mass concentrations of the exposure groups at the different time endpoints were slightly higher than the mass concentrations of the control groups. The mass concentration of 4800 nm PSPs in *L. benedeni* did not change significantly ($p > 0.05$) among the exposure groups with time, but was significantly higher than in the control group ($p < 0.05$). This implied that PSPs were retained in the predator. The difference in the average mass concentration between the exposure groups and control groups is supported by the appearance of a fluorescent signal in the PSP-exposed groups observed in the biodistribution (Figure 4.4). Generally, during the 48 h depuration period, the order of magnitude of the average mass concentration was 4800 nm > 500 nm > 26 nm, which

corresponds to the order of mass concentration of PSPs during the feeding exposure period. Furthermore, as shown in Table 4.1, the elimination rate derived from cutting off the background data was found to be relatively low for all treatments. No significant difference in elimination rate constants between PSPs of different sizes was found ($p > 0.05$). This suggests that the particle size of PSPs did not influence the kinetics of depuration process.
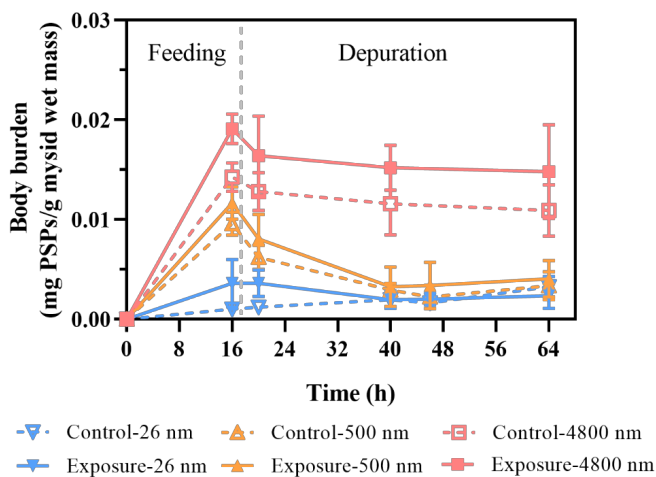

Figure 4.3 Concentration of PSPs (26, 500 and 4800 nm) in *L. benedeni* after a 16 h exposure period and a 48 h depuration period.

The biodistribution of PSPs (26, 500 and 4800 nm) in *L. benedeni* was observed over the 16 h feeding exposure period and 48 h depuration period, as shown in Figure S4.4 (Supplementary data). All controls remained non-fluorescent in the studied areas of *L. benedeni* tissues during all timepoints. After 16 and 20 h of exposure, a strong fluorescence was observed in the organisms exposed to the small sized PSPs (26 nm), while weak fluorescence was detected in the feeding

exposure treatments of 500 and 4800 nm PSPs. The strong intensity of fluorescence of the 26 nm PSPs was in correspondence to the high number concentration of particles in the mysids transferred from daphnids. This is also associated with the initial exposure to a greater particle number of 26 nm PSPs. It is worth mentioning that fluorescent particles were mainly visible in the digestive tract (stomach and intestine) over time, and no translocation of any of the studied PSPs into other tissues was observed in *L. benedeni*. This finding was similar to a previous study on brine shrimp *Artemia franciscana* larvae exposed to 40 and 50 nm PSPs, which were found to be considerably accumulated in the guts of *A. franciscana* (Brun et al., 2017).
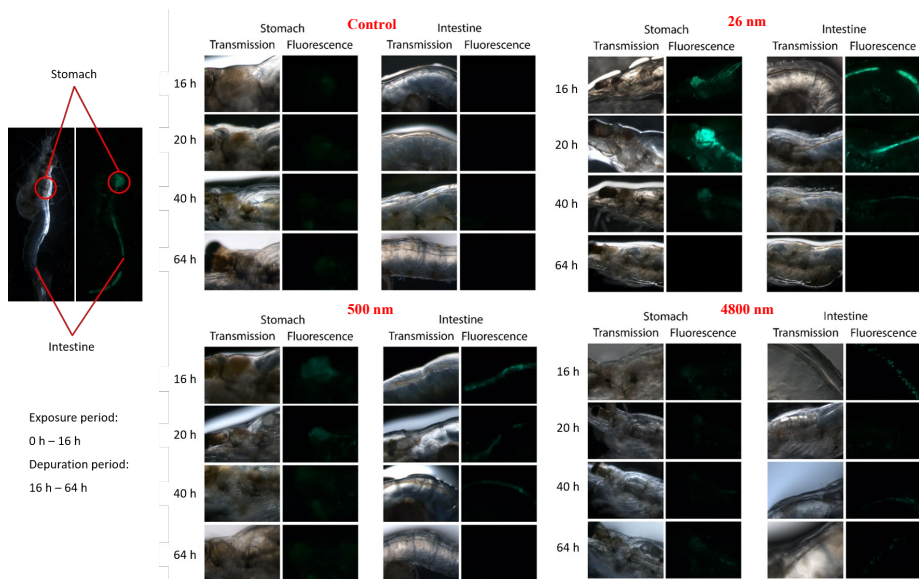

Figure 4.4 Representative images demonstrating the accumulation of PSPs (26, 500 and 4800 nm) in the stomach and intestine of *L. benedeni* over a 16 h feeding exposure period and a 48 h depuration period.

TTFs based on the mass concentration during the feeding and depuration periods were evaluated, as shown in Table 4.2. All TTF values were found to be less than 1, regardless of the size of the PSPs and the exposure time. Hence, the extent of transfer of PSPs from *D. magna* to *L. benedeni* was limited and not associated with their particle sizes. In other kinds of food chains, a low extent of NMPs transfer was also observed. For instance, a TTF value < 1 was determined for 6 μm PSPs as they were transferred from *D. magna* to *Pimephales promelas* (Elizalde-Velázquez et al., 2020a). The biomagnification of 6 μm PSPs from mussels to crabs did not occur as well (Wang et al., 2021).

Table 4.1 Trophic transfer factor (TTF) for the PSPs with sizes of 26, 500 and 4800 nm at the different time intervals [a].

Time (h)	PSPs		
	26 nm	500 nm	4800 nm
16	0.001 ± 0.001	0.000 ± 0.000	0.000 ± 0.000
20	0.001 ± 0.000	0.000 ± 0.001	0.000 ± 0.000
40	0.000 ± 0.000	0.000 ± 0.000	0.000 ± 0.000
64	0.000 ± 0.000	0.000 ± 0.000	0.000 ± 0.000

[a] Data were derived by comparing experimental values to the background auto-fluorescence values.

A challenge in using fluorescently labelled PSPs in uptake and elimination studies is the potential dissociation of dye from the particles (Schür et al., 2019) and Catarino et al. (2019), which can result in false-negative identification of particles in the examined medium, matrix or cell culture when using fluorometric methods for detection. If dye-release contributed to a large extent to the regarding uptake,

elimination and biodistribution, similar kinetic patterns would likely have been observed regardless of particle size (assuming that particle size is not determining the rate of dye-release). In the current experiment, large differences were observed in fluorescent signals in tissues from organisms exposed to different particle sizes, also when accounting for differences in exposure concentrations expressed as fluorescence intensity. In particular, comparisons of fluorescence intensities of PSPs between 26 nm and 4800 nm and between 500 nm and 4800 nm detected after 2 hours exposure to daphnia (uptake reaching to plateau) demonstrated a statistically significant difference ($p < 0.001$), as shown in Table S4.3. There is no a statistically significant difference in the fluorescence intensities of PSPs between 26 nm and 500 nm (Table S4.3), whereas the averaged fluorescence intensities of 26 nm PSPs were higher than the averaged fluorescence intensities of 500 nm PSPs. These evidences indicated that the PSP particles alone considerably contributed to the uptake process rather than the leaching dye, otherwise similar fluorescence intensities should be found between the PSPs with different particle size. Consequently, the labelled PSP particles can be determined in the organisms.

4.4 Conclusions

This work showed that particle size influenced the extent of accumulation and trophic transfer of PSPs from the prey (*D. magna*) to the predator (*L. benedeni*) in the simulated aquatic system. The increase of the mass concentration of PSPs with a large size (4800 nm) was higher than the increase of the mass of internalized PSPs with a small size (26 or 500 nm). Moreover, the uptake rate of 26 and 4800

nm PSPs in *D. magna* was significantly higher than the uptake rate of the 500 nm PSPs. It was estimated that a small fraction of each PSP introduced by *D. magna* was transferred to *L. benedeni*, whereas a large fraction of the PSPs was released in the aqueous phase (26 and 500 nm PSPs) and in the depositional phase (4800 nm PSPs). The extent of trophic transfer from *D. magna* to *L. benedeni* decreased in the order of 4800 nm > 26 nm > 500 nm PSPs. Moreover, there was no significant difference in elimination rate constants between PSPs of different sizes. Furthermore, fluorescence observations in *L. benedeni* revealed that PSPs accumulate mainly in the intestinal tract. In addition, the TTF values of all the studied PSPs were less than 1, implying that trophic transfer was limited in the simulated aquatic food chain. In summary, the study provides evidence that the role of particle size cannot be neglected in regulating the bioaccumulation and fate of PSPs in the aquatic environment.

References

Adam, N.; Schmitt, C.; Galceran, J.; Companys, E.; Vakurov, A.; Wallace, R.; Knapen, D.; Blust, R. The chronic toxicity of ZnO nanoparticles and ZnCl$_2$ to *Daphnia magna* and the use of different methods to assess nanoparticle aggregation and dissolution. Nanotoxicology 2014, 8, 709-717.

Al-Reasi, H. A.; Wood, C. M.; Smith, D. S. Physicochemical and spectroscopic properties of natural organic matter (NOM) from various sources and implications for ameliorative effects on metal toxicity to aquatic biota. Aquat. Toxicol. 2011, 179-190.

Baker, B. J. Investigation of the competitive effects of copper and zinc on fulvic acid complexation: Modeling analytical approaches, Colorado School of Mines, 2012.

Bliss, C. I. The toxicity of poisons applied jointly. Ann. Appl. Biol. 1939, 26, 585-615.

Bondarenko, O.; Juganson, K.; Ivask, A.; Kasemets, K.; Mortimer, M.; Kahru, A. Toxicity of Ag, CuO and ZnO nanoparticles to selected environmentally relevant test organisms and mammalian cells *in vitro*: A critical review. Arch. Toxicol. 2013, 1181-1200.

Bossuyt, B. T.; Janssen, C. R. Copper regulation and homeostasis of *Daphnia magna* and *Pseudokirchneriella subcapitata*: Influence of acclimation. Environ. Pollut. 2005, 136: 135-144.

Clifford, M.; McGeer, J. C. Development of a biotic ligand model for the acute toxicity of zinc to *Daphnia pulex* in soft waters. Aquat. Toxicol. 2009, 91, 26-32.

Cooper, N. L.; Bidwell, J. R.; Kumar, A. Toxicity of copper, lead, and zinc mixtures to *Ceriodaphnia dubia* and *Daphnia carinata*. Ecotoxicol. Environ. Saf. 2009, 72, 1523-1528.

Crémazy, A.; Brix, K. V.; Wood, C. M. Using the biotic ligand model framework to investigate binary metal interactions on the uptake of Ag, Cd, Cu, Ni, Pb and Zn in the freshwater snail *Lymnaea Stagnalis*. Sci. Total Environ. 2019, 647, 1611-1625.

Cronholm, P.; Karlsson, H.L.; Hedberg, J.; Lowe, T.A.; Winnberg, L.; Elihn, K.; Wallinder, I.O.; Möller, L. Intracellular uptake and toxicity of Ag and CuO nanoparticles: a comparison between nanoparticles and their corresponding metal ions. Small. 2013, 9: 970-982.

Cupi, D.; Hartmann, N. B.; Baun, A. The influence of natural organic matter and aging on suspension stability in guideline toxicity testing of silver, zinc oxide, and titanium dioxide nanoparticles with *Daphnia magna*. Environ. Toxicol. Chem. 2015, 34, 497-506.

Deng, R.; Lin, D.; Zhu, L.; Majumdar, S.; White, J. C.; Gardea-Torresdey, J. L.; Xing, B. Nanoparticle interactions with co-existing contaminants: Joint toxicity, bioaccumulation and risk. Nanotoxicology. 2017, 11, 591-612.

DePalma, S. G. S.; Ray Arnold, W.; McGeer, J. C.; George Dixon, D.; Scott Smith, D. Effects of dissolved organic matter and reduced sulphur on copper bioavailability in coastal marine environments. Ecotoxicol. Environ. Saf. 2011, 74, 230-237.

Fabrega, J.; Fawcett, S. R.; Renshaw, J. C.; Lead, J. R. Silver nanoparticle impact on bacterial growth: effect of pH, concentration, and organic matter. Environ. Sci. Technol. 2009, 43, 7285-7290.

Field, S.; Sea, S. W. B. Stabilization of Metals and Shooting Range Soils - the Metalloids in Contaminated Effect of Iron-Based Amendments, University of Oslo, 2014.

Geller, W.; Müller, H. The filtration apparatus of cladocera: Filter mesh-sizes and their implications on food selectivity. Oecologia 1981, 49, 316-321.

Gheorghiu, C.; Smith, D. S.; Al-Reasi, H. A.; McGeer, J. C.; Wilkie, M. P. Influence of natural organic matter (NOM) quality on Cu-gill binding in the rainbow trout (*Oncorhynchus mykiss*). Aquat. Toxicol. 2010, 97, 343-352.

Green, N. W.; Mcinnis, D.; Hertkorn, N.; Maurice, P. A.; Perdue, E. M. Suwannee River Natural Organic Matter: Isolation of the 2R101N Reference Sample by Reverse Osmosis.

Guinée, J. B.; Heijungs, R.; Vijver, M. G.; Peijnenburg, W. J. G. M. Setting the stage for debating the roles of risk assessment and life-cycle assessment of engineered nanomaterials. Nat. Nanotechnol. 2017, 12, 727-733.

Gustafsson, J. P. Visual MINTEQ 3.1. https://vminteq.lwr.kth.se/: KTH, Sweden.

Ho, K. T.; Portis, L.; Chariton, A. A.; Pelletier, M.; Cantwell, M.; Katz, D.; Cashman, M.; Parks, A.; Baguley, J. G.; Conrad-Forrest, N.;

Boothman, W.; Luxton, T.; Simpson, S. L.; Fogg, S.; Burgess, R. M. Effects of micronized and nano-copper azole on marine benthic communities. Environ. Toxicol. Chem. 2018, 37, 362-375.

Hyne, R. V.; Pablo, F.; Julli, M.; Markich, S. J. Influence of water chemistry on the acute toxicity of copper and zinc to the cladoceran *Ceriodaphnia cf dubia*. Environ. Toxicol. Chem. 2005, 24, 1667-1675.

Liu, Y.; Baas, J.; Peijnenburg, W. J. G. M.; Vijver, M. G. Evaluating the combined toxicity of Cu and ZnO nanoparticles: Utility of the concept of additivity and a nested experimental design. Environ. Sci. Technol. 2016, 50, 5328-5337.

Komjarova, I.; Blust, R. Multi-metal interactions between Cd, Cu, Ni, Pb and Zn in water flea Daphnia magna, a stable isotope experiment. Aquat. Toxicol. 2008, 90, 138-144.

Lee, B. T.; Ranville, J. F. The effect of hardness on the stability of citrate-stabilized gold nanoparticles and their uptake by *Daphnia magna*. J. Hazard. Mater. 2012, 213-214, 434-439.

Lopes, S.; Ribeiro, F.; Wojnarowicz, J.; Lojkowski, W.; Jurkschat, K.; Crossley, A.; Soares, A. M. V. M.; Loureiro, S. Zinc oxide nanoparticles toxicity to *Daphnia magna*: Size-dependent effects and dissolution. Environ. Toxicol. Chem. 2014, 33, 190-198.

Lorenzo, J. I.; Beiras, R.; Mubiana, V. K.; Blust, R. Copper uptake by Mytilus edulis in the presence of humic acids. Environ. Toxicol. Chem. 2005, 24, 973-980.

Lores, E. M.; Snyder, R. A.; Pennock, J. R. The effect of humic acid on uptake/adsorption of copper by a marine bacterium and two marine ciliates. Chemosphere 1999, 38, 293-310.

Ma, D. Hybrid nanoparticles: An introduction - ScienceDirect. 2019.

Meyer, J. S.; Ranville, J. F.; Pontasch, M.; Gorsuch, J. W.; Adams, W. J. Acute toxicity of binary and ternary mixtures of Cd, Cu, and Zn to *Daphnia magna*. Environ. Toxicol. Chem. 2015, 34, 799-808.

Minteq, V.; Agency, E. P. Visual MINTEQ - a Brief Tutorial. 2000, 1-5.

Mitrano, D. M.; Motellier, S.; Clavaguera, S.; Nowack, B. Review of nanomaterial aging and transformations through the life cycle of nano-enhanced products. Environ. Int. 2015, 77: 132-147.

Nadella, S. R.; Fitzpatrick, J. L.; Franklin, N.; Bucking, C.; Smith, S.; Wood, C. M. Toxicity of dissolved Cu, Zn, Ni and Cd to developing embryos of the blue mussel (*Mytilus trossolus*) and the protective effect of dissolved organic carbon. Comp. Biochem. Physiol. - C Toxicol. Pharmacol. 2009, 149, 340-348.

Nogueira, L. S.; Bianchini, A.; Smith, S.; Jorge, M. B.; Diamond, R. L.; Wood, C. M. Physiological effects of five different marine natural organic matters (NOMs) and three different metals (Cu, Pb, Zn) on early life stages of the blue mussel (*Mytilus galloprovincialis*). PeerJ 2017, 5: e3141.

OECD. Guideline for Testing of Chemicals. Daphnia sp., Acute Immobilization Test. OECD 202. Paris, 2004.

Ogunsuyi, O. I.; Fadoju, O. M.; Akanni, O. O.; Alabi, O. A.; Alimba, C. G.; Cambier, S.; Eswara, S.; Gutleb, A. C.; Adaramoye, O. A.; Bakare, A. A. Genetic and systemic toxicity induced by silver and copper oxide nanoparticles, and their mixture in Clarias gariepinus (Burchell, 1822). Environ. Sci. Pollut. Res. 2019, 26, 27470-27481.

Qiao, R.; Lu, K.; Deng, Y.; Ren, H.; Zhang, Y. Combined effects of polystyrene microplastics and natural organic matter on the accumulation and toxicity of copper in zebrafish. Sci. Total Environ. 2019, 682, 128-137.

Sani-Kast, N.; Labille, J.; Ollivier, P.; Slomberg, D.; Hungerbühler, K.; Scheringer, M. A network perspective reveals decreasing material diversity in studies on nanoparticle interactions with dissolved organic matter. Proc. Natl. Acad. Sci. U. S. A. 2017, 114, E1756-E1765.

Sharma, V. K.; Sayes, C. M.; Guo, B.; Pillai, S.; Parsons, J. G.; Wang, C.; Yan, B.; Ma, X. Interactions between silver nanoparticles and other metal nanoparticles under environmentally relevant conditions: A review. Sci. Total Environ. 2019, 653, 1042-1051.

Tervonen, K.; Waissi, G.; Petersen, E. J.; Akkanen, J.; Kukkonen, J. V. K. Analysis of fullerene-C60 and kinetic measurements for its accumulation and depuration in *Daphnia magna*. Environ. Toxicol. Chem. 2010, 29, 1072-1078.

Unsworth, E. R.; Warnken, K. W.; Zhang, H.; Davison, W.; Black, F.; Buffle, J.; Cao, J.; Cleven, R.; Galceran, J.; Gunkel, P.; et al. Model predictions of metal speciation in freshwaters compared

to measurements by in situ techniques. Environ. Sci. Technol. 2006, 40, 1942-1949.

Wang, Z.; Chen, J.; Li, X.; Shao, J.; Peijnenburg, W. J. G. M. Aquatic toxicity of nanosilver colloids to different trophic organisms: contributions of particles and free silver ion. Environ. Toxicol. Chem. 2012, 31, 2408-2413.

Wang, Z.; Li, J.; Zhao, J.; Xing, B. Toxicity and internalization of CuO nanoparticles to prokaryotic alga *Microcystis aeruginosa* as affected by dissolved organic matter. Environ. Sci. Technol. 2011, 45, 6032-6040.

Wang, Z.; Zhang, L.; Zhao, J.; Xing, B. Environmental processes and toxicity of metallic nanoparticles in aquatic systems as affected by natural organic matter. Environ. Sci. Nano 2016, 3, 240-255.

Wilke, C. M.; Wunderlich, B.; Gaillard, J. F.; Gray, K. A. Synergistic bacterial stress results from exposure to nano-Ag and nano-TiO$_2$ mixtures under light in environmental media. Environ. Sci. Technol. 2018, 52, 3185-3194.

Wu, J., Wang, G., Vijver, M.G., Bosker, T., Peijnenburg, W.J.G.M. Foliar versus root exposure of AgNPs to lettuce: Phytotoxicity, antioxidant responses and internal translocation. Environ. Pollut. 2020, 261, 114117.

Xiao, Y.; Peijnenburg, W. J. G. M.; Chen, G.; Vijver, M. G. Impact of water chemistry on the particle-specific toxicity of copper nanoparticles to *Daphnia magna*. Sci. Total Environ. 2018, 610-611, 1329-1335.

Xiao, Y.; Vijver, M. G.; Chen, G.; Peijnenburg, W. J. G. M. Toxicity and accumulation of Cu and ZnO nanoparticles in *Daphnia magna*. Environ. Sci. Technol. 2015, 49, 4657-4664.

Ye, N.; Wang, Z.; Wang, S.; Peijnenburg, W. J. G. M. Toxicity of mixtures of zinc oxide and graphene oxide nanoparticles to aquatic organisms of different trophic level: particles outperform dissolved ions. Nanotoxicology 2018, 12, 423-438.

Yu, R.; Wu, J.; Liu, M.; Zhu, G.; Chen, L.; Chang, Y.; Lu, H. Toxicity of binary mixtures of metal oxide nanoparticles to *Nitrosomonas Europaea*. Chemosphere 2016, 153, 187-197.

Zhang, Y.; Chen, Y.; Westerhoff, P.; Crittenden, J. Impact of natural organic matter and divalent cations on the stability of aqueous nanoparticles. Water Res. 2009, 43, 4249-4257.

Supplementary Information

Table S4.1 Survival (%) of *D. magna* exposed to various concentrations of PSPs with different sizes of 26 nm, 500 nm and 4800 nm after 24 h of exposure [a]

Exposure concentrations (mg/L)	PSPs		
	26 nm	500 nm	4800 nm
0	100 ± 0%	100 ± 0%	100 ± 0%
0.5	100 ± 0%	100 ± 0%	100 ± 0%
1	100 ± 0%	96 ± 9%	100 ± 0%
2	100 ± 0%	100 ± 0%	96 ± 9%
4	100 ± 0%	96 ± 9%	92 ± 18%
8	96 ± 9%	100 ± 0%	100 ± 0%

[a] Values are expressed as mean ± standard deviation (n = 5). Each replicate contained five daphnids.

Table S4.2 Levels for significant (p) comparison between the concentrations of PSPs in *L. benedeni* between control groups [a] and exposure groups [b] ($p < 0.05$ indicates a significant difference)

Time (h)	26 nm	500 nm	4800 nm
16	0.00	0.03	0.00
20	0.00	0.06	0.01
40	0.95	0.71	0.00
46	0.12	0.14	--
64	0.07	0.42	0.02

[a] Treatments without exposure.

[b] Treatments fed up with daphnids exposed PSPs with different sizes of 26 nm, 500 nm and 4800 nm.

Table S4.3 Levels for significant (p) comparison among the fluorescence intensities (FI) of PSPs in *D. magna* after 2 hours exposure (p < 0.05 indicates a significant difference) [a]

(I) group	log *FI*	(J) group	p
4800 nm	4.209 ± 0.165	500 nm	0.000
		26 nm	0.000
500 nm	4.041 ± 0.133	4800 nm	0.000
		26 nm	0.777
26 nm	4.064 ± 0.121	4800 nm	0.000
		500 nm	0.777

[a] Fluorescence data were Log10 transformed to assure that the requirements for residual- and variance distributions were met.
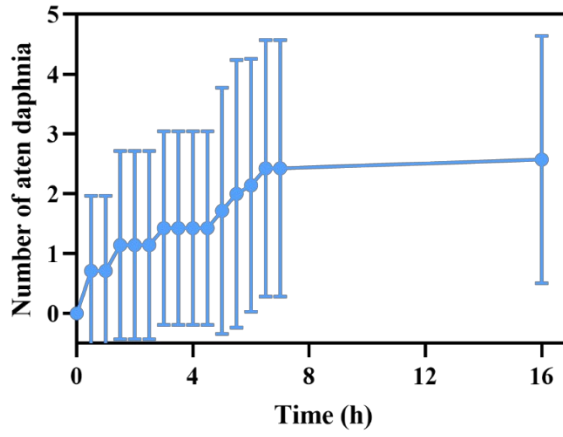
Figure S4.1 The number of the waterflea (*D. magna*) eaten over time by the mysid (*L. benedeni*).
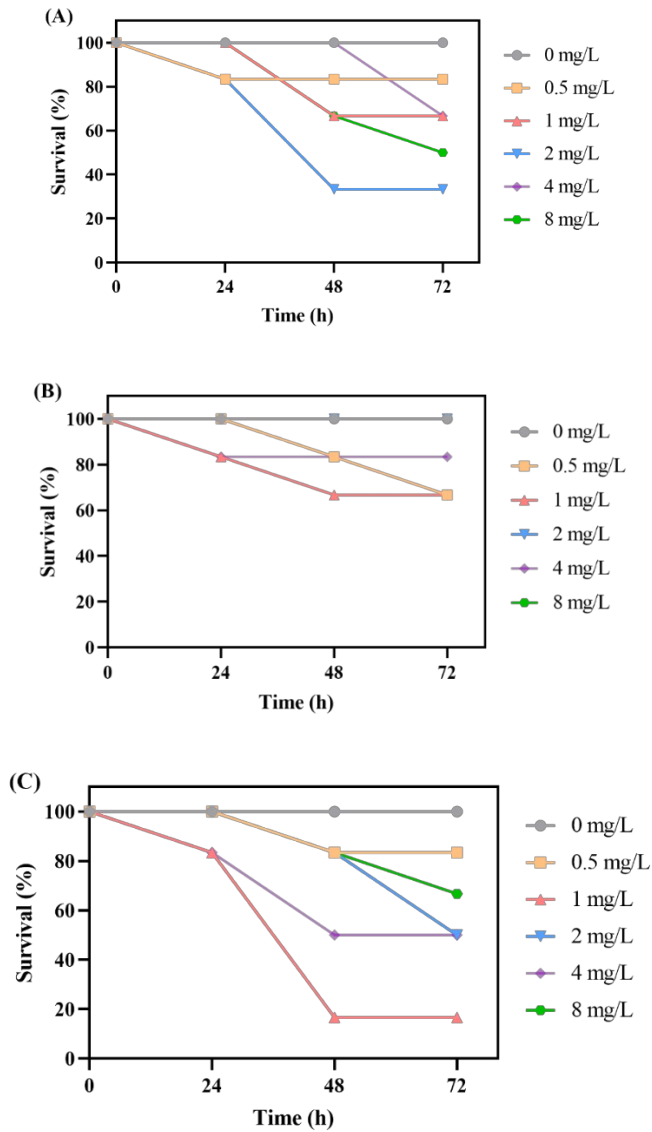
Figure S4.2 Survival (%) of the mysid (*L. benedeni*) exposed to PSPs with sizes of 26 nm (A), 500 nm (B) and 4800 nm (C). The exposure concentrations of PSPs were 0, 0.5, 1, 2, 4 and 8 mg/L. Each treatment contained ten shrimps.
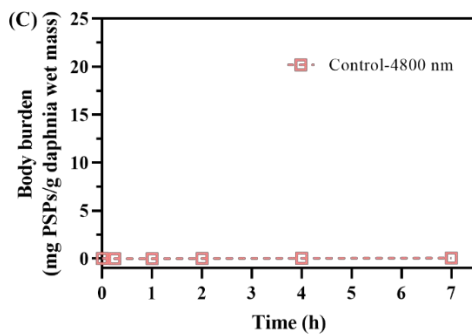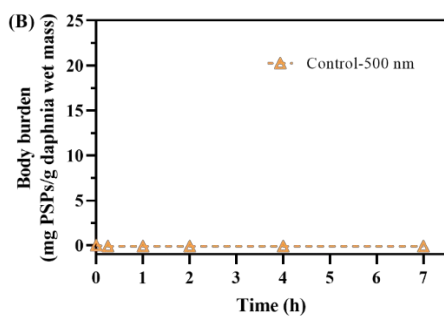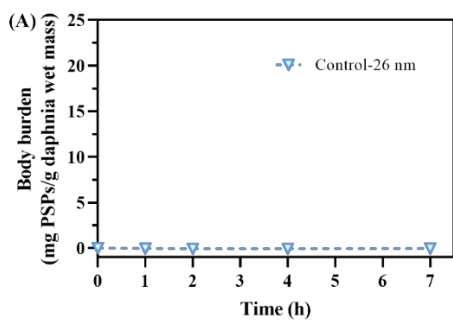
Figure S4.3 Control group data for the accumulation of PSPs (26, 500 and 4800 nm) in *D. magna* neonates over 7 h exposure period.
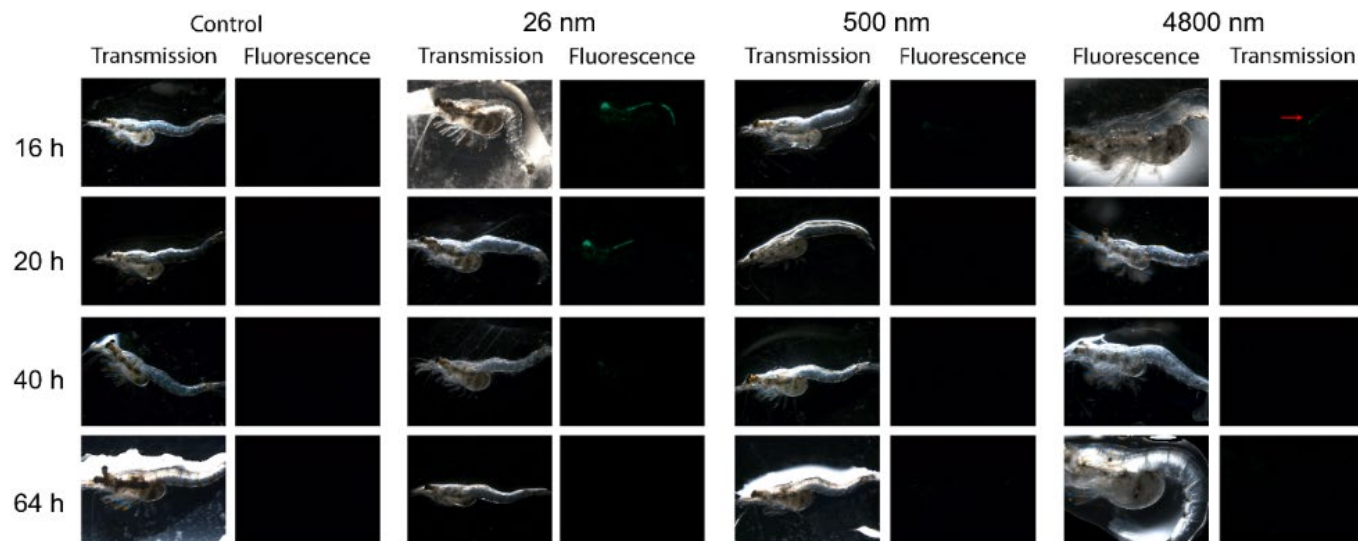
Figure S4.4 Representative images demonstrating the accumulation of PSPs (26, 500 and 4800 nm) in *L. benedeni* over a 16 h exposure period and a 48 h depuration period.

Chapter 5

Trophic transfer of Cu nanoparticles in a simulated aquatic food chain

Qi Yu, Zhenyan Zhang, Fazel Abdolahpur Monikh, Juan Wu, Zhuang Wang, Martina G. Vijver, Thijs Bosker, Willie J. G. M. Peijnenburg

Abstract

The goal of the current study was to quantify the trophic transfer of copper nanoparticles (CuNPs) in a food chain consisting of the microalgae *Pseudokirchneriella subcapitata* as a representative of primary producers, the grazer *Daphnia magna,* and the omnivorous mysid *Limnomysis benedeni.* To quantify the size and number concentration of CuNPs in the biota, tissue extraction with tetramethylammonium hydroxide (TMAH) was performed and quantification was done by single particle inductively coupled plasma mass spectrometry (sp-ICP-MS). The bioconcentration factor (BCF) of the test species for CuNPs varied between $10^2 - 10^3$ L/kg dry weight when expressing the internal concentration on a mass basis, which was lower than BCF values reported for Cu^{2+} ($10^3 - 10^4$ L/kg dry weight). The particle size of CuNPs determined by sp-ICP-MS ranged from 22 to 40 nm in the species. No significant changes in the particle size were measured throughout the food chain. Moreover, the measured number of CuNPs in each trophic level was in the order of 10^{13} particles/kg wet weight. The calculated trophic transfer factor (mass concentration basis) was > 1. This indicates biomagnification of particulate Cu from *P. subcapitata* to *L. benedeni.* It was also found that the uptake of particulate Cu (based on the particle number concentration) was mainly from the dietary route rather than from direct aqueous exposure. Furthermore, dietary exposure to CuNPs had a significant effect on the feeding rate of mysid during their transfer from daphnia to mysid and from algae through daphnia to mysid. This work emphasizes the importance of tracing the particulate fraction of metal-based engineered nanoparticles when studying their uptake and trophic transfer.

5.1 Introduction

Copper nanoparticles (CuNPs) are known for their excellent thermophysical properties and their fairly inexpensive synthesis. As a result, CuNPs have many applications, including in semiconductors, electronic chips, and heat transfer nanofluids (Kim et al., 2016; Li et al., 2021). However, CuNPs can be released into the aquatic environment (Holden et al., 2016; Keller and Lazareva, 2013). This way, CuNPs can be taken up by a variety of organisms and might also be transferred along a food chain (Siddiqui and Bielmyer-Fraser, 2019; Tangaa et al., 2016). Examples reported in literature evidenced that metal-based NPs can affect multiple levels in the food chain, e.g. primary producers and herbivorous consumers following exposure to AgNPs (Kalman et al., 2015; Sharma et al., 2019; Yan and Wang, 2021), quantum dots (Rocha et al., 2017) and TiO_2NPs (Chen et al., 2015; Wang et al., 2017). Several studies reported that dietary uptake of NPs can induce more severe effects compared to direct waterborne exposure (Jackson et al., 2012; Kalman et al., 2015; Wu et al., 2017). However, the data available for the trophic transfer of CuNPs through a multiple-level aquatic food chain are limited and inconclusive.

Distinguishing the differences in uptake pathways and trophic transfer processes between the particulate form of CuNPs and their dissolved-release ions is a critical gap in existing research. Trophic transfer ability can be quantified from the ratio of the mass concentration of NPs in the body of a predator and the mass concentration of these NPs in the prey (Chen et al., 2015; Lee et al., 2015; Yan and Wang, 2021). Body mass concentrations are generally quantified as the total metal content including both the NPs and the dissolved metal ions (Baccaro et al., 2018). However, some studies

have reported that NPs cause as much effect or even more effect than the ionic form of the same metal (Shoults-Wilson et al., 2011; Xiao et al., 2015). For instance, Xiao et al. (2015) found that Cu particles rather than the dissolved Cu ions were the major source of toxicity for water-exposed daphnids. Others found that the dissolved fraction of metal ions causes most of the effects when evaluating NPs toxicity (Adam et al., 2014; Jo et al., 2012). To evaluate the environmental risks of the particulate form of Cu, we expressed the transfer of CuNPs through the food chain based on the particle's number and size distribution in biota of different trophic levels. We also did the same by using mass as the basis for expressing transfer. To date, a limited number of studies (Monikh et al., 2019a; Heringa et al., 2018; Monikh et al., 2021; Taboada-López et al., 2018) have reported on particle number based transfer. This can be explained by the analytical challenges of quantifying particle numbers in complex media such as the whole body and specific tissues of biota.

In the present study, we aim to investigate: (1) whether CuNPs transfer through an aquatic food chain and undergo biomagnification in consumers; (2) to what extent CuNPs can transfer in particulate, and ionic forms and how the particle size and number change in different organisms; and (3) the effect of dietary CuNPs exposure on the survival and feeding rate of the predator (mysids). Accordingly, we used the mass and particle number of the CuNPs as dose metrics. The microalga *Pseudokirchneriella subcapitata* (Kalman et al., 2015; Wang et al., 2019) was selected as a primary producer and the zooplankton *Daphnia magna* (Chen et al., 2015; Dalai et al., 2014; Lee et al., 2015; Ribeiro et al., 2017; Wu et al., 2017) as being representative of consumers grazing on algae. The omnivorous mysid *Lymnomysis benedeni* (Boda and Borza, 2013; Gergs et al., 2008; Hanselmann,

2012) was selected as the predator. The predator *L. benedeni* can provide information on three food transfer cases: case-1 from *P. subcapitata* to *L. benedeni*, case-2 from *D. magna* to *L. benedeni*, and case-3 from *P. subcapitata* to *D. magna* to *L. benedeni*. Moreover, we developed a multistep sample preparation method consisting of the extraction of particles from tissues with tetramethylammonium hydroxide (TMAH). Then, the extracted samples were used to quantify the separated CuNPs by single particle inductively coupled plasma mass spectrometry (sp-ICP-MS). The obtained findings emphasize the roles of particle number and size of particulate Cu in the aquatic organisms in assessing the trophic transfer of CuNPs. Hence, this work will gain a better understanding of the risk of soluble NPs to ecosystems.

5.2 Materials and Method

5.2.1 Test materials

Spherical CuNPs were purchased from IoLiTecGmbh (Heibronn, Germany) with a specific surface area of 30-50 m²/g, > 99.5% purity and the nominal size of 25 nm. TMAH (25% w/w) and nitric acid (HNO$_3$, 65%) were obtained from Sigma-Aldrich (Zwijndrecht, The Netherlands).

5.2.2 Physicochemical characterization

The morphology and size of the CuNPs were determined using transmission electron microscopy (TEM, JEOL 1010, JEOL Ltd., Japan). The hydrodynamic diameter (Z-average) and zeta potential

(mV) of 1 mg/L NPs in Milli-Q water and in different exposure media were analyzed using a ZetaSizer Nano-ZS instrument (Malvern, Instruments Ltd., UK). Furthermore, sp-ICP-MS (PerkinElmer, NexION 2000 ICP-MS operating in sp mode) was applied to measure the particle number concentration and the size distribution of the particles. The method development and validation have been performed in-house and published lately (Monikh et al., 2021). To measure the number of the particles, CuNPs were mixed with Woods Hole Medium (Janet Stein, 1982) and Elendt M7 medium (OECD, 2004; Samel et al., 1999) (submerging 1 mL of a 100 mg/L stock suspension into 99 mL) for 24 h. During the 24 h of incubation, all suspensions were stored in a climate chamber under a 16:8 h light-dark cycle (temperature: 22 ± 1 °C, RH: 80.0%). The samples were collected at the top 1.5-2 cm layer of the dispersions at 0 and 24 h. Meanwhile, the ion release profiles and the particle aggregation kinetics of the CuNPs were evaluated. The results are shown in Supplementary data.

5.2.3 Trophic transfer experiments

The assembled food chains consisting of either 2 or 3 levels were examined, using *P. subcapitata, D. magna* and *L. benedeni.* The details of the culturing of the organisms are described in the Supplementary data.

Case-1: 2-level food chain from *P. subcapitata* to *L. benedeni.* The algal (*P. subcapitata*) cells at a density of 5.0×10^6 cells/mL were first exposed for 24 h in a suspension of 1 mg/L CuNPs as prepared in the Woods Hole Medium (Janet Stein, 1982). The compositions of Woods Hole Medium are listed in Table S5.1, Supplementary data. The

treatment group contained 10 replicates with 6 controls, containing only test medium and algae. All test glass vials (200 mL) with algae and test solutions (50 mL) were covered using cotton to allow for CO_2 diffusion. The containers were placed on a shaker (110-120 rpm) at 22 ± 2°C and continuously illuminated at a density of 31-51 μmol m^{-2} s^{-1} as measured via Apogee line quantum sensors (Apogee Instruments, MQ-301). The pH of the test media was measured at the beginning and end of the exposure period. The harvested algal cells pre-contaminated with NPs in the Woods Hole Medium were introduced as food to the mysids for 24 h after washing 3 times. As part of the washing procedure, the algae were centrifuged at 2000 rpm for 5 min with 0.05 M ethylene diamine-tetra acetic acid (EDTA) twice and then once with clean Elendt M7 medium. As a chelating agent, EDTA has been frequently used to complex and remove Cu bound to the surface of organisms in previous studies (Bossuyt and Janssen, 2005; Canuel et al., 2021; Gonzalez-Estrella et al., 2017; Wang et al., 2017; Wu et al., 2017). The targeted algal concentration was around 1.0×10^6 cells/mL in each beaker containing one *L. benedeni* individual in 50 mL Elendt M7 medium. The used mysids were allowed to clean their guts one day before exposure. Four replicates were used for each treatment and 20 mysids were included in each replicate. There were also four replicates for the control (without CuNPs or metal nanoparticles). The exposed *P. subcapitata* and *L. benedeni* were washed with 0.05 M EDTA twice and with PBS/Milli-Q water once, then they were directly snap frozen with liquid nitrogen and stored at -80 °C before characterization using sp-ICP-MS.

Case-2: 2-level food chain from _D. magna_ to _L. benedeni._ *D. magna* (< 24 h) was exposed to 1 mg/L CuNPs for 24 h and washed thrice using clean Elendt M7 medium. Then each *L. benedeni* (without feeding for

24 h) was fed with 5 exposed daphnids once during the 24 h feeding period. Each mysid was placed in a beaker with 50 mL Elendt M7 medium. Four replicates were used for each treatment and 20 mysids were included in each replicate. There were also four replicates for the control (non-exposure). After 24 h, *D. magna* and *L. benedeni* were sampled and washed with 0.05 M EDTA twice and once with Milli-Q water, then directly snap frozen with liquid nitrogen and stored at -80 °C for characterization with sp-ICP-MS.

Case-3: 3-level food chain from *P. subcapitata* to *L. benedeni* through *D. magna*. The harvested algal cells pre-contaminated with CuNPs in an aqueous medium were introduced as food to the daphnids for 24 h after washing 3 times with clean Elendt M7 medium. The targeted algal concentration was around 1.0×10^6 cells/mL in each beaker containing 10 *D. magna* individuals (< 24 h). These daphnids were gut cleaned beforehand in 100 mL Elendt M7 medium. Then five of these daphnids were fed to each *L. benedeni* for 24 h as mentioned above for the other food chains.

To quantify the particle or mass concentrations of CuNPs in organisms, three replicates with each treatment containing > 100 daphnids or 15-20 alive mysids were used. To assess the survival of fed mysids, each treatment contained 10 replicates with 15 - 20 alive mysids. For the feeding behavior of mysids on account of the number of ingested daphnia, each treatment contained more than 45 alive mysids.

5.2.4 Extraction of CuNPs from biological tissues

In order to extract CuNPs from the organisms, samples of species of different trophic level were treated with 1 mL of 20% (w/w) TMAH.

This TMAH concentration has already been successfully applied in previous studies (Gray et al., 2013; Jiménez-Lamana et al., 2014; Johnson et al., 2017; Loeschner et al., 2013) and was checked in our test as compared to 5% TMAH. The extraction scheme includes several steps as shown in Figure 5.1. First, biota samples were put into 1 mL of 20% (w/w) TMAH and the suspensions were vortexed for 30 s. Second, the samples were sonicated for 30 minutes in a water bath to speed up the breaking down of the tissue and to prevent particle aggregation. Next, the samples were incubated on a Thermoshaker for 24 h at 70 °C and 800 rpm in order to allow the tissue to interact deeply with TMAH instead of allowing the tissue to settle down on the bottom. To extract the particles adsorbed to the carapace, the samples were sonicated for another 30 min after the incubation. After the digestion procedure, all tissues were dissolved whereas the carapaces of the daphnids and the mysids remained in suspension. Therefore, the samples were centrifuged at 4000 rpm for 10 min to separate the solution and the carapaces. The suspension was transferred to a new tube and the remaining carapaces were washed twice with Milli-Q water. The remaining solution was finally diluted to 5 mL and stored at -80 °C before measurement. The carapace was digested with HNO_3 (65%) at a temperature above 170 °C for around 2 h and then diluted with Milli-Q water to 5 mL. Atomic Absorption Spectroscopy (AAS; Perkin Elmer 1100B) was used to check whether there were still particles or ions left in the digested carapace solutions. The results are shown in Table S5.2.
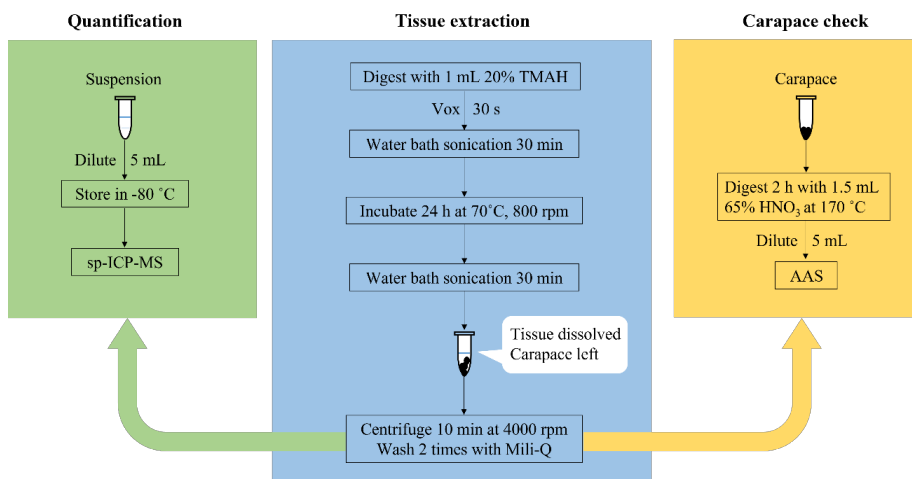
Figure 5.1 Extraction scheme employed in this study.

5.2.5 Particle analysis by sp-ICP-MS

The details of the settings of the instrument and the evaluation of the performance of the extraction method for particles were processed based on previous studies (Monikh et al., 2019a; Cui et al., 2019). The instrumental parameters of the sp-ICP-MS are presented in Table S5.3. The CuNPs suspensions were diluted 1000-fold using ultrapure water to bring the CuNP concentration to a final concentration of within 5000–200000 particles/mL before analysis. The instrument was calibrated using a blank (deionized water) and at least five soluble Cu standards ranging from 0 to 10 ng/g Cu.

5.2.6 Total Cu determination

To measure the total concentration of Cu in the tissues, organism samples were dried to constant weight at 80 °C in an oven (MOV-212S,

SANYO Electric Co., Ltd.) and then digested with HNO_3 (65%) at a temperature exceeding 170 °C for around 2 h. After samples were fully dissolved and the remaining solutions were transparent. They were then transferred to a clean tube and diluted to 5 mL with Milli-Q water. Cu concentrations in all digested samples were determined by ICP-MS (PerkinElmer, NexION 2000). To evaluate the contamination in the used water, blank samples of Milli-Q water were measured. After running the samples of each treatment, the instrument was cleaned by running 2.5% acid nitric in Milli-Q water followed by samples of Milli-Q water. The biological samples without any treatment were also digested and measured to assure that the samples were free of particulate Cu. There are no standard particles available for CuNPs. Thus, AuNPs of 30, 60, and 100 nm were used for calibration of sp-ICP-MS for measuring the size distribution. Standard Cu solutions of 1 ppb, 10 ppb, 50 ppb, and 100 ppb were used to provide the calibration cure using the ICP-MS. Blanks and standard Cu solutions were determined before analysis and between every 20 samples during the analysis. The limit of detection for Cu was 1 ng/L. The relative standard deviation (RSD) of the measurement was less than 5% for all cases.

5.2.7 Calculation of bioconcentration factor and trophic transfer factor

For aqueous exposure, a bioconcentration factor (BCF) was derived as the ratio between the concentration of NPs in biota and the actual concentration in the medium:

$$\text{BCF (L/kg)} = \frac{C_{\text{biota}} \, (\mu g/kg)}{C_{\text{medium}} \, (\mu g/L)} \tag{1}$$

where C_{biota} (μg/kg dry weight) is the metal concentration in the organism and C_{medium} (μg/L) is the metal concentration in the exposure medium.

In addition, the trophic transfer factor (TTF) is a measure of the trophic transfer potential of any substance from one trophic level to the next level in a food chain (Ma et al., 2018). The TTF was determined as the ratio of the NP concentration in the higher lever organism to the concentration in the lower level organism:

$$TTF = \frac{C_{predator}}{C_{prey}} \qquad (2)$$

A value higher than 1 is indicative of a trend of biomagnification, whereas a value less than or equal to 1 indicates that the extent of transfer is limited. More detail of the data processing and the calculations performed are presented in the Supplementary data.

5.2.8 Statistical analysis

All experiments were performed in four replicates, and the data were expressed as mean ± standard deviation. The differences among various groups were assessed using one-way analysis of variance (ANOVA) by Tukey's range test with the IBM SPSS statistics program, and $p < 0.05$ is defined as the significance level.

5.3 Results and discussion

5.3.1 Physicochemical characterizations of CuNPs

Table 5.1 provides the primary particle size, the mode size, and the hydrodynamic size of CuNPs characterized by TEM, sp-ICP-MS, and dynamic light scattering, respectively. The primary sizes of CuNPs were around 20-30 nm, which were similar to their mode sizes (21-31 nm). The hydrodynamic sizes of CuNPs in the Woods Hole Medium and Elendt M7 medium were greater than their primary particle sizes, implying that CuNPs agglomerated in the test media. The characterization of morphology of pristine CuNPs in the test media also indicated that the spherical CuNPs tended to form irregularly shaped agglomerates (Figure S5.1, Supplementary data).

Table 5.1 Particle sizes and zeta potential of 1 mg/L CuNPs suspended in the Woods Hole Medium and Elendt M7 medium [a]

Test medium	Primary particle size (nm) measured by TEM	Mode size (nm) measured by sp-ICP-MS	Hydrodynamic size (nm) measured by dynamic light scattering	Zeta potential (mV)
Woods Hole Medium	24 ± 6	22 ± 1	682 ± 43	-14 ± 0
Elendt M7	24 ± 4	28 ± 3	1046 ± 81	-8 ± 1

[a] Values are expressed as mean ± standard deviation ($n = 3$).

The hydrodynamic size of the CuNPs in the Woods Hole Medium was observed to be lower than the hydrodynamic size of CuNPs in the Elendt M7 medium, as shown in Table 5.1. Moreover, the zeta potential of CuNPs in the Woods Hole Medium was more negative than the zeta

potential of CuNPs in the Elendt M7 medium (Table 5.1). The increase in the absolute zeta potential can result in a high rate of particle movement by inducing the growth of the energy barrier, and then preventing the agglomeration of particles (Guo et al., 2018). Furthermore, the hydrodynamic size of CuNPs in the Woods Hole Medium did not change over time (Figure S5.2, Supplementary data). However, the hydrodynamic size of CuNPs in the Elendt M7 medium shifted from 1336 ± 182 nm to 603 ± 82 nm over 30 min of incubation (Figure S5.2). A reasonable explanation for the decrease in the hydrodynamic size may be due to the sedimentation of larger agglomerates (Arenas-Lago et al., 2019). These findings indicated that the stability of CuNPs in the Woods Hole Medium was higher than their stability in the Elendt M7 medium.
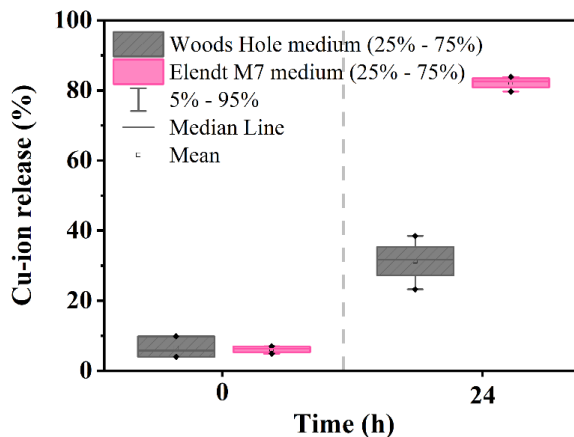

Figure 5.2 Percentage of dissolved Cu released from 1 mg/L CuNPs suspensions after 0 and 24 h of incubation in the Woods Hole Medium and Elendt M7 medium. Values are expressed as mean ± standard deviation (n = 3).

The Cu-ion release profiles from the CuNPs in the test media after 0 and 24 h of incubation are presented in Figure 5.2. The percentages of Cu ions in the CuNPs suspensions were both around 6% at the start of the experiment. However, the percentage of Cu ions in the CuNPs suspensions shifted to 31% in the Woods Hole Medium and even to 82% in the Elendt M7 medium after 24 h of incubation. It can be concluded that particulate Cu might play a more important role in the food chain starting from *P. subcapitata*.

5.3.2 Trophic transfer of CuNPs in the food chain

The actual Cu exposure concentrations in the Woods Hole Medium and Elendt M7 medium were 514 ± 27 μg/L and 355 ± 23 μg/L, respectively, after exposure to CuNPs at a nominal concentration of 1 mg/L. Considering the ion release profiles of CuNPs suspensions, parallel exposure experiments to 10 μg Cu/L $Cu(NO_3)_2$ were conducted to examine the uptake and transfer of dissolved Cu and to compare these properties with the behavior of particulate Cu. Similar to what was done in previous studies (Wang et al., 2015, 2011; Zhang et al., 2018), stable Cu^{2+} ions instead of unstable Cu^+ ions were selected to represent released ionic Cu. This may be due to the fact that: 1) Cu^{2+} has greater a hydration enthalpy than Cu^+, and 2) Cu^+ can spontaneously form Cu and Cu^{2+} ions ($2Cu^+ (aq) \rightarrow Cu^{2+} + Cu$). The amount of Cu taken up from the exposure media by each species and the calculated BCF values are presented in Table 5.2. The amount of CuNPs taken up by the organisms directly from the aquatic exposure medium decreased in the order of *L. benedeni > D. magna ≈ P. subcapitata*. This order was in good agreement with the order of the

degree of uptake of Cu^{2+} in the organisms. Note that the uptake of Cu in *P. subcapitata* and *D. magna* was similar, although the exposure concentration of Cu in the algae medium is higher than the Cu concentration for the daphnids. This provided a similar start for all food chains. As shown in Table 5.2, the BCFs of CuNPs in our test species were all in the range of 10^2 - 10^3 L/kg dry weight. The BCFs of Cu^{2+} were significantly higher than the BCFs of the CuNPs in each trophic level. This suggests a higher bioavailability of Cu in its ionic form than in its particulate form, taking into account the presence of the essential Cu in the organisms. A similar conclusion was reported by Makama et al. (2015) for ionic Ag and particulate Ag in earthworms exposed via (pore) water.

Table 5.2 Cu concentration (μg/g dry weight) in algae (*P. subcapitata*), daphnids (*D. magna*) and mysids (*L. benedeni*), and their bioconcentration factors (BCF, L/kg dry weight) [a]

		Cu. conc. (µg/g dw)	BCF (L/kg dw)
	Control	50 ± 1	
P. subcapitata	CuNPs	344 ± 98	670 ± 191
	Cu^{2+}	84 ± 10	8434 ± 1034
	Control	71 ± 23	
D. magna	CuNPs	380 ± 39	1072 ± 110
	Cu^{2+}	92 ± 4	9199 ± 428
	Control	96 ± 10	
L. benedeni	CuNPs	878 ± 346	2476 ± 975
	Cu^{2+}	527 ± 116	52658 ± 11553

[a] These species were not exposed (control) and exposed to 1 mg/L CuNPs and 0.01 mg/L $Cu(NO_3)_2$ solution, respectively. Values are

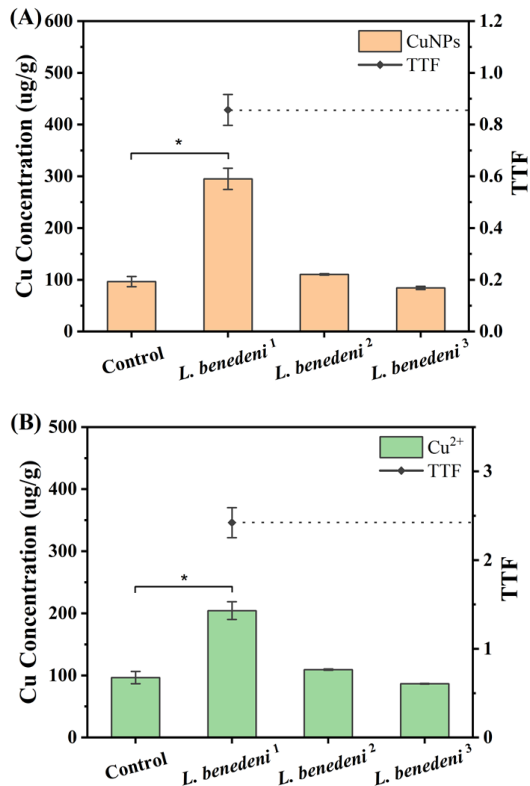expressed as mean ± standard deviation (n = 3). Each replicate contained > 100 daphnids or 15-20 alive mysids.

Figure 5.3 Cu concentrations (µg/g dry weight) for CuNPs (A) and Cu^{2+} (B) in mysids (*L. benedeni*) and their mass-based trophic transfer factors (TTF). *L. benedeni* [1], *L. benedeni* [2] and *L. benedeni* [3] stand for the predators in case-1 (from algae to mysid), case-2 (from daphnia to mysid), and case-3 (from algae through daphnia to mysid). Control stands for the mysid fed by unexposed food. Bars represent mean ± standard deviation (n = 3). The asterisk indicates statistical significance versus control group ($p < 0.05$).

The Cu concentrations in the predator from each food chain exposed to CuNPs and Cu^{2+} and the calculated TTFs are presented in Figure 5.3. As shown in Figure 5.3A, the Cu concentration in *L. benedeni*[1] fed with *P. subcapitata* was significantly higher compared to the Cu concentration in the control ($p < 0.05$). Hence, the trophic transfer of CuNPs was observed in case-1, rather than in case-2 and case-3. A similar finding was observed in the trophic transfer of Cu^{2+} (Figure 5.3B). These results indicated that both the food source and the length of the food chain can influence the trophic transfer potential of CuNPs and Cu ions. On the one hand, although the uptake of *L. benedeni*[1] was 3 times higher compared to the control, CuNPs did not biomagnify, as indicated by a TTF < 1. The comparison of TTF values showed that Cu ions were easier transferred across food chains. In addition, aqueous exposure resulted in higher uptake of Cu than in the case of ingestion of Cu-contaminated algae. Croteau et al. (2014) also found that the uptake of CuONPs in a freshwater snail could be accounted for mostly by diet-borne exposures. The accumulation and trophic transfer of NPs are commonly evaluated based on the mass concentration of metal accumulated in the predator. Mass might, however, not be necessarily the best metric to quantify bioaccumulation and trophic transfer of NPs and will for instance not reflect the possibility of preferential uptake of particles of different sizes or different morphology (Monikh et al., 2019b). Therefore, to quantify the size and number concentration of particulate Cu in prey and predator, we determined the particle size and particle number using sp-ICP-MS. Our finding for the performance check of the method showed that the addition of TMAH slightly decreased the sizes of particles and increased the number concentrations of particles (Table S5.4).

Table 5.3 Mode size (nm) and number particle concentrations (# particles/g wet weight) of Cu particles in biota, bioconcentration factors (BCF) in each test species, and trophic transfer factor (TTF) from algae to mysids [a]

	Mode size (nm)	Part. Conc. (10^{13} parts/kg ww)	Part. BCF (L/kg ww)	Part. TTF
P. subcapitata	34 ± 4	2 ± 2^{b}	429 ± 364	
D. magna	28 ± 2	2 ± 4	1689 ± 2766	
L. benedeni[o]	28 ± 6	2 ± 1^{b}	445 ± 102	
L. benedeni[1]	31 ± 9	4 ± 2^{c}		2 ± 1

[a] *L. benedeni*[o] and *L. benedeni*[1] stand for the mysids directly exposed to CuNPs in the aqueous phase and the predators in case-1 (from algae to mysid), respectively. The results are expressed as mean ± standard deviation ($n = 3$). Each replicate contained > 100 daphnids or 15-20 alive mysids. The different superscript letters indicate statistically significant ($p < 0.05$) differences between the treatments.

The mode size, number concentration, BCF, and TTF of CuNPs in each test species are shown in Table 5.3. The particle size of CuNPs did not change significantly after uptake, with the mode sizes of CuNPs among the test species in the range of 22 - 40 nm. Compared to the uptake order in biota (mysids > daphnia ≈ algae) based on the total mass concentration, the uptake of Cu particles based on number concentration directly from the aqueous phase in the different biota was similar and for all species roughly in the level of 10^{10} particles/g wet weight. The order of the BCF values based on the dose metric of particle number was *D. magna* > *L. benedeni* ≈ *P. subcapitata*. It was

also found that the order of the BCF values based on the dose metric of particle number was different from the order based on mass concentration (*L. benedeni* > *D. magna* > *P. subcapitata*, as shown in Table 5.2). Furthermore, the calculated TTF value of particulate Cu was greater than 1, indicating that the biomagnification of particulate Cu was observed in case-1. Mysids exposed to CuNPs via food (algae) showed higher uptake than mysids exposed via water. This result was in contrast with the total Cu content in the mysids (including both ionic Cu and particulate Cu) which originated mainly via waterborne exposure. Expressed based on the total Cu concentration, biomagnification was not found to occur (TTF < 1). This may be associated with the influence of the biophysiological factors of the predators on the uptake and bioaccumulation of CuNPs. It has been confirmed that several biophysiological factors such as feeding mode, digestive physiology, assimilation, and subcellular fractionation can affect the uptake and bioaccumulation of NPs in organisms (Ohe and Zwart, 2013; Tangaa et al., 2016). For instance, the internal location and subcellar fractionation of soluble metal-based NPs in daphnia distributed in the guts mostly (Yan and Wang, 2021). From this scenario, the extent of Cu uptake by the daphnia and mysid could depend on the conditions in the gut and the gut residence time. In contrast, Brun et al. (2017) found NPs in the lipid droplets around the gut tissue and in the brood pouch rather than in the gut of *D. magna*.
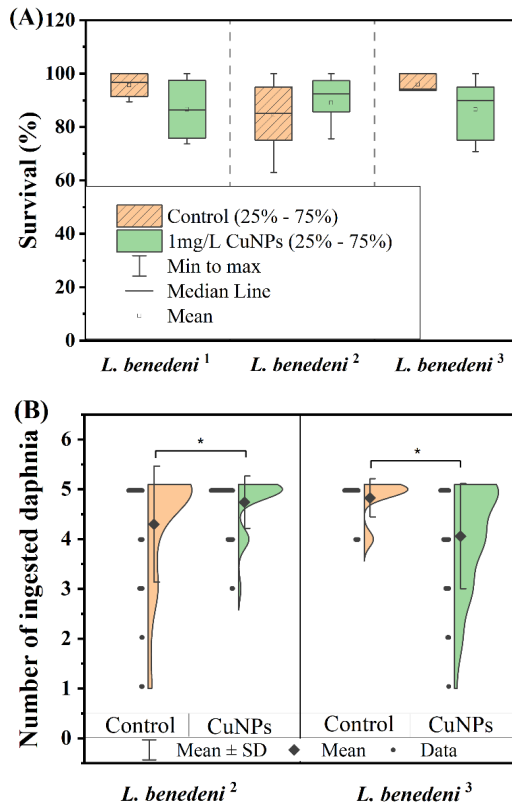
Figure 5.4 Survival (A, %) of mysids (*L. benedeni*) in the three food chains. Each survival test group contained 10 replicates with 15 - 20 alive mysids. The half violin figure (B) describes the distribution of mysids according to the number of ingested daphnia. Dots in the left part of the violin figure stand for the mysids hunting a different number of daphnia. The width of the right part represents the distribution of these data. Each group contained more than 45 alive mysids. *L. benedeni* [1], *L. benedeni* [2] and *L. benedeni* [3] stand for the predators in case-1 (from algae to mysid), case-2 (from daphnia to mysid), and case-3 (from algae through daphnia to mysid), respectively. The asterisk indicates statistical significance versus control group ($p <$ 0.05).

Figure 5.4 depicts the effects of dietary CuNPs exposure on the survival (%) and feeding rate (%) of mysids in the food chain. As shown in Figure 5.4A, there was no significant difference in the mysid survival between each treatment and the corresponding control group ($p > 0.05$). In case-1, a high amount of Cu was detected in the mysids and particulate Cu even biomagnified in the predator (Figure 5.3). However, the levels of Cu transferred from algae to mysids did not affect the survival of mysids. In addition, in terms of the feeding, no significant effect of the dietary uptake of CuNPs on the ingestion of algae by the mysids was observed. As shown in Figure 5.4B, a significant effect of the dietary uptake of CuNPs on the feeding rate calculated from the number of hunting the daphnia by the mysids was found in case-2 and case-3 ($p < 0.05$). Compared with the control, the dietary uptake of CuNPs induced an increase in the feeding rate in case-2, while the dietary uptake of CuNPs induced a decrease in the feeding rate in case-3. Since CuNPs were not found to be transferred to the predators (mysids) in the present study, the observed changes in feeding rate may be mainly related to the toxic effects of CuNPs on the prey (algae or daphnia). In our previous studies, the median lethal concentration of CuNPs for *D. magna* was found to be around 0.4 mg Cu/L (Yu et al., 2022). When the studied daphnids were exposed to around 355 µg Cu/L CuNPs, it was observed that some of the alive daphnids tended to swim slowly and became easier to catch during the 24 h exposure period. Therefore, an increase in the feeding ratio was observed in case-2. In addition, the algae (*P. subcapitata*) can compete with *D. magna* for the uptake of CuNPs, which could lead to a decrease in eating the daphnids exposed to CuNPs by the mysids in case-3.

In addition to the hydrosphere, the fate, behavior and effects of CuNPs in other environmental spheres such as the pedosphere and the biosphere are also of equal interest (Al-zharani et al., 2021; Bakshi and Kumar, 2021; Gao et al., 2019; Liu et al., 2018; Rizwan et al., 2017; Wang et al., 2022). A relatively high uptake of Cu and altered nutrient quality in soybean (*Glycine max*) grown in agricultural soil amended with CuNPs (Xiao et al., 2022) were reported. Moreover, natural organic matter increased the dissolution of CuNPs, and mitigated the phytotoxicity of CuNPs more significantly than that of Cu salt (Xiao et al., 2021). The increasing use of Cu-based NP_S in agricultural, industrial and environmental applications will undoubtedly lead to their spread in terrestrial ecosystems (Bakshi and Kumar, 2021). Thus, the dynamic transport of CuNPs may occur from soil to plants and then to food chain. To thoroughly understand the chemical behavior of Cu and potential risk of Cu-based NPs, further research is needed regarding the transport and transformation of CuNPs along terrestrial food chains in plant-soil environments.

5.4 Conclusions

The trophic transfer of CuNPs or Cu^{2+} was found in the direct route from the microalgae *P. subcapitata* to the mysid *L. benedeni*, but the extent of transfer of Cu was limited (TTF < 1). The size of the Cu particles was stable in the range of $22 - 40$ nm throughout the food chain. Consequently, particle number and mass were found to be equally suited to express bioaccumulation in the food chains studied. Unique was the quantification of particulate Cu within organisms. The uptake of Cu particles from the exposure medium in the organisms of

different trophic levels based on number concentrations was in the same order of magnitude of 10^{13} particles/kg wet weight. Furthermore, the biomagnification (TTF > 1) of particulate Cu occurred from the algae to the mysids. For the predator mysids, the uptake of total Cu from the aqueous exposure was higher than the uptake via the dietary exposure, while the uptake of particulate Cu was mainly via dietary uptake. Furthermore, the dietary CuNPs exposure showed significant effects on the feeding rates of mysids in the transfer processes from daphnia to mysid and from algae through daphnia to mysid. Taken together, this work exhibited that CuNPs transfer across trophic chains and show a limited extent of biomagnification. It is worthwhile to note that in the real world CuNPs could be excreted by organisms due to their own physiological and biochemical processes, and afterwards CuNPs would re-enter the environment upon excretion and pose an ecological risk to other organisms.

References

Adam, N.; Schmitt, C.; Galceran, J.; Companys, E.; Vakurov, A.; Wallace, R.; Knapen, D.; Blust, R. The chronic toxicity of ZnO nanoparticles and ZnCl$_2$ to *Daphnia magna* and the use of different methods to assess nanoparticle aggregation and dissolution. Nanotoxicology 2014, 8, 709-717.

Al-Reasi, H. A.; Wood, C. M.; Smith, D. S. Physicochemical and spectroscopic properties of natural organic matter (NOM) from various sources and implications for ameliorative effects on metal toxicity to aquatic biota. Aquat. Toxicol. 2011, 179-190.

Baker, B. J. Investigation of the competitive effects of copper and zinc on fulvic acid complexation: Modeling analytical approaches, Colorado School of Mines, 2012.

Bliss, C. I. The toxicity of poisons applied jointly. Ann. Appl. Biol. 1939, 26, 585-615.

Bondarenko, O.; Juganson, K.; Ivask, A.; Kasemets, K.; Mortimer, M.; Kahru, A. Toxicity of Ag, CuO and ZnO nanoparticles to selected environmentally relevant test organisms and mammalian cells *in vitro*: A critical review. Arch. Toxicol. 2013, 1181-1200.

Bossuyt, B. T.; Janssen, C. R. Copper regulation and homeostasis of *Daphnia magna* and *Pseudokirchneriella subcapitata*: Influence of acclimation. Environ. Pollut. 2005, 136: 135-144.

Clifford, M.; McGeer, J. C. Development of a biotic ligand model for the acute toxicity of zinc to *Daphnia pulex* in soft waters. Aquat. Toxicol. 2009, 91, 26-32.

Cooper, N. L.; Bidwell, J. R.; Kumar, A. Toxicity of copper, lead, and zinc mixtures to *Ceriodaphnia dubia* and *Daphnia carinata*. Ecotoxicol. Environ. Saf. 2009, 72, 1523-1528.

Crémazy, A.; Brix, K. V.; Wood, C. M. Using the biotic ligand model framework to investigate binary metal interactions on the uptake of Ag, Cd, Cu, Ni, Pb and Zn in the freshwater snail *Lymnaea Stagnalis*. Sci. Total Environ. 2019, 647, 1611-1625.

Cronholm, P.; Karlsson, H.L.; Hedberg, J.; Lowe, T.A.; Winnberg, L.; Elihn, K.; Wallinder, I.O.; Möller, L. Intracellular uptake and toxicity of Ag and CuO nanoparticles: a comparison between nanoparticles and their corresponding metal ions. Small. 2013, 9: 970-982.

Cupi, D.; Hartmann, N. B.; Baun, A. The influence of natural organic matter and aging on suspension stability in guideline toxicity testing of silver, zinc oxide, and titanium dioxide nanoparticles with *Daphnia magna*. Environ. Toxicol. Chem. 2015, 34, 497-506.

Deng, R.; Lin, D.; Zhu, L.; Majumdar, S.; White, J. C.; Gardea-Torresdey, J. L.; Xing, B. Nanoparticle interactions with co-existing contaminants: Joint toxicity, bioaccumulation and risk. Nanotoxicology. 2017, 11, 591-612.

DePalma, S. G. S.; Ray Arnold, W.; McGeer, J. C.; George Dixon, D.; Scott Smith, D. Effects of dissolved organic matter and reduced sulphur on copper bioavailability in coastal marine environments. Ecotoxicol. Environ. Saf. 2011, 74, 230-237.

Fabrega, J.; Fawcett, S. R.; Renshaw, J. C.; Lead, J. R. Silver nanoparticle impact on bacterial growth: effect of pH, concentration, and organic matter. Environ. Sci. Technol. 2009, 43, 7285-7290.

Field, S.; Sea, S. W. B. Stabilization of Metals and Shooting Range Soils - the Metalloids in Contaminated Effect of Iron-Based Amendments, University of Oslo, 2014.

Geller, W.; Müller, H. The filtration apparatus of cladocera: Filter mesh-sizes and their implications on food selectivity. Oecologia 1981, 49, 316-321.

Gheorghiu, C.; Smith, D. S.; Al-Reasi, H. A.; McGeer, J. C.; Wilkie, M. P. Influence of natural organic matter (NOM) quality on Cu-gill binding in the rainbow trout (*Oncorhynchus mykiss*). Aquat. Toxicol. 2010, 97, 343-352.

Green, N. W.; Mcinnis, D.; Hertkorn, N.; Maurice, P. A.; Perdue, E. M. Suwannee River Natural Organic Matter: Isolation of the 2R101N Reference Sample by Reverse Osmosis.

Guinée, J. B.; Heijungs, R.; Vijver, M. G.; Peijnenburg, W. J. G. M. Setting the stage for debating the roles of risk assessment and life-cycle assessment of engineered nanomaterials. Nat. Nanotechnol. 2017, 12, 727-733.

Gustafsson, J. P. Visual MINTEQ 3.1. https://vminteq.lwr.kth.se/: KTH, Sweden.

Ho, K. T.; Portis, L.; Chariton, A. A.; Pelletier, M.; Cantwell, M.; Katz, D.; Cashman, M.; Parks, A.; Baguley, J. G.; Conrad-Forrest, N.;

Boothman, W.; Luxton, T.; Simpson, S. L.; Fogg, S.; Burgess, R. M. Effects of micronized and nano-copper azole on marine benthic communities. Environ. Toxicol. Chem. 2018, 37, 362-375.

Hyne, R. V.; Pablo, F.; Julli, M.; Markich, S. J. Influence of water chemistry on the acute toxicity of copper and zinc to the cladoceran *Ceriodaphnia cf dubia*. Environ. Toxicol. Chem. 2005, 24, 1667-1675.

Liu, Y.; Baas, J.; Peijnenburg, W. J. G. M.; Vijver, M. G. Evaluating the combined toxicity of Cu and ZnO nanoparticles: Utility of the concept of additivity and a nested experimental design. Environ. Sci. Technol. 2016, 50, 5328-5337.

Komjarova, I.; Blust, R. Multi-metal interactions between Cd, Cu, Ni, Pb and Zn in water flea Daphnia magna, a stable isotope experiment. Aquat. Toxicol. 2008, 90, 138-144.

Lee, B. T.; Ranville, J. F. The effect of hardness on the stability of citrate-stabilized gold nanoparticles and their uptake by *Daphnia magna*. J. Hazard. Mater. 2012, 213-214, 434-439.

Lopes, S.; Ribeiro, F.; Wojnarowicz, J.; Lojkowski, W.; Jurkschat, K.; Crossley, A.; Soares, A. M. V. M.; Loureiro, S. Zinc oxide nanoparticles toxicity to *Daphnia magna*: Size-dependent effects and dissolution. Environ. Toxicol. Chem. 2014, 33, 190-198.

Lorenzo, J. I.; Beiras, R.; Mubiana, V. K.; Blust, R. Copper uptake by Mytilus edulis in the presence of humic acids. Environ. Toxicol. Chem. 2005, 24, 973-980.

Lores, E. M.; Snyder, R. A.; Pennock, J. R. The effect of humic acid on uptake/adsorption of copper by a marine bacterium and two marine ciliates. Chemosphere 1999, 38, 293-310.

Ma, D. Hybrid nanoparticles: An introduction - ScienceDirect. 2019.

Meyer, J. S.; Ranville, J. F.; Pontasch, M.; Gorsuch, J. W.; Adams, W. J. Acute toxicity of binary and ternary mixtures of Cd, Cu, and Zn to *Daphnia magna*. Environ. Toxicol. Chem. 2015, 34, 799-808.

Minteq, V.; Agency, E. P. Visual MINTEQ - a Brief Tutorial. 2000, 1-5.

Mitrano, D. M.; Motellier, S.; Clavaguera, S.; Nowack, B. Review of nanomaterial aging and transformations through the life cycle of nano-enhanced products. Environ. Int. 2015, 77: 132-147.

Nadella, S. R.; Fitzpatrick, J. L.; Franklin, N.; Bucking, C.; Smith, S.; Wood, C. M. Toxicity of dissolved Cu, Zn, Ni and Cd to developing embryos of the blue mussel (*Mytilus trossolus*) and the protective effect of dissolved organic carbon. Comp. Biochem. Physiol. - C Toxicol. Pharmacol. 2009, 149, 340-348.

Nogueira, L. S.; Bianchini, A.; Smith, S.; Jorge, M. B.; Diamond, R. L.; Wood, C. M. Physiological effects of five different marine natural organic matters (NOMs) and three different metals (Cu, Pb, Zn) on early life stages of the blue mussel (*Mytilus galloprovincialis*). PeerJ 2017, 5: e3141.

OECD. Guideline for Testing of Chemicals. Daphnia sp., Acute Immobilization Test. OECD 202. Paris, 2004.

Ogunsuyi, O. I.; Fadoju, O. M.; Akanni, O. O.; Alabi, O. A.; Alimba, C. G.; Cambier, S.; Eswara, S.; Gutleb, A. C.; Adaramoye, O. A.; Bakare, A. A. Genetic and systemic toxicity induced by silver and copper oxide nanoparticles, and their mixture in Clarias gariepinus (Burchell, 1822). Environ. Sci. Pollut. Res. 2019, 26, 27470-27481.

Qiao, R.; Lu, K.; Deng, Y.; Ren, H.; Zhang, Y. Combined effects of polystyrene microplastics and natural organic matter on the accumulation and toxicity of copper in zebrafish. Sci. Total Environ. 2019, 682, 128-137.

Sani-Kast, N.; Labille, J.; Ollivier, P.; Slomberg, D.; Hungerbühler, K.; Scheringer, M. A network perspective reveals decreasing material diversity in studies on nanoparticle interactions with dissolved organic matter. Proc. Natl. Acad. Sci. U. S. A. 2017, 114, E1756-E1765.

Sharma, V. K.; Sayes, C. M.; Guo, B.; Pillai, S.; Parsons, J. G.; Wang, C.; Yan, B.; Ma, X. Interactions between silver nanoparticles and other metal nanoparticles under environmentally relevant conditions: A review. Sci. Total Environ. 2019, 653, 1042-1051.

Tervonen, K.; Waissi, G.; Petersen, E. J.; Akkanen, J.; Kukkonen, J. V. K. Analysis of fullerene-C60 and kinetic measurements for its accumulation and depuration in *Daphnia magna*. Environ. Toxicol. Chem. 2010, 29, 1072-1078.

Unsworth, E. R.; Warnken, K. W.; Zhang, H.; Davison, W.; Black, F.; Buffle, J.; Cao, J.; Cleven, R.; Galceran, J.; Gunkel, P.; et al. Model predictions of metal speciation in freshwaters compared

to measurements by in situ techniques. Environ. Sci. Technol. 2006, 40, 1942-1949.

Wang, Z.; Chen, J.; Li, X.; Shao, J.; Peijnenburg, W. J. G. M. Aquatic toxicity of nanosilver colloids to different trophic organisms: contributions of particles and free silver ion. Environ. Toxicol. Chem. 2012, 31, 2408-2413.

Wang, Z.; Li, J.; Zhao, J.; Xing, B. Toxicity and internalization of CuO nanoparticles to prokaryotic alga *Microcystis aeruginosa* as affected by dissolved organic matter. Environ. Sci. Technol. 2011, 45, 6032-6040.

Wang, Z.; Zhang, L.; Zhao, J.; Xing, B. Environmental processes and toxicity of metallic nanoparticles in aquatic systems as affected by natural organic matter. Environ. Sci. Nano 2016, 3, 240-255.

Wilke, C. M.; Wunderlich, B.; Gaillard, J. F.; Gray, K. A. Synergistic bacterial stress results from exposure to nano-Ag and nano-TiO₂ mixtures under light in environmental media. Environ. Sci. Technol. 2018, 52, 3185-3194.

Wu, J., Wang, G., Vijver, M.G., Bosker, T., Peijnenburg, W.J.G.M. Foliar versus root exposure of AgNPs to lettuce: Phytotoxicity, antioxidant responses and internal translocation. Environ. Pollut. 2020, 261, 114117.

Xiao, Y.; Peijnenburg, W. J. G. M.; Chen, G.; Vijver, M. G. Impact of water chemistry on the particle-specific toxicity of copper nanoparticles to *Daphnia magna*. Sci. Total Environ. 2018, 610-611, 1329-1335.

Xiao, Y.; Vijver, M. G.; Chen, G.; Peijnenburg, W. J. G. M. Toxicity and accumulation of Cu and ZnO nanoparticles in *Daphnia magna*. Environ. Sci. Technol. 2015, 49, 4657-4664.

Ye, N.; Wang, Z.; Wang, S.; Peijnenburg, W. J. G. M. Toxicity of mixtures of zinc oxide and graphene oxide nanoparticles to aquatic organisms of different trophic level: particles outperform dissolved ions. Nanotoxicology 2018, 12, 423-438.

Yu, R.; Wu, J.; Liu, M.; Zhu, G.; Chen, L.; Chang, Y.; Lu, H. Toxicity of binary mixtures of metal oxide nanoparticles to *Nitrosomonas Europaea*. Chemosphere 2016, 153, 187-197.

Zhang, Y.; Chen, Y.; Westerhoff, P.; Crittenden, J. Impact of natural organic matter and divalent cations on the stability of aqueous nanoparticles. Water Res. 2009, 43, 4249-4257.

Supplementary data

Nanoparticle dissolution and aggregation testing

To determine the dissolution profile of CuNPs, we monitored the concentration of ionic Cu in the test media over 24 h. The samples were collected at 0 and 24 h from a suspension of 1 mg/L CuNPs prepared in Woods Hole Medium (Janet Stein, 1982) and in ElendtM7 medium (Samel et al., 1999). The samples were obtained from the top 1.5-2 cm layer of the dispersions., The samples for the measurement of the total Cu concentration were acidified by addition of 2 drops of 65% nitric acid. Samples for the measurement of Cu-ions released from the CuNPs were firstly centrifuged at 15,000 rpm for 30 min at 4 °C, and then 5 mL of supernatant was transferred to another tube for analysis. The actual concentration of total Cu and the Cu-ions released from the CuNPs were determined via Atomic Absorption Spectroscopy (AAS; Perkin Elmer 1100B).

Aggregation kinetics during 30 min of changes were monitored using dynamic light scattering (DLS, Malvern, Instruments Ltd., UK). Suspensions of 10 mg/L CuNPs as used for the DLS measurements were prepared in the Wood Hole Medium and in the ElendtM7 medium, respectively. The hydrodynamic diameters of the CuNPs were determined immediately after the dispersions were sonicated for 15 min. During the 30 min observation of aggregation, the DLS measurements were performed with an interval of 2 min.

Culture of test organisms

Pseudokirchneriella subcapitata used as a test organism were maintained in a climate room. OECD Guideline 201 was used as the procedure for culturing of the algae with some slight modification (Andrews and Walsh, 2007). The algae were cultured in autoclaved Woods Hole Medium at 22 ± 1 °C with a 16:8 light-dark cycle. The algae were continuously aerated to provide sufficient CO_2 and the algae suspension was stirred to avoid settling down.

Daphnia magna was originally obtained from Leiden University. According to OECD Guideline 202 (OECD, 2004), the daphnia culture medium ElendtM7 medium (Samel et al., 1999) was prepared at pH 8.4 ± 0.4. *D. magna* were cultured at a temperature of 22 ± 1 °C with a 16:8 light-dark cycle. The density of the culture was around 1 individual/500 mL medium and daphnids were fed with *P. subcapitata* every 2 days.

Lymnomysis benedeni, a widespread species in Western Europe, was collected from a pond (Leiden, The Netherlands) at a size of around 1.1 cm, and the collection included both male and female species. *L. benedeni* was acclimated in the lab for 3 days prior to the test by means of the following 3 steps: 1) culturing in combined natural water and in the ElendtM7 medium with a small amount of sediment originating from the pond for the first day; 2) culturing in the ElendtM7 medium with sediment from the pond for the second day; 3) culturing in the ElendtM7 medium without sediment and without food for the third day to clean the guts. *L. benedeni* was cultured with continuously aeration, using the same condition as for *D. magna*.
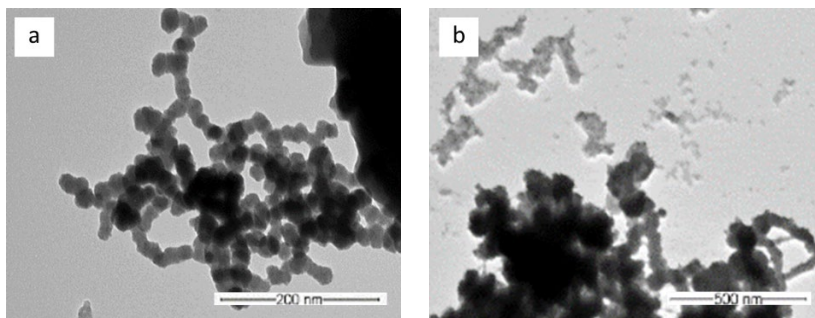
Figure S5.1 TEM images of 1 mg/L Cu NP suspensions in (a) Woods Hole Medium and (b) ElendtM7 medium (Yu et al., 2022)
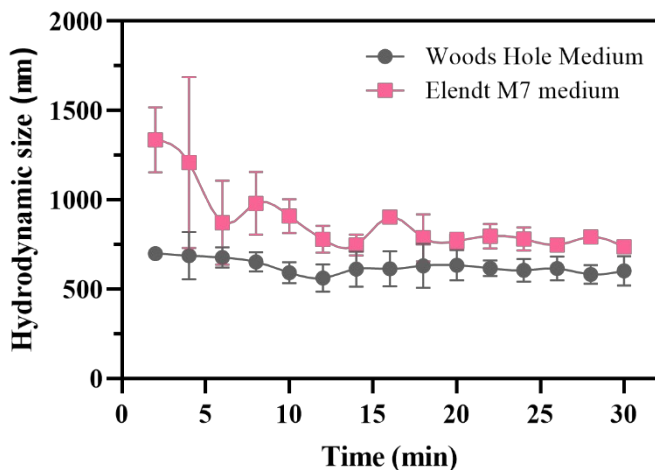

Figure S5.2 Hydrodynamic sizes of the suspension of 10 mg/L CuNPs dispersed in Woods Hole Medium and in ElendtM7 medium over 30 min, as measured by dynamic light scattering. The values reported are expressed as mean ± standard deviation (n = 3)

Table S5.1 Chemical Composition of Woods Hole Medium (Janet Stein, 1982)

Chemicals	Concentration (g/L)
CaCl·2H$_2$O	3.676
MgSO$_4$·4H$_2$O	3.698
NaHCO$_3$	1.26
K$_2$HPO$_4$	0.872
NaNO3	8.502
MnCl$_2$·4H$_2$O	0.02
ZnSO$_4$·7H$_2$O	0.002
NaMoO·2H$_2$O	0.00012
CoCl$_2$·6H$_2$O	0.001
CuSO$_4$·5H$_2$O	0.001
NaEDTA	0.436
FeCl$_3$·6H$_2$O	0.316
Vitamins	0.5 mL of the stock[*]

*The vitamin stock was prepared according to Lehman (1976).

Table S5.2 Concentration of Cu (µg/g) left on the daphnia and shrimp after extraction

Carapace		Cu concentration (µg/g)
daphnia	Control	8.6 ± 5.6
	Exposure	3.3 ± 1.6
shrimp	Control	0.5 ± 0.2
	Exposure	0.0 ± 0.0

Table S5.3 Instrumental parameters for single particle inductively coupled plasma mass spectrometry (sp-ICP-MS) analysis

Nebulizer Gas Flow [NEB]	1.12 L/min
Auxiliary Gas Flow	1.2 L/min
Plasma Gas Flow	18 L/min
ICP RF Power	1600 W
Flow Rate	0.34 g/min
Transport Efficiency	13.62 %
Dwell Time	50 us

Table S5.4 Particle size and particle number concentration of suspensions of 1 mg/L CuNPs in 20% TMAH and Milli-Q water

Solution	Mean size (nm)	Part. Conc. (10^8 parts/mL)
20% TMAH	25.7 ± 1.0	2.6 ± 0.8
Milli-Q water	39.5 ± 11.1	0.1 ± 0.2

References

Andrews, S., Walsh, K., 2007. Experiences merging two university websites. Proc. ACM SIGUCCS User Serv. Conf. 4–7.

Janet Stein, 1982. Handbook of phycological methods, Culture methods and Growth measurement, Cambridge. ed. Cambridge University Press, London, UK.

Lehman, J.T., 1976. Ecological and nutritional studies on Dinobryon Ehrenb.: Seasonal periodicity and the phosphate toxicity problem. Limnol. Oceanogr. 21, 646–658.

OECD, 2004. Oecd Guideline for testing of chemicals Daohnia sp., Acute Immobilisation Test, OECD.

Samel, A., Ziegenfuss, M., Goulden, C.E., Banks, S., Baer, K.N., 1999. Culturing and bioassay testing of *Daphnia magna* using Elendt M4, Elendt M7, and COMBO media. Ecotoxicol. Environ. Saf. 43, 103–110.

Yu, Q., Wang, Z., Wang, G., Peijnenburg, W.J.G.M., Vijver, M.G., 2022. Effects of natural organic matter on the joint toxicity and accumulation of Cu nanoparticles and ZnO nanoparticles in *Daphnia magna*. Environ. Pollut. 292, 118413.

Chapter 6

General Discussion

Nanotechnology is considered part of a new renaissance in science, as it has been identified as a key enabling technology that brings prosperity and innovation within a wide range of commercial and industrial applications (European Commission, 2012; Song et al., 2017). However, it is crucial to unravel the fate and effects of ENPs in aqueous media in a world where nanotechnology is accelerating and hence unintended ENPs will be emitted into surface waters. Evaluating nanosafety, making use of standardized first tier screening assays, has shown not to be not sufficient accurate. ENPs will undergo physicochemical processes in freshwater media, which can influence the bio-uptake and -accumulation of ENPs and modify their toxic effects.

In addition, within natural settings it is not unlikely that mixtures of nanoparticle suspensions can be found. Moreover, the presence of natural organic material (NOM) is known to impact the fate and subsequent processes of ENPs up to the potential of trophic transfer through food chains. To add experimental data as well as new knowledge to address the inevitable questions and challenges for the environmental risk assessment of ENPs, we systematically investigated 1) the impact of NOM on the fate, bioaccumulation and single/joint toxic actions of ENPs, 2) the transfer of ENPs from lower trophic levels to higher trophic levels, and the subsequently occurring effect on predators.

6.1. Findings in this thesis

We investigated the individual toxicity of CeO_2NPs in three organisms. A relationship between exposure characteristics with the toxicity of

CeO$_2$NPs was found. The joint toxic action of CuNPs + ZnONPs was additive or more-than-additive for *D. magna*. A similar pattern was found in the toxicity of the mixtures of Cu- and Zn-salts.

The individual and joint toxicity were affected in the presence of NOM. Different concentrations of humic substances (HS) alleviated CeO$_2$NPs toxicity to *R. subcapitata* and to *C. sphaericus*. The joint effects of HS and CeO$_2$NPs were additive and synergistic to *D. rerio*. Additionally, NOM increased the relative contribution of dissolved metal-ions to the joint toxicity. NOM enhanced metal bioaccumulation in the mixtures of CuNPs and ZnONPs.

Trophic transfer was observed for PSPs from algae to mysids, and for CuNPs from daphnids to mysids. A limited extent (TTF < 1) of trophic transfer of total CuNPs or Cu ions was observed from algae to the mysid. Biomagnification of particulate Cu occurred from algae to mysids. The extent of trophic transfer was found to be affected by particle size and the type of food chain. Particle size of CuNPs determined by sp-ICP-MS ranged from 22 to 40 nm in species. No significant changes in the particle size of CuNPs were measured during uptake.

6.2. Implications and future perspectives

Assessing the environmental risk of ENPs is the key to nanosafety and green design (Savolainen et al., 2013). The European Commission emphasized that understanding the effects and concentrations of ENPs in complex and realistic situations is required to better and more effectively assess the risks of manufactured nanomaterials (Science for Environment Policy, 2017). As described above, investigations were

performed in this thesis to help unravel the toxicity of ENPs exposed in single and mixture settings, explicitly considering the impact of NOM on the accumulation and toxicity of ENPs and their potential to transfer through food chains. These findings are crucial when developing predictive models for ENPs based on the processes that jointly determine the fate of ENPs and their relationship to uptake and trophic transfer potential. Understanding of the exposure and hazard risk of ENPs can ultimately provide basic data for safe design and process-based environmental risk assessment (Figure 6.1).
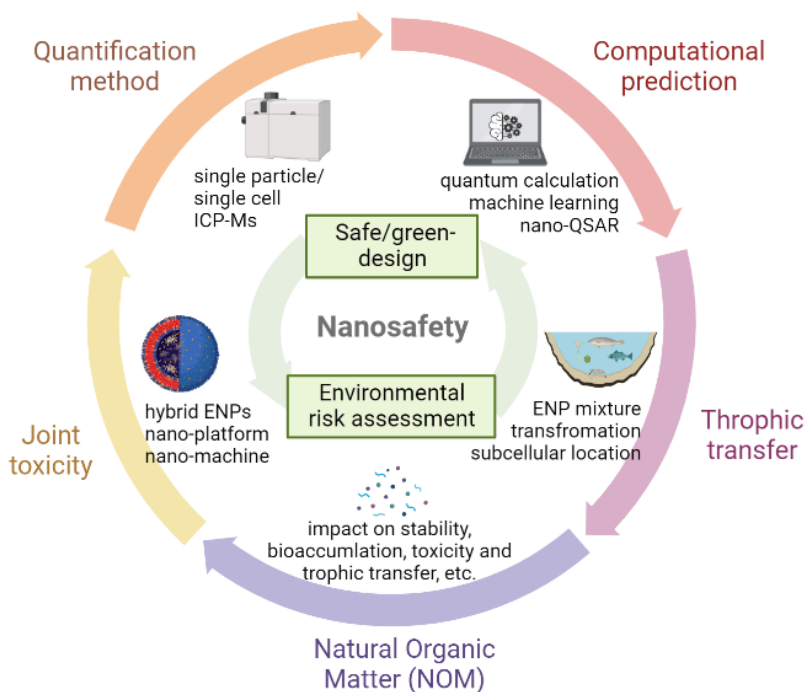
Figure 6.1 Schematic illustration of the implications and future perspectives of ENPs on safe/green-design and environmental risk assessment in this thesis.

6.2.1 Joint toxicity of ENPs

The data obtained on the joint impacts of two ENPs in a mixture could be the stepping stone for prospective new innovations. Nowadays, metal alloys and hybrid nanoparticles are already synthesized, going a step beyond the 1st generation of single element nanomaterials. Consequently, the future co-release of multiple ENPs will inevitably result in mixtures of ENPs in the environment. As found in our case study (**Chapter 2**), the joint toxicity of CuNPs + ZnONPs was greater than the single toxicity of CuNPs or ZnONPs toward water fleas. The mode of action of toxicity induced by CuNPs + ZnONPs was additive or more-than-additive. Synergistic and antagonistic actions were found in other researches, as listed in Table 1.1 (Chapter 1). Hence, the toxic potential of ENP mixtures could be distinct from the summed toxicity of individual ENPs. The risk assessment and risk management should include the joint toxicity of ENP mixtures in complex conditions or under environmentally realistic conditions.

In addition, we found that the toxic mode of action of CuNPs + ZnONPs was similar to the toxic mode of action of Cu^{2+} + Zn^{2+}. This finding indicates that the joint toxic mode of metal salts could be the reference for the evaluation of metal-based ENPs of similar chemical composition. However, the contribution of particles should not be neglected as well. Furthermore, the presence of CuNPs will enhance the bioaccumulation of ZnONPs as found in **Chapter 2**. Previous studies proved that the bioaccumulation of Cu ions was promoted with the addition of Zn ions (Komjarova and Blust, 2008). This suggests that the hazard of Zn-based ENPs will increase in the presence of Cu-

based ENPs. For the purpose of safe/green design, Cu and Zn should not be included into the same nano-product.

6.2.2 Trophic transfer

Within our study results we have found that trophic transfer occurred only under specific conditions. The exposure pathway of ENPs to organisms was an important descriptor in this respect (**Chapters 4 and 5**) The confirmed biomagnification of particulate Cu further highlights the potential hazard to human beings. Specifically, the extent of transfer depended on the type of food chains and particle size. CuNPs were found to transfer from algae to mysids, rather than from daphnia to mysids or from algae to daphnia to mysids (**Chapter 4**). Also the larger the particle size of PSPs, the higher the extent of transfer in the food chain, which is counterintuitive and currently lots of researchers are investigating this issue (**Chapter 5**). The study provides evidence that the role of particle size should not be neglected in regulating the bioaccumulation and trophic transfer of ENPs in the aquatic environment. We echo Tangaa et al. (2016) in this respect and plea for a larger scientific understanding on the trophic transfer of ENPs and the affecting factors such as food chain types and particle size. To reveal the availability of ENPs for transfer in a more realistic and complex system, understanding how ENPs transfer through the food web or micro-ecosystem is meaningful and challenging. Furthermore, investigations on the transfer of ENP mixtures along food chains or the food web are warranted in future study, are still a research area.

6.2.3 An inevitable factor —— NOM

Natural organic matter (NOM) is ubiquitous in field setting. Soils, sediments, air and water are carrying large amounts of NOM, whereas organisms for instance shed off skin, mucus and other body fluids. This provides NOM as well death biota (plants, microbes and biota) that are later turned into NOM. It turns out that when translating simplified screening laboratory tests towards realistic settings this parameter is an inevitable and key parameter to consider. Additionally, NOM is also crucial for the fate of ENPs because NOM stabilizes nano-suspensions (**Chapter 2)** and thus have a huge impact on CeO_2NPs toxicity, as it differs across different aquatic organisms. Our research emphasizes how the stabilization of particles with NOM or any other type of NOM affects the toxicity of ENPs. A key element of our findings is that the interactions between NOM and ENPs or other water chemistry factors affecting particle stability can be utilized to reduce the toxicity of ENPs. In addition, we highlighted that NOM enhances the toxicity to fish larvae but inhibits the toxicity induced by CeO_2NPs to algae and water fleas. Further investigations of the role of NOM on the fate of ENPs is thus an essential part of the exposure characterization of specific organisms in the aquatic environment. The same is true for considering multiple ENPs in an exposure media (**Chapter 3**).

6.2.4 Other implications and research area

One main limitation of risk assessment frameworks for ENPs is the lack of a quantitative uncertainty assessment to improve transparency

(Jahnel, 2015). To determine ENPs in aquatic columns and biota, constructing an accurate and suitable quantification method combined with an extraction procedure is crucial. In **Chapter 4**, we used sp-ICP-MS quantified the size and number concentration of CuNPs in the biota using tissue extraction with TMAH. Particle number and mass were found to be equally suited to express bioaccumulation and to trace the ENPs in food chains. Moreover, a newly developed mode of the time-resolved inductively coupled plasma mass spectrometry (ICP-MS) technique, described as single-cell (sc)-ICP-MS, was recently introduced to measure the concentration of elements in cells (Monikh et al., 2019, 2021). However, there is still a lack of a recognized and systematic quantitative analysis method for environmental risk assessment and management. It is a critical challenge to develop more reliable and reproducible measurement techniques and standards for small size and particulate materials (Shatkin, 2020).

Tools for predictive risk assessment and risk management including databases and ontologies were described as one of the research needs and priorities of ENPs for the coming 10 years in the "Nanosafety in Europe 2015–2025" report (Savolainen et al., 2013). Alternative methods of toxicity assessment were proposed by the US National Research Council in "Toxicity Testing in the 21st Century: A Vision and a Strategy" (National Research Council, 2007). There are currently many researchers focusing on the development of these predictive models; what we learned from the thesis results is that also emphasis should be put on the joint toxicity of ENPs in suspension. There is thus an urgent need to create curated and publicly accessible data sets for ENP mixtures (Shatkin, 2020).

To conclude, the research results described in this thesis are stepping stones towards improving the understanding of the processes that determine the actual exposure of a suite of aquatic organisms to exposure media of different compositions, mimicking to an increasing extent natural aquatic systems. Our findings provide a basis, i.e. joint toxicity, trophic transfer potential and effect of NOM, for environmental risk assessment and management in a more realistic and natural aquatic environment. From the evaluation endpoint, feedback and reference were generated for predictive risk assessment as well as building blocks for a green/safe-design of ENPs. Based on current studies, research priorities include further investigations on the toxicity of ENP mixtures, trophic transfer of ENP mixtures, the influence of NOM on trophic transfer of multiple ENPs, development of quantitative analysis methods and standards, and prediction of nanotoxicity.

References

European Commission, 2012. Internal Market, Industry, Entrepreneurship and SMEs - Nanomaterials [WWW Document]. https://ec.europa.eu/growth/sectors/chemicals/reach/nanomaterials_en

Jahnel, J., 2015. Addressing the Challenges to the Risk Assessment of Nanomaterials, Nanoengineering: Global Approaches to Health and Safety Issues. Elsevier B.V.

Komjarova, I., Blust, R., 2008. Multi-metal interactions between Cd, Cu, Ni, Pb and Zn in water flea Daphnia magna, a stable isotope experiment. Aquat. Toxicol. 90, 138–144.

Monikh, F.A., Chupani, L., Vijver, M.G., Peijnenburg, W.J.G.M., 2021. Parental and trophic transfer of nanoscale plastic debris in an assembled aquatic food chain as a function of particle size. Environ. Pollut. 269, 116066.

Monikh, F.A., Fryer, B., Arenas-Lago, D., Vijver, M.G., Krishna Darbha, G., Valsami-Jones, E., Peijnenburg, W.J.G.M., 2019. A dose metrics perspective on the association of gold nanomaterials with algal cells. Environ. Sci. Technol. Lett. 6, 732–738.

National Research Council, 2007. Toxicity Testing in the 21st Century: A Vision and a Strategy. Washington, DC: The National Academies Press.

Savolainen, K., Backman, U., Brouwer, D., Fadeel, B., Fernandes, T., Kuhlbusch, T., Landsiedel, R., Lynch, I., Pylkkanen, L., 2013. Nanosafety in Europe 2015–2025: Towards safe and sustainable nanomaterials and nanotechnology innovations. Finnish institute of occupational health.

Science for Environment Policy, 2017. *Assessing the environmental safety of manufactured nanomaterials.* In-depth Report 14 produced for the European Commission, DG Environment by the Science Communication Unit,. UWE, Bristol.

Shatkin, J.A., 2020. The Future in Nanosafety. Nano Lett. 20, 1479–1480.

Song, R., Qin, Y., Suh, S., Keller, A.A., 2017. Dynamic Model for the Stocks and Release Flows of Engineered Nanomaterials. Environ. Sci. Technol. 51, 12424–12433.

Tangaa, S.R., Selck, H., Winther-Nielsen, M., Khan, F.R., 2016. Trophic transfer of metal-based nanoparticles in aquatic environments: A review and recommendations for future research focus. Environ. Sci. Nano 3, 966–981.

Summary

In the last two decades, the field of nanotechnology has been rapidly expanding and has been experimented with in various applications, such as consumer products, nanomedicine, as well as engineering and materials. The growing concern of potential health and environmental risks associated with ENPs has triggered various safety regulations around the world. However, the understanding of the toxicity level of these ENPs is still underestimated as the influence of water chemistry such as NOM on the fate and toxicity of ENPs, the quantification of ENPs trophic transfer through food chains and relative affecting factors are still poorly studied. In accordance with the scientific questions, the main conclusions reached in this thesis are summarized below:

1) How does NOM affect the stability and toxicity of **individual ENPs** to aquatic organisms?

The case study of **Chapter 2** determined the impacts of humic substances (HS) as a NOM analog on the aquatic stability and single toxicity of CeO_2NPs to three organisms with different exposure characteristics. With the addition of HS at a concentration ranging from 0.5 to 40 mg C/L, the stability of CeO_2NPs was significantly improved, and the stabilization depended on the concentration of HS. Toxic effects of CeO_2NPs on algae and on daphnids were reduced by different concentrations of HS, while the toxicity towards zebrafish larvae was enhanced. A concentration-dependent influence of the addition of HS on the toxicity of CeO_2NPs was observed to different organisms. Furthermore, relationships between particle stability with

toxicity and between aquatic species with toxicity were found in the condition of HS. These findings emphasize the important role of NOM in stabilizing the nano-suspensions and the different impact on CeO_2NPs toxicity towards different aquatic organisms.

2) How does NOM affect the fate, accumulation and toxicity of **ENP mixtures**?

In **Chapter 3**, the fate, joint toxicity and accumulation of a mixture of CuNPs and ZnONPs in *Daphnia magna* influenced by the presence of Suwannee River natural organic matter (SR-NOM) were investigated. Different concentrations of SR-NOM have no significant impact on the hydrodynamic diameter and zeta potential of the binary mixtures. The only exception was that the co-agglomeration behavior of ENP mixtures was significantly alleviated after adding 20 mg/L SR-NOM. The addition of SR-NOM didn't affect significantly the apparent joint toxicity of CuNPs + ZnONPs. Whereas, SR-NOM changed the contribution to total toxicity and enhanced metal bioaccumulation of ENP mixtures. The presence of SR-NOM increased the relative contribution of dissolved metal-ions released from metal-based ENPs to the joint toxicity. Particularly, the released Zn-ions dominated the toxicity of the binary ENP mixtures with the co-existence of SR-NPM. This is due to the agglomeration and sedimentation of CuNPs and the complexation of the released Cu-ions with SR-NOM. Moreover, the accumulation of Cu and Zn in the mixtures of CuNPs and ZnONPs in daphnia was both remarkably increased by the addition of SR-NOM.

3) To what extent do ENPs **transfer** in particulate, and ionic forms and how does the particle size and number change in different organisms?

The trophic transfer of CuNPs through an aquatic food chain consisting of algae, daphnia, and mysid was quantified in **Chapter 4**. The number-based concentration and size of Cu particles in different tropic level species were quantify by single particle inductively coupled plasma mass spectrometry (sp-ICP-MS). A limited extent of trophic transfer of total CuNPs or Cu ions was observed from algae to the mysid. Meanwhile, the particulate Cu biomagnified from the algae to the mysids as a result of the trophic transfer factor value higher than 1. Additionally, the number concentrations of Cu particles in different trophic levels were in the order of 10^{13} particles/kg wet weight. The size of the particulate Cu was determined from 22 to 40 nm throughout the food chain without significant changes. These results exhibited that tracing the particulate fraction of ENPs is as important as tracing the ionic fraction along the trophic transfer.

4) How do **particle sizes** and **food chain types** affect the trophic transfer of ENPs and their subsequently biodistribution and toxicity to the predators?

In order to compare the influence of food chain types on the trophic transfer extent, the length and food source were considered in **Chapter 4 and 5**. The transfer of CuNPs through three simulated freshwater food chains were constructed including from algae to daphnia to mysids, from algae to mysids, and from daphnids to mysids (**Chapter 4**). Trophic transfer was only found in the 2-level food chain from algae to mysids, rather than the other two types food chain. This provided evidence that both the position in the length of the chain as well as the food source have impact on the trophic transfer potential of CuNPs. Moreover, the significant effects on the feeding rates of predator mysids by the dietary CuNPs was found in the transfer

processes from daphnia to mysid and from algae through daphnia to mysid.

The trophic transfer of polystyrene particles (PSPs) from daphnia to mysids as a function of particle size (26, 500 and 4800 nm) was investigated (**Chapter 5**). Only a small fraction ranged from 1 to 5% of all sized PSPs ingested by daphnia was transferred to mysids. The extent of trophic transfer is size-dependent decreased in the order of 4800 nm > 500 nm > 26 nm PSPs. No tropic transfer was observed in the predator for all sized PSP treatments. Furthermore, all PSPs were mainly accumulated in the intestinal tract (stomach and intestine) of mysids. Consequently, our findings emphasized that different sized PSPs can transfer along the daphnia-mysids food chain, and the impact of particle size on the potential of trophic transfer shouldn't be neglected.

In conclusion, the findings in this thesis improve the understanding of 1) the relationship between exposure characteristics and toxicity of ENPs, 2) the joint toxic action of ENP mixtures and the comparison to metal salt mixtures, 3) how NOM affects the individual and joint toxicity of ENPs, 4) the extent of trophic transfer of ENPs along aquatic food chains, 5) the influence factors on trophic transfer, and 6) bioaccumulation, distribution and toxic effect on predators. This knowledge would provide a basis for data on individual and joint toxicity, bioaccumulation, and trophic transfer of ENPs for more realistic environmental risk assessment.

Samenvatting

In de afgelopen twee decennia heeft het gebied van de nanotechnologie zich snel uitgebreid en is er geëxperimenteerd met verschillende toepassingen, zoals het gebruik van nanodeeltjes in consumenten producten, nanogeneeskunde en electrotechnologie. De toenemende bezorgdheid over de potentiële gezondheids- en milieurisico's van gesynthetiseerde nanodeeltjes (ENP's) heeft wereldwijd tot diverse veiligheidsvoorschriften geleid. Het inzicht in de processen die ten grondslag liggen aan de toxiciteit van deze ENP's wordt echter nog steeds onderschat en zijn dan ook het onderwerp van dit proefschrift. Dit betreft onder andere de invloed van de waterchemie op het lot en de toxiciteit van ENP's, alsmede op de trofische overdracht van ENP's via voedselketens. Voor wat betreft de waterchemie kan hierbij gedacht worden aan parameters zoals de pH en het gehalte aan natuurlijk organisch materiaal (NOM) in het blootstellingsmedium.

In overeenstemming met de wetenschappelijke vragen worden de belangrijkste conclusies van dit proefschrift hieronder samengevat:

1) Hoe beïnvloedt NOM de stabiliteit en toxiciteit van individuele ENP's voor waterorganismen?

De case studie van hoofdstuk 2 gaf inzicht in de effecten van humusstoffen (HS) als NOM-analoog op de aquatische stabiliteit en enkelvoudige toxiciteit van ceriumdioxide nanodeeltjes (CeO_2NPs) voor drie organismen met verschillende blootstellingskarakteristieken. Met de toevoeging van HS in een concentratie variërend van 0,5 tot 40 mg C/L werd de stabiliteit van de suspensies van CeO_2NPs aanzienlijk verbeterd, waarbij de stabilisatie afhing van de HS concentratie. De

toxische effecten van CeO$_2$NPs op algen en watervlooien werden verminderd door verschillende concentraties HS, terwijl de toxiciteit voor zebravislarven werd versterkt. Er werd een concentratie-afhankelijke invloed van de toevoeging van HS op de toxiciteit van CeO$_2$NPs voor verschillende organismen waargenomen. Voorts werden relaties gevonden tussen de deeltjesstabiliteit en toxiciteit en tussen aquatische soorten en toxiciteit na toevoegen van HS. Deze bevindingen benadrukken de belangrijke rol van NOM bij het stabiliseren van de nano-suspensies en de verschillende invloed op de toxiciteit van CeO$_2$NPs voor verschillende waterorganismen.

2) Hoe beïnvloedt NOM het lot, de accumulatie en de toxiciteit van ENP-mengsels?

In hoofdstuk 3 werden het lot, de gezamenlijke toxiciteit, en de accumulatie van een mengsel van CuNPs en ZnONPs in *Daphnia magna* onder invloed van de aanwezigheid van natuurlijk organisch materiaal van de Suwannee River (SR-NOM) onderzocht. Verschillende concentraties SR-NOM hebben geen significante invloed op de hydrodynamische diameter en zetapotentiaal van de binaire mengsels. De enige uitzondering was dat het co-agglomeratiegedrag van ENP-mengsels aanzienlijk werd verminderd na toevoeging van 20 mg/L SR-NOM. De toevoeging van SR-NOM had geen significante invloed op de schijnbare gezamenlijke toxiciteit van CuNPs + ZnONPs. SR-NOM verhoogde de metaal bioaccumulatie van ENP-mengsels. De aanwezigheid van SR-NOM verhoogde de relatieve bijdrage aan de gezamenlijke toxiciteit van opgeloste metaalionen die uit metaalhoudende ENP's vrijkwamen. Met name de vrijgekomen Zn-

ionen domineerden de toxiciteit van de binaire ENP-mengsels in aanwezigheid van SR-NOM. Dit komt door de agglomeratie en sedimentatie van CuNP's en de complexatie van de vrijgekomen Cu-ionen met SR-NOM. Bovendien werd de accumulatie van Cu en Zn in de mengsels van CuNP's en ZnONP's in watervlooien opmerkelijk verhoogd door de toevoeging van SR-NOM.

3) In welke mate gaan ENP's over in deeltjes- en ionische vormen en hoe verandert de deeltjesgrootte en het aantal opgenomen deeltjes in verschillende organismen?

De trofische overdracht van CuNPs door een aquatische voedselketen bestaande uit algen, watervlooien en mysiden werd gekwantificeerd in hoofdstuk 4. De op aantal gebaseerde concentratie en grootte van Cu-deeltjes in verschillende tropische soorten werden gekwantificeerd met behulp van inductief gekoppelde plasmamassaspectrometrie met één deeltje (sp-ICP-MS). Een beperkte mate van trofische overdracht van totale CuNP's of Cu-ionen werd waargenomen van algen naar de mysiden. Ondertussen zagen we biomagnificatie van de Cu deeltjes van de algen naar de mysiden, hetgeen leidde tot een waarde van de trofische overdracht factor die hoger was dan 1.De aantallen Cu deeltjes in verschillende trofische niveaus in de orde van 1013 deeltjes/kg nat gewicht. De grootte van de Cu-deeltjes werd vastgesteld in een range van 22 tot 40 nm in de gehele voedselketen zonder significante veranderingen. Uit deze resultaten blijkt dat het traceren van de deeltjesfractie van ENP's even belangrijk is als het traceren van de ionische fractie langs de trofische overdracht.

4) Hoe beïnvloeden de deeltjesgrootte en het type voedselketen de trofische overdracht van ENP's en hun daaropvolgende biodistributie en toxiciteit voor de predatoren?

Om de invloed van typen voedselketens op de omvang van de trofische overdracht te vergelijken, zijn in hoofdstuk 4 en 5 de lengte van de voedselketen en de voedselbron beschouwd. De overdracht van CuNP's via drie gesimuleerde zoetwatervoedselketens werd geconstrueerd: van algen naar watervlooien naar mysiden, van algen naar mysiden, en van watervlooien naar mysiden (hoofdstuk 4). Trofische overdracht werd alleen aangetroffen in de voedselketen met twee niveaus van algen naar mysiden, en niet in de twee andere typen voedselketens. Dit leverde het bewijs dat zowel de positie in de voedselketen als de voedselbron van invloed zijn op het trofisch overdrachtspotentieel van CuNP's. Bovendien werden de significante effecten op de opnamesnelheid van voedsel van roofzuchtige mysiden door de CuNPs in het dieet gevonden in de overdrachtsprocessen van watervlooien naar de mysiden en van algen via watervlooien naar de mysiden.

De trofische overdracht van polystyreendeeltjes (PSP's) van watervlo naar mysiden als functie van de deeltjesgrootte (26, 500 en 4800 nm) werd onderzocht (hoofdstuk 5). Slechts een kleine fractie, variërend van 1 tot 5 % van alle door watervlooien ingenomen PSP's van alle afmetingen, werd overgedragen op mysiden. De mate van trofische overdracht is grootte-afhankelijk en nam af in de orde van 4800 nm > 500 nm > 26 nm PSP's. Bij de predator werd voor alle PSP-behandelingen met grootte geen trofische overdracht (trofische overdrachtsfactoren kleiner dan 1) waargenomen. Bovendien werden alle PSP's voornamelijk geaccumuleerd in het darmkanaal (maag en darm) van de mysiden. Onze bevindingen wijzen er bijgevolg op dat

PSP van verschillende grootte kan worden overgedragen in de voedselketen watervlo - mysids, en dat de invloed van de deeltjesgrootte op de potentiële trofische overdracht niet mag worden verwaarloosd.

Concluderend kan worden gesteld dat de bevindingen van het onderzoek in dit proefschrift het inzicht verbeteren in 1) de relatie tussen blootstellingskenmerken en toxiciteit van ENP's, 2) de gezamenlijke toxische werking van ENP-mengsels en de vergelijking met metaalzoutmengsels, 3) hoe NOM de individuele en gezamenlijke toxiciteit van ENP's beïnvloeden, 4) de mate van trofische overdracht van ENP's langs aquatische voedselketens, 5) de invloedsfactoren op de trofische overdracht, en 6) bioaccumulatie, distributie en toxisch effect op predatoren. Deze kennis heeft een basis opgeleverd voor gegevens over individuele en gezamenlijke toxiciteit, bioaccumulatie en trofische overdracht van ENP's voor een meer realistische risicobeoordeling voor het milieu.

Curriculum Vitae

Qi Yu was born on May 28th, 1992 in Qitaihe, Heilongjiang Province, China. She graduated from Qitaihe Experimental Senior High School in 2010, and started her Bachelor study in Ecology in Northeast Normal University from 2010 to 2014. After then, she continued her Master study in Environmental Science and Engineering in Dalian University of Technology from 2014 to 2017. She was supervised by Prof. Hong-Bin Xie in the group of Prof. Jingwen Chen. Her Master thesis was entitled "Atmospheric transformation mechanism and kinetics of alternatives of polybrominated diphenyl ethers initiated by OH radical". During her Master period, she presented her research findings in the 11th National Conference on Environmental Chemistry Conference in Guangzhou, and she was nominated for the "Outstanding Presentation". Her thesis was awarded one of the "Excellent Master's Thesis (2017016)" of Liaoning Province, and she was one of the "Outstanding Graduates" of Dalian University of Technology. After her Master study, she was awarded a scholarship by the "Chinese Scholarship Council" to continue PhD research in the Institute of Environmental Sciences in Leiden University in 2017 under the supervision of Prof. dr. Willie Peijnenburg, Prof. dr. Martina Vijver and Dr. Thijs Bosker. Her PhD research focused on the fate, bioaccumulation, toxicity and trophic transfer of nanoparticles, and the impact of natural organic matters. She presented her research findings in the Anniversary symposium of MilieuChemTox in Utrecht. She was a board member of "Leiden Science China" society.

Publication list

Qi Yu, Zhenyan Zhang, Fazel Abdolahpur Monikh, Juan Wu, Zhuang Wang, Martina G. Vijver, Thijs Bosker & Willie J. G. M. Peijnenburg (2022), Trophic transfer of Cu nanoparticles in a simulated aquatic food chain, *Ecotoxicology and Environmental Safety*, 242: 113920.

Qi Yu, Zhuang Wang, Guiyin Wang, Willie J.G.M. Peijnenburg & Martina G. Vijver (2021), Effects of natural organic matter on the joint toxicity and accumulation of Cu nanoparticles and ZnO nanoparticles in *Daphnia magna*, *Environmental Pollution*, 292: 118413.

Qi Yu, Zhuang Wang, Yujia Zhai, Fan Zhang, Martina G. Vijver & Willie J.G.M. Peijnenburg (2021), Effects of humic substances on the aqueous stability of cerium dioxide nanoparticles and their toxicity to aquatic organisms, *Science of the Total Environment*, 781: 146583.

Qi Yu, Tom A.P. Nederstigt, Zhuang Wang, Juan Wu, Aranka Kolmas, Thijs Bosker, Zuzanna Filipiak, Willie J.G.M. Peijnenburg & Martina G. Vijver, Accumulation kinetics of polystyrene nano- and micro-plastics in the waterflea *Daphnia magna* and trophic transfer to the mysid *Limnomysis benedeni*. In preparation

Qi Yu, Pan Wang, Fangfang Ma, Hong-Bin Xie, Ning He & Jingwen Chen. (2017), Computational investigation of the nitrosation mechanism of piperazine in CO_2 capture, *Chemosphere*, 186:341-349.

Qi Yu, Hong-Bin Xie, Tianchi Li, Fangfang Ma, Zihao Fu, Zhongyu Wang, Chao Li, Zhiqiang Fu, Deming Xia & Jingwen Chen (2017), Atmospheric chemical reaction mechanism and kinetics of 1,2-bis(2,4,6-tribromophenoxy)ethane initiated by oh radical: a computational study, *RSC Advances*, 7(16): 9484-9494.

Qi Yu, Hong-Bin Xie & Jingwen Chen (2016), Atmospheric chemical reactions of alternatives of polybrominated diphenyl ethers initiated by OH: A case study on triphenyl phosphate, *Science of the Total Environment*, 571:1105-1114.

Zhenyan Zhang, Xiaoji Fan, Willie J.G.M. Peijnenburg, Meng Zhang, Liwei Sun, Yujia Zhai, **Qi Yu**, Juan Wu, Tao Lu, Haifeng Qian (**2021**), Alteration of dominant cyanobacteria in different bloom periods caused by abiotic factors and species interactions, *Journal of Environmental Sciences*, 99: 1-9.

Juan Wu, **Qi Yu**, Thijs Bosker, Martina G. Vijver & Willie J.G.M. Peijnenburg (**2020**), Quantifying the relative contribution of particulate versus dissolved silver to toxicity and uptake kinetics of silver nanowires in lettuce: impact of size and coating, *Nanotoxicology,* 14(10): 1399-1414.

Zhuang Wang, Lan Song, Nan Ye, **Qi Yu**, Yujia Zhai, Fan Zhang, Martina G. Vijver & Willie J.G.M. Peijnenburg (**2020**), Oxidative stress actuated by cellulose nanocrystals and nanofibrils in aquatic organisms of different trophic levels, *NanoImpact,* 17: 100211.

Fangfang Ma, Zhezheng Ding, Jonas Elm, Hong-Bin Xie, **Qi Yu**, Cong Liu, Chao Li, Zhiqiang Fu, Lili Zhang & Jingwen Chen (**2018**). Atmospheric oxidation of piperazine initiated by cl: unexpected high nitrosamine yield, *Environmental Science and Technology*, 52(17), 9801-9809.

Zhongyu Wang, Zhiqiang Fu, **Qi Yu** & Jingwen chen (**2017**), Oxidation reactivity of 1,2-bis(2,4,6-tribromophenoxy)ethane (BTBPE) by Compound I model of cytochrome P450s, *Journal of Environmental Sciences*, 62(12):11-21.

Hong-Bin Xie, Fangfang Ma, **Qi Yu**, Ning He & Jingwen Chen (**2017**). Computational study of the reactions of chlorine radicals with atmospheric organic compounds featuring nhx–π-bond (x = 1, 2) structures, *Journal of Physical Chemistry A*, 121(8), 1657.

Zihao Fu, Ning He, Putian Zhou, Jiaxu Liu, Hong-Bin Xie, **Qi Yu**, Fangfang Ma, Zhiqiang Fu, Zhongyu Wang & Jingwen Chen (**2017**), Adsorption of nitrobenzene on the surface of ice: A grand canonical monte carlo simulation study, *Journal of Physical Chemistry C*, 121: 15746-15755.

Hong-Bin Xie, Fangfang Ma, Yuanfang Wang, Ning He, **Qi Yu** & Jingwen Chen (**2015**). Quantum chemical study on ·cl-initiated atmospheric degradation of monoethanolamine, *Environmental Science & Technology*, 13246-55.

Acknowledgement

I would like to express my sincere appreciation to my promotors Prof. dr. Willie Peijnenburg and Prof. dr. Martina Vijver for their guidance and support. They are marvelous scientists with immense knowledge, professional work spirit and high efficiency. I could not finish this thesis without their critical scientific feedback, continuous inspiration and infinite patience. I would also like to thank my supervisor Dr. Thijs Bosker for the motivation, advice on experiment design and the help in writing. He always gives me valuable encouragement with a big smile. It is my great honor to do my PhD research under their supervision.

I am grateful to my thesis committee: Prof.dr.ir. P.M. van Bodegom, Prof.dr. N.J. de Voogd, Dr. S.H. Barmentlo, Prof.dr. M.S. Sepúlveda and Prof.dr. Z. Wang for their time and expertise in reviewing my thesis.

Thanks to China Scholarship Council (CSC) for the financial support of my PhD study.

Special thanks to Dr. Zhuang Wang who provides invaluable help in the investigation, methodology, formal analysis, writing - review & editing. I am so lucky to receive support from Zhuang, a wise senior and selfless mentor. He is just like my other supervisor offering consistent guidance. Thanks to all co-authors for their efforts and contributions. I am also grateful to have had the opportunity to learn in the group of Prof. dr. Jingwen Chen in my Master study. Many many thanks to my Master supervisor Prof. dr. Hong-Bin Xie who opened the door of the scientific world for me.

I would like to thank my parents for their unfailing care and support. Thanks to my elder brother and my sister-in-law for their contribution to the family. I wish my nephew healthy and happy growth! Thanks to my cat S for the company and fun time. 爸、妈，谢谢你们无私的爱；哥、嫂子，你们辛苦了；大侄儿，请健康快乐的长大吧！

I would like to say thank you to myself as well. Thanks so much for your insistence, forgiveness, tolerance and acceptance. Thanks for slowing your steps to think and respect who you are and what you want. You are still weak but strong enough to go forwards.

Life is not as bad or good as you expect. Just go ahead. All is well or will be well.